

The Supporting Information for

**Solvent-Dependent *fac/mer*-Isomerization and Self-Assembly
of Triply Helical Complexes Bearing a Pivot Part**

Takuma Morozumi, Ryota Matsuoka, Takashi Nakamura, Tatsuya Nabeshima*

Faculty of Pure and Applied Sciences

and Tsukuba Research Center for Energy Materials Science (TREMS),

University of Tsukuba, 1-1-1 Tennodai, Tsukuba, Ibaraki 305-8571, Japan

*Corresponding Author. E-mail: nabesima@chem.tsukuba.ac.jp

Contents

Materials and methods	3
Synthesis and characterization of the compounds	4
Solvent dependence in the <i>fac/mer</i> -isomerization of [2bFe](TFPB) ₂	53
van't Hoff study of the <i>fac/mer</i> -isomerization in various solvents	55
DOSY-NMR spectra of [2bFe](TFPB) ₂ in CD ₃ CN or CDCl ₃	58
Comparison of solvent dependence between [2bFe](TFPB) ₂ and the others	60
Regression analyses with various solvent parameters	63
X-ray diffraction analysis	64
Cycle characteristics of exchanging solvent	65
Synthesis of imine-linked dimer and tetramer	66
References for the Supplementary Information	74

Materials and methods

Unless otherwise noted, the solvents and reagents were purchased from TCI Co., Ltd., FUJIFILM Wako Pure Chemical Industries, Ltd., Kanto Chemical Co., Inc., Nacalai Tesque, Inc., Cambridge Isotope Laboratories, Inc., or Sigma-Aldrich Co., and used without further purification. Dry THF and DMF were purified by Glass Contour Ultimate Solvent System 3S-TCN 1. Silica gel and amine-functionalized silica gel for column chromatography were purchased from Kanto Chemical Co. Inc. (Silica Gel 60 N (spherical, 63–210 μm) and Silica Gel 60 N (spherical, 40–50 μm) NH_2 , respectively). GPC purification was performed by a JAI LC-9210 II NEXT system with JAIGEL-1HH/2HH columns using CHCl_3 as the eluent.

Measurements were performed at 298 K unless otherwise noted. ^1H , ^{13}C , ^{11}B , ^{19}F , ^{31}P NMR, and other 2D NMR spectra were recorded by a Bruker AVANCE III-600 (600 MHz) spectrometer or a Bruker AVANCE III-400 (400 MHz) spectrometer. Negative values were depicted in red in the spectra. Tetramethylsilane was used as the internal standard (δ 0.00 ppm) for the ^1H and ^{13}C NMR measurements when CDCl_3 or a mixed solvent of $\text{CDCl}_3/\text{CD}_3\text{CN} = 1/1$ was used as the solvent. In the other deuterium solvents, the residual solvent signal was used as the internal standard for the ^1H NMR and ^{13}C NMR measurements. $\text{BF}_3 \cdot \text{Et}_2\text{O}$ in CDCl_3 (1 wt%) was used as the external standard (δ 0.00 ppm) for the ^{11}B NMR measurements. Hexafluorobenzene in CDCl_3 (1 wt%) was used as the external standard (δ -163.0 ppm) for the ^{19}F NMR measurements. Triphenylphosphine oxide in CDCl_3 (1 wt%) was used as an external standard (δ 30.0 ppm) for the ^{31}P NMR measurements. The assignments of the ^1H and ^{13}C signals were based on ^1H - ^1H COSY, ^1H - ^1H ROESY, ^1H - ^{13}C HSQC, and ^1H - ^{13}C HMBC measurements.

The ESI-TOF mass data were recorded by an AB SCIEX TripleTOF 4600 system. The HRMS values of iron complexes were calculated for the strongest peak using PeakView 1.2.0.3 software (AB SCIEX, 2012).

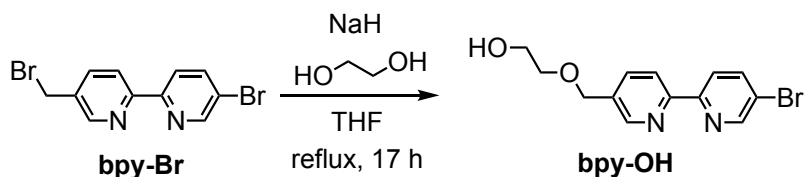
The single-crystal X-ray crystallographic measurements were performed using a Bruker APEX II ULTRA with $\text{MoK}\alpha$ radiation (graphite-monochromated, $\lambda = 0.71073 \text{ \AA}$) at 120 K. The collected diffraction images were processed by a Bruker APEX2. The initial structure was solved using SHELXT-2018^[S1] and refined using SHELXL-2018^[S2], which were running on Yadokari-XG crystallographic software^[S3]. CCDC 2067281 contain the data for this paper. The data can be obtained free of charge from The Cambridge Crystallographic Data Centre via www.ccdc.cam.ac.uk/getstructures.

The calculation of the structure of *mer*-[**1a**Fe]²⁺ was performed on a Spartan'18 software (Wavefunction Inc.). The initial structure was obtained by an equilibrium conformer search based on a molecular mechanics calculation (Forcefield: MMFF). The obtained initial structure was optimized by a DFT calculation (B3LYP/6-31G*, vacuum).

The elemental analysis was performed by a Yanaco MT-6 analyzer with tin boats purchased from Elementar. We appreciate Mr. Masao Sasaki of the University of Tsukuba for the elemental analyses.

Synthesis and characterization of the compounds

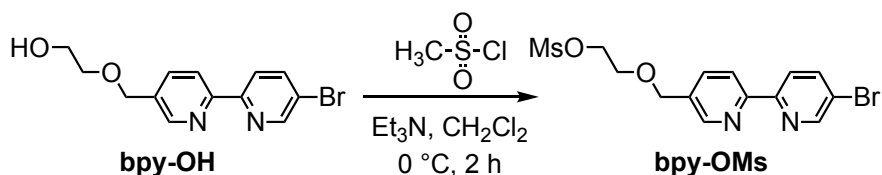
Synthesis of **bpy-OH**



To a suspension of NaH (60 wt% dispersion in mineral oil, 3.60 g, 90.0 mmol) in dry THF (150 mL) was added dry ethylene glycol (15.0 mL, 270 mmol), and the mixture was refluxed under an argon atmosphere. After 1 h, a suspension of **bpy-Br**^[S4] (9.84 g, 30.0 mmol) in dry THF (150 mL) was added to the suspension dropwise over 3 h. Then the reaction mixture was further refluxed for 17 h. After cooling to room temperature, the mixture was concentrated *in vacuo*. The residue was suspended in satd. NH₄Cl aq. (500 mL) and extracted with EtOAc (150 mL × 3). The combined organic layer was dried over MgSO₄, filtered, and concentrated *in vacuo*. The crude product was purified by column chromatography on amine-functionalized silica gel (EtOAc/hexane = 2/1) to give **bpy-OH** as a colorless solid (7.98 g, 25.8 mmol, 86%).

bpy-OH: colorless solid; ¹H NMR (600 MHz, CDCl₃) δ 8.72 (d, *J* = 2.4 Hz, 1H), 8.63 (d, *J* = 2.4 Hz, 1H), 8.37 (d, *J* = 8.4 Hz, 1H), 8.31 (d, *J* = 8.4 Hz, 1H), 7.94 (dd, *J* = 8.4, 2.4 Hz, 1H), 7.82 (dd, *J* = 8.4, 2.4 Hz, 1H), 4.64 (s, 2H), 3.82–3.79 (m, 2H), 3.66 (t, *J* = 4.5 Hz, 2H), 2.09 (br t, *J* = 5.7 Hz, 1H); ¹³C NMR (151 MHz, CDCl₃) δ 154.8, 154.4, 150.2, 148.6, 139.5, 136.5, 133.8, 122.3, 121.2, 120.8, 71.8, 70.6, 61.9; Anal. Calcd for C₁₃H₁₃BrN₂O₂: C, 50.51; H, 4.24; N, 9.06. Found: C, 50.26; H, 4.04; N, 8.91.

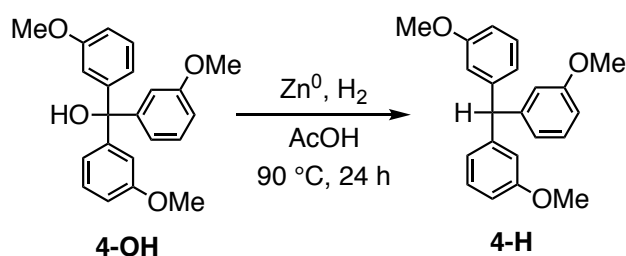
Synthesis of **bpy-OMs**



To a solution of **bpy-OH** (6.95 g, 22.5 mmol) in CH₂Cl₂ (150 mL) was added Et₃N (3.6 mL, 25.9 mmol) and methanesulfonyl chloride (2.0 mL, 25.9 mmol) at 0 °C under an argon atmosphere. The mixture was stirred at 0 °C for 2 h. 0.1 M HCl aq. (50 mL) was added to the reaction mixture, and the organic layer was separated, washed with satd NaHCO₃ aq. (50 mL), dried over MgSO₄, filtered, and concentrated *in vacuo*. The residue was washed with diethyl ether to give **bpy-OMs** as a pale yellow solid (7.48 g, 19.3 mmol, 86%).

bpy-OMs: pale yellow solid; ¹H NMR (600 MHz, CDCl₃) δ 8.72 (d, *J* = 1.8 Hz, 1H), 8.63 (d, *J* = 1.8 Hz, 1H), 8.38 (d, *J* = 8.4 Hz, 1H), 8.31 (d, *J* = 8.4 Hz, 1H), 7.94 (dd, *J* = 8.4, 1.8 Hz, 1H), 7.82 (dd, *J* = 8.4, 1.8 Hz, 1H), 4.66 (s, 2H), 4.43–4.42 (m, 2H), 3.82–3.80 (m, 2H), 3.05 (s, 3H); ¹³C NMR (151 Hz, CDCl₃) δ 155.0, 154.3, 150.2, 148.6, 139.5, 136.5, 133.3, 122.4, 121.2, 120.8, 70.7, 68.7, 68.3, 37.7; HRMS (ESI): *m/z* calcd for C₁₄H₁₆BrN₂O₄S⁺ ([**bpy-OMs**•H]⁺): 387.0010; found: 387.0005.

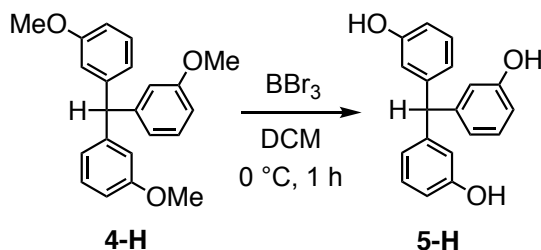
Synthesis of **4-H**



A suspension of **4-OH**^[S5] (3.50 g, 10.0 mmol) and Zn powder (11.3 g, 173 mmol) in acetic acid (50 mL) was stirred at 90 °C for 24 h under a hydrogen atmosphere. The reaction mixture was filtered, and H₂O (100 mL) was added to the filtrate. The suspension was extracted with CHCl₃ (50 mL × 3). The organic layer was washed with satd NaHCO₃ aq. (100 mL × 2), dried over MgSO₄, filtered, and concentrated *in vacuo*. The crude product was purified by column chromatography on silica gel (CH₂Cl₂/hexane = 2/1) to give **4-H** as a colorless solid (1.46 g, 4.36 mmol, 44%).

4-H: colorless solid; ¹H NMR (600 MHz, CDCl₃) δ 7.19 (dd, *J* = 7.8, 7.8 Hz, 3H), 6.75 (dd, *J* = 7.8 Hz, 2.4 Hz, 3H), 6.72 (d, *J* = 7.8 Hz, 3H), 6.67 (dd, *J* = 2.4, 2.4 Hz, 3H), 5.44 (s, 1H), 3.73 (s, 9H); ¹³C NMR (151 MHz, CDCl₃) δ 159.7, 145.3, 129.3, 122.1, 115.7, 111.5, 57.0, 55.2; Anal. Calcd for C₂₂H₂₂O₃: C, 79.02; H, 6.63; N, 0.00. Found: C, 78.87; H, 6.71; N, 0.00.

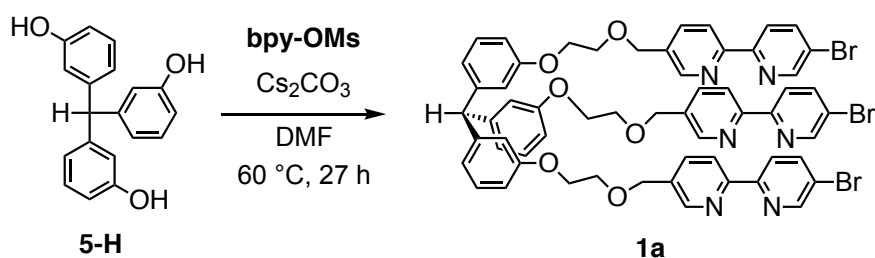
Synthesis of **5-H**



To a solution of **4-H** (0.846 g, 2.53 mmol) in dry CH₂Cl₂ (12.3 mL) was added BBr₃ (0.80 mL, 8.4 mmol) at 0 °C under an argon atmosphere. After being stirred at 0 °C for 1 h, the reaction mixture was quenched with brine (50 mL) and extracted with THF (50 mL × 2). The combined organic layer was dried over Na₂SO₄, filtered, and concentrated *in vacuo* at 150 °C for 12 h to give **5-H** (0.731 g, 2.50 mmol, 99%) as a colorless solid.

5-H: colorless solid; ¹H NMR (600 MHz, DMSO-*d*₆) δ 9.25 (s, 3H), 7.07 (dd, *J* = 7.8, 7.8 Hz, 3H), 6.58 (dd, *J* = 7.8, 1.8 Hz, 3H), 6.53 (d, *J* = 7.8 Hz, 3H), 6.50 (dd, *J* = 1.8, 1.8 Hz, 3H), 5.29 (s, 1H); ¹³C NMR (151 MHz, CDCl₃) δ 157.1, 145.2, 129.0, 119.8, 116.0, 113.1, 55.6; Anal. Calcd for C₁₉H₁₇O_{3.5} (**5-H**·0.5H₂O): C, 75.73; H, 5.69; N, 0.00. Found: C, 75.92; H, 5.47; N, 0.00.

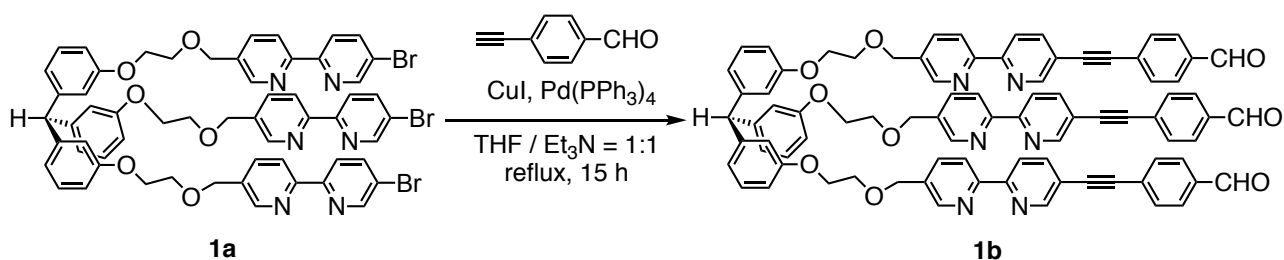
Synthesis of **1a**



A suspension of **5-H** (0.694 g, 2.37 mmol) and Cs₂CO₃ (2.32 g, 7.12 mmol) in dry DMF (25 mL) was stirred at 60 °C under an argon atmosphere. After 30 min, a solution of **bpy-OMs** (2.77 g, 7.16 mmol) in dry DMF (40 mL) was added to the reaction mixture, and the mixture was further stirred for 27 h. H₂O (200 mL) was added to the mixture, and the mixture was extracted with a mixed solvent of EtOAc/hexane = 1/1 (50 mL × 3). The combined organic layer was washed with H₂O (100 mL), dried over MgSO₄, filtered, and concentrated *in vacuo*. The crude product was purified by column chromatography on amine-functionalized silica gel (EtOAc/hexane = 1/2) to give **1a** as a pale brown solid (0.853 g, 0.732 mmol, 31%).

1a: pale brown solid; ¹H NMR (600 MHz, CDCl₃) δ 8.70 (d, *J* = 2.4 Hz, 3H), 8.60 (d, *J* = 1.8 Hz, 3H), 8.32 (d, *J* = 8.4 Hz, 3H), 8.29 (d, *J* = 8.4 Hz, 3H), 7.91 (dd, *J* = 8.4, 2.4 Hz, 3H), 7.45 (dd, *J* = 8.2, 1.8 Hz, 3H), 7.18 (dd, *J* = 7.8, 7.8 Hz, 3H), 6.76 (dd, *J* = 7.8, 1.8 Hz, 3H), 6.73–6.69 (m, 6H), 5.42 (s, 1H), 4.65 (s, 6H), 4.09 (t, 4.8 Hz, 6H), 3.82 (t, 4.8 Hz, 6H); ¹³C NMR (151 MHz, CDCl₃) δ 158.9, 154.8, 154.6, 150.3, 148.7, 145.3, 139.6, 136.6, 134.1, 129.4, 122.5, 122.4, 121.2, 120.8, 116.4, 112.3, 70.9, 69.2, 67.4, 57.0; ESI-MS: *m/z* calcd for C₅₈H₄₉Br₃N₆O₆⁺ ([**1a**•H]⁺): 1163.13; found:1163.12.

Synthesis of **1b**

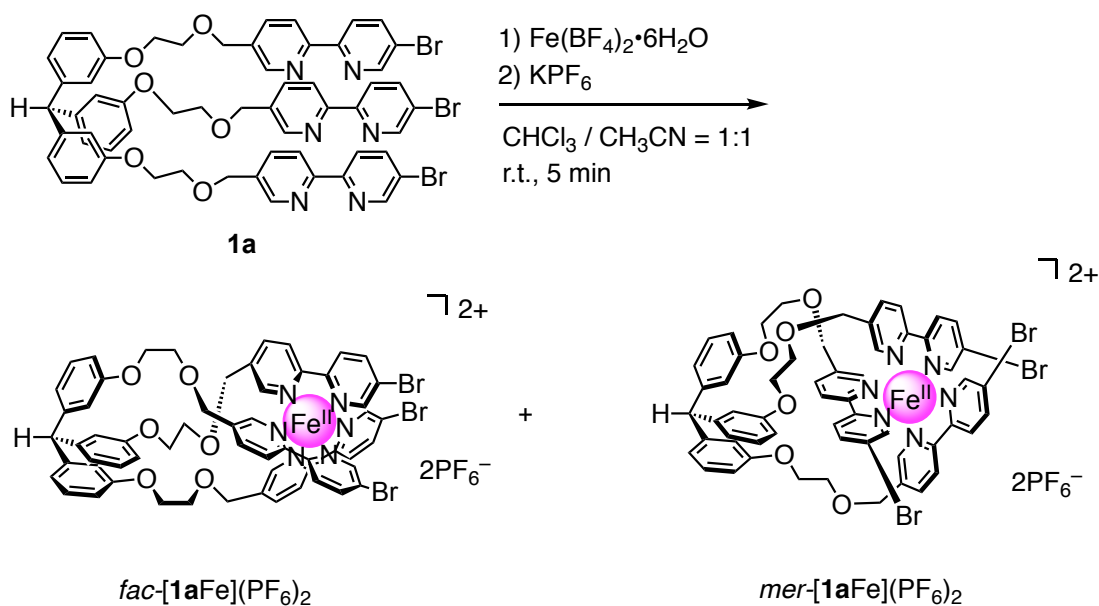


A solution of **1a** (0.227 g, 0.195 mmol), 4-ethynylbenzaldehyde^[S7] (0.153 g, 1.17 mmol), Pd(PPh₃)₄ (0.169 g, 0.146 mmol), and CuI (28.4 mg, 0.146 mmol) in a mixed solvent of dry THF (20 mL) and Et₃N (20 mL) was refluxed under an argon atmosphere. After 15 h, the mixture was concentrated *in vacuo*. The residue was suspended in a solution of EDTA•4Na•4H₂O (0.689 g, 1.52 mmol) in H₂O (50 mL) and extracted with CHCl₃ (30 mL × 3). The combined organic layer was dried over Na₂SO₄, filtered, and concentrated *in vacuo*. The crude product was purified by GPC (using CHCl₃ as an eluent) and reprecipitation from CHCl₃/diethyl ether to give **1b** as a pale brown solid (0.0671 g, 51.1 μmol, 26%).

1b: pale brown solid; ¹H NMR (600 MHz, CDCl₃) δ 10.04 (s, 3H), 8.81 (br s, 3H), 8.64 (br s, 3H), 8.42 (d, *J* = 8.4 Hz, 3H), 8.40 (d, *J* = 8.4 Hz, 3H), 7.94 (dd, *J* = 8.4, 1.8 Hz, 3H), 7.89 (d, *J* = 7.8 Hz, 6H), 7.82 (dd, *J* = 8.4, 1.8 Hz, 3H), 7.71 (d, *J* = 7.8 Hz, 6H), 7.19 (dd, *J* = 7.8, 7.8 Hz, 3H), 6.78 (br d, *J* = 7.8 Hz, 3H), 6.74–6.71 (m, 6H), 5.43 (s, 1H), 4.68 (s, 6H), 4.11 (t, *J* = 4.2 Hz, 6H), 3.83 (t, *J* = 4.2 Hz, 6H); ¹³C NMR (151 MHz, CDCl₃) δ 191.3, 158.9, 155.5, 154.9, 151.9, 148.8, 145.3, 139.6, 136.5, 136.0, 134.2, 132.4, 129.7, 129.4, 128.9, 122.5, 121.3, 120.5, 119.6, 116.5, 112.4, 92.6, 90.4, 86.0, 70.9, 69.2, 67.5, 57.0.

Although we tried to characterize **1b** by ESI-MS and MALDI-MS in various conditions, but **1b** was not observed under any investigated conditions.

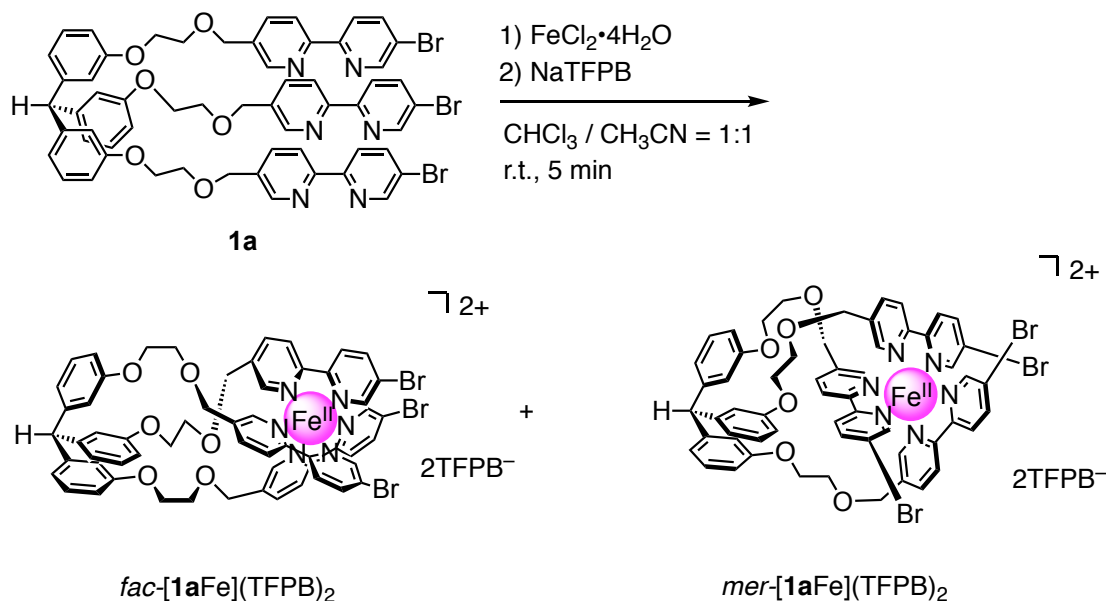
Synthesis of [1aFe](PF₆)₂



A solution of **1a** (0.122 g, 0.100 mmol) and Fe(BF₄)₂·6H₂O (41.5 mg, 0.123 mmol) in a mixed solvent of CH₃CN/CHCl₃ = 1/1 (30 mL) was sonicated for 5 min. A solution of KPF₆ (1.84 g, 10.0 mmol) in H₂O (100 mL) was added to the reaction mixture, and the mixture was extracted with a mixed solvent of CH₃CN/CHCl₃ = 1/2 (50 mL × 3). The combined organic layer was dried over Na₂SO₄, filtered, and concentrated *in vacuo*. The crude product was purified by column chromatography on silica gel (CH₃CN/CHCl₃ = 1/4) to give [1aFe](PF₆)₂ as a red solid (0.104 g, 0.068 mmol, 68%).

[1aFe](PF₆)₂: red solid; ¹H NMR (600 MHz, CD₃CN, the signals for the *fac*-isomer are shown) δ 8.51 (d, *J* = 8.4 Hz, 3H), 8.38 (d, *J* = 8.4 Hz, 3H), 8.29 (dd, *J* = 8.4, 2.4 Hz, 3H), 8.17 (dd, *J* = 8.4, 1.2 Hz, 3H), 7.46 (d, *J* = 2.4 Hz, 3H), 7.26 (dd, *J* = 7.8, 7.8 Hz, 3H), 7.18 (d, *J* = 1.2 Hz, 3H), 6.87 (d, *J* = 7.8 Hz, 3H), 6.76 (dd, *J* = 7.8, 1.8 Hz, 3H), 6.39 (dd, *J* = 1.8, 1.8 Hz, 3H), 5.55 (s, 1H), 4.39 (dd, *J* = 83.4, 12.6 Hz, 3H), 4.13 (dd, *J* = 9.0, 9.0 Hz, 3H), 4.00–3.92 (m, 6H), 3.75–3.70 (m, 3H); ¹³C NMR (151 MHz, CD₃CN, the signals for the *fac*-isomer are shown) δ 159.5, 159.0, 158.6, 156.4, 153.4, 146.1, 142.9, 140.2, 139.4, 131.0, 125.7, 125.6, 123.8, 123.2, 117.6, 110.5, 70.9, 70.5, 68.8, 56.3; ¹⁹F NMR (376 MHz, CD₃CN) δ -73.0 (d, ¹*J*_{F-P} = 707 Hz); ³¹P NMR (243 MHz, CD₃CN) δ -144.6 (septet, ¹*J*_{P-F} = 707 Hz); HRMS (ESI-MS): *m/z* calcd for C₅₈H₄₉Br₃FeN₆O₆²⁺ ([1aFe]²⁺): 608.0324; found: 608.0335.

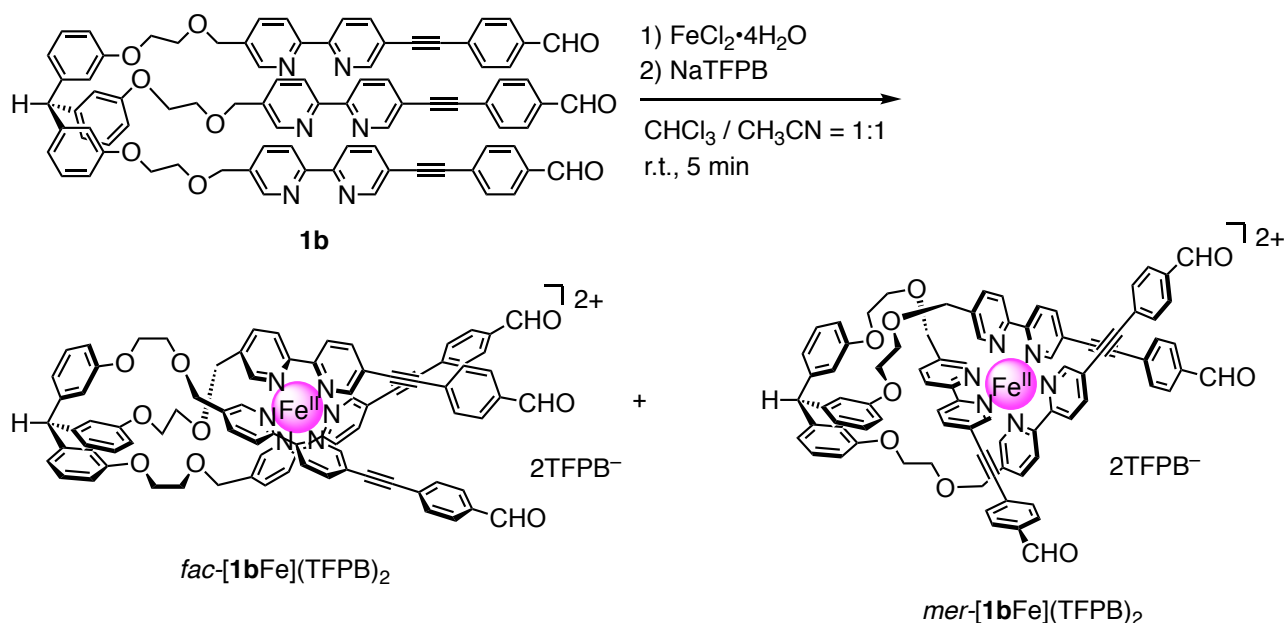
Synthesis of [1aFe](TFPB)₂



A solution of **1a** (0.122 g, 0.100 mmol) and FeCl₂·4H₂O (24.3 mg, 0.122 mmol) in a mixed solvent of CH₃CN/CHCl₃ = 1/1 (30 mL) was sonicated for 5 min. A solution of sodium tetrakis[3,5-bis(trifluoromethyl)phenyl]borate (NaTFPB) (0.806 g, 0.909 mmol) in H₂O (100 mL) was added to the reaction mixture, and the mixture was extracted with a mixed solvent of CH₃CN/CHCl₃ = 1/2 (50 mL × 3). The combined organic layer was dried over Na₂SO₄, filtered, and concentrated *in vacuo*. The crude product was purified by column chromatography on silica gel (CH₃CN/CHCl₃ = 1/4) to give [1aFe](TFPB)₂ as a red solid (0.236 g, 80 μmol, 80%).

[1aFe](TFPB)₂: red solid; ¹H NMR (600 MHz, CD₃CN, the signals for the *fac*-isomer are shown) δ 8.50 (d, *J* = 8.4 Hz, 3H), 8.38 (d, *J* = 8.4 Hz, 3H), 8.28 (dd, *J* = 8.4, 3.0 Hz, 3H), 8.16 (dd, *J* = 8.4, 1.8 Hz, 3H), 7.69 (br s, 16H), 7.66 (s, 8H), 7.46 (d, *J* = 1.8 Hz, 3H), 7.25 (dd, *J* = 8.4, 8.4 Hz, 3H), 7.18 (d, *J* = 1.8 Hz, 3H), 6.87 (br d, *J* = 8.4 Hz, 3H), 6.83 (dd, *J* = 8.4, 3.0 Hz, 3H), 6.39 (dd, *J* = 3.0, 3.0 Hz, 3H), 5.55 (s, 1H), 4.31 (dd, *J* = 85.2, 17.4 Hz, 6H), 4.16–4.09 (m, 3H) 4.01–3.91 (m, 6H), 3.75–3.68 (m, 3H); ¹³C NMR (151 MHz, CD₃CN, the signals for the *fac*-isomer are shown) δ 162.7 (q, ¹*J*_{C-B} = 49.8 Hz), 159.5, 159.0, 158.6, 156.4, 153.5, 146.1, 142.9, 140.2, 139.4, 135.7 (br s), 131.0, 130.0 (qq, ²*J*_{C-F} = 31.9 Hz, ³*J*_{C-F} = 3.8 Hz), 125.7, 125.6, 125.5 (q, ¹*J*_{C-F} = 272 Hz), 123.8, 123.2, 118.7 (septet, ³*J*_{C-F} = 3.8 Hz), 117.6, 110.4, 70.9, 70.5, 68.8, 56.4; ¹¹B NMR (192 MHz, CD₃CN) δ -6.65; ¹⁹F NMR (376 MHz, CD₃CN) δ -63.3; HRMS (ESI-MS): *m/z* calcd for C₅₈H₄₉Br₃FeN₆O₆²⁺ ([1aFe]²⁺): 608.0324; found: 608.0310.

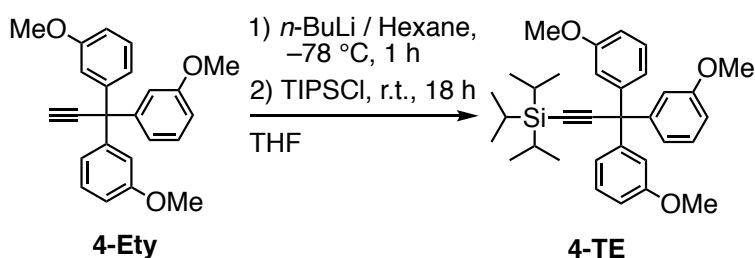
Synthesis of [1bFe](TFPB)₂



A solution of **1b** (0.104 g, 79.2 μmol) and FeCl₂·4H₂O (26.9 mg, 135 μmol) in a mixed solvent of CH₃CN/CHCl₃ = 1/1 (10 mL) was sonicated for 5 min. A solution of NaTFPB (0.489 g, 0.552 mmol) in H₂O (50 mL) was added to the reaction mixture, and the mixture was extracted with a mixed solvent of CH₃CN/CHCl₃ = 1/2 (20 mL × 3). The combined organic layer was dried over Na₂SO₄, filtered, and concentrated *in vacuo*. The crude product was purified by column chromatography on silica gel (CH₃CN/CHCl₃ = 1/4) to give [1bFe](TFPB)₂ as a purple solid (0.104 g, 33.6 μmol, 42%).

[1bFe](TFPB)₂: purple solid; ¹H NMR (600 MHz, CD₃CN, the signals for the *fac*-isomer are shown) δ 10.00 (s, 3H), 8.56 (d, *J* = 8.4 Hz, 3H), 8.54 (d, *J* = 8.4 Hz, 3H), 8.25 (d, *J* = 8.4 Hz, 3H), 8.19 (d, *J* = 8.4 Hz, 3H), 7.89 (d, *J* = 7.8 Hz, 6H), 7.69 (br s, 16H), 7.68–7.62 (m, 17H), 7.30–7.23 (m, 6H), 6.88 (d, *J* = 7.8 Hz, 3H), 6.77 (d, *J* = 7.8 Hz, 3H), 6.41 (s, 3H), 5.56 (s, 1H), 4.42 (dd, *J* = 85.2, 12.6 Hz, 6H) 4.17–4.11 (m, 6H), 4.02–3.93 (m, 6H), 3.78–3.71 (m, 3H); ¹³C NMR (151 MHz, CD₃CN, the signals for the *fac*-isomer are shown) δ 192.8, 162.7 (q, ¹*J*_{C-B} = 49.8 Hz), 159.6, 159.5, 158.8, 157.4, 153.7, 146.2, 142.2, 140.3, 139.4, 137.9, 135.7 (br s), 133.3, 131.0, 130.6, 130.1 (qq, ²*J*_{C-F} = 31.9 Hz, ³*J*_{C-F} = 3.8 Hz), 128.1, 125.8, 125.5 (q, ¹*J*_{C-F} = 272 Hz), 124.9, 124.1, 123.3, 118.7 (septet, ³*J*_{C-F} = 3.8 Hz), 117.7, 110.6, 96.1, 88.2, 71.0, 70.6, 68.8, 56.5; ¹¹B NMR (192 MHz, CD₃CN) δ –6.68; ¹⁹F NMR (376 MHz, CD₃CN) δ –63.2; HRMS (ESI): *m/z* calcd for C₈₅H₆₄FeN₆O₉²⁺ ([1bFe]²⁺): 683.2060; found: 683.2072.

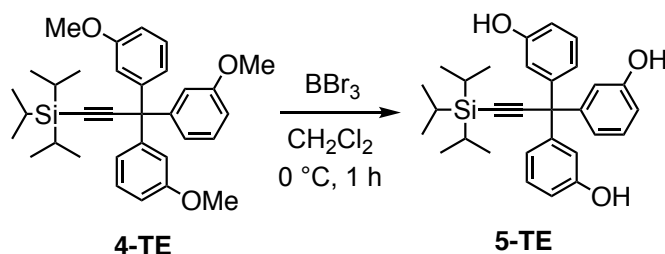
Synthesis of 4-TE



To a solution of **4-Ety**^[S5] (3.58 g, 9.98 mmol) in dry THF (100 mL) was added a solution of *n*-BuLi in hexane (1.57 M, 7.0 mL, 11.0 mmol) at -78 °C under an argon atmosphere. After the mixture was stirred at -78 °C for 1 h, triisopropylsilyl chloride (2.4 mL, 11.7 mmol) was added at r.t. After being stirred at r.t. for 18 h, the reaction mixture was diluted with H₂O (200 mL) and extracted with CHCl₃ (100 mL × 3). The combined organic layer was dried over MgSO₄, filtered, and concentrated *in vacuo*. The crude product was recrystallized from methanol to give **4-TE** (4.84 g, 9.42 mmol, 94%) as a colorless solid.

4-TE: colorless solid, m.p. 91.2–92.2 °C; ¹H NMR (600 MHz, CDCl₃) δ 7.16 (dd, *J* = 7.8, 7.8 Hz, 3H), 6.93 (dd, *J* = 1.8, 1.8 Hz, 3H), 6.82 (d, *J* = 7.8 Hz, 3H), 6.77 (dd, *J* = 7.8, 1.8 Hz, 3H), 3.73 (s, 9H), 1.10–1.09 (m, 21H); ¹³C NMR (151 MHz, CDCl₃) δ 159.2, 146.6, 128.6, 121.8, 115.0, 113.3, 112.4, 85.7, 56.8, 55.1, 18.8, 11.4; Anal. Calcd for C₃₃H₄₂O₃Si: C, 77.00; H, 8.22; N, 0.00. Found: C, 76.93; H, 8.22; N, 0.00.

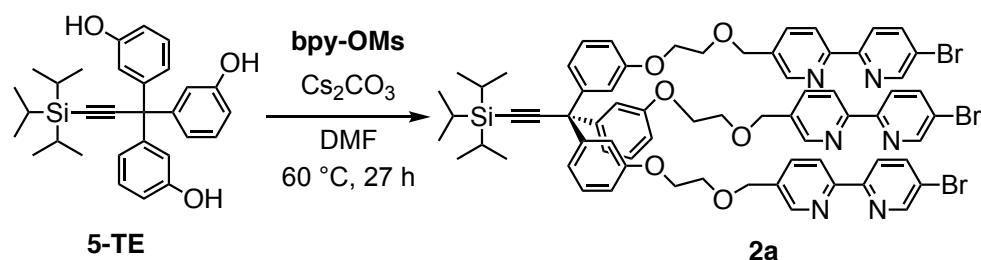
Synthesis of 5-TE



To a solution of **4-TE** (9.30 g, 17.5 mmol) in dry CH₂Cl₂ (78 mL) was added BBr₃ (6.0 mL, 64.5 mmol) at 0 °C under an argon atmosphere. After being stirred at 0 °C for 1 h, the reaction mixture was quenched with H₂O (200 mL), and extracted with diethyl ether (100 mL × 3). The combined organic layer was dried over Na₂SO₄, filtered, and concentrated *in vacuo*. The crude product was recrystallized from diethyl ether/hexane to give **5-TE** (7.46 g, 15.8 mmol, 90%) as a colorless solid.

5-TE: colorless solid, m.p. 196–197 °C; ¹H NMR (600 MHz, DMSO-*d*₆) δ 9.35 (s, 3H), 7.10 (dd, *J* = 7.8, 7.8 Hz, 3H), 6.68 (d, *J* = 7.8 Hz, 3H), 6.65 (dd, *J* = 7.8, 1.8 Hz, 3H), 6.60 (dd, *J* = 1.8, 1.8 Hz, 3H), 1.08–1.04 (m, 21H); ¹³C NMR (151 MHz, DMSO-*d*₆) δ 157.3, 146.6, 129.1, 119.8, 116.5, 114.3, 114.2, 84.9, 56.3, 19.0, 11.4; Anal. Calcd for C₃₀H_{36.8}O_{3.4}Si (**5-TE**·0.4H₂O): C, 75.08; H, 7.73; N, 0.00. Found: C, 75.05; H, 7.67; N, 0.00.

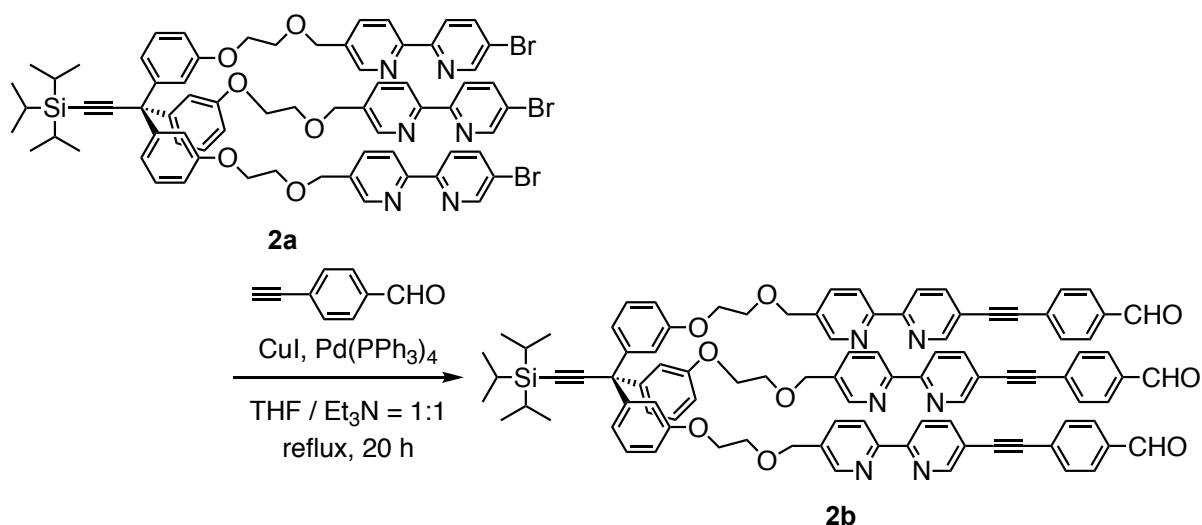
Synthesis of **2a**



A suspension of **5-TE** (1.18 g, 2.50 mmol) and Cs_2CO_3 (2.61 g, 8.00 mmol) in dry DMF (50 mL) was stirred at 60 °C under an argon atmosphere. After 30 min, a solution of **bpy-OMs** (3.10 g, 8.00 mmol) in dry DMF (40 mL) was added, and the reaction mixture was further stirred at 60 °C for 27 h. H_2O (200 mL) was added, and the mixture was extracted with a mixed solvent of ethyl acetate/hexane = 1/1 (50 mL \times 3). The combined organic layer was washed with H_2O (100 mL), dried over MgSO_4 , filtered, and concentrated *in vacuo*. The crude product was purified by column chromatography on amine-functionalized silica gel (ethyl acetate/hexane = 1/2) to give **2a** as a pale brown solid (1.66 g, 1.23 mmol, 49%).

2a: pale brown solid; ^1H NMR (600 MHz, CDCl_3) δ 8.68 (d, $J = 1.8$ Hz, 3H), 8.59 (d, $J = 1.8$ Hz, 3H), 8.32 (d, $J = 8.4$ Hz, 3H), 8.27 (d, $J = 8.4$ Hz, 3H), 7.87 (dd, $J = 8.4, 1.8$ Hz, 3H), 7.76 (dd, $J = 8.4, 1.8$ Hz, 3H), 7.18 (dd, $J = 7.8, 7.8$ Hz, 3H), 6.98 (s, 3H), 6.89 (d, $J = 7.8$ Hz, 3H), 6.81 (dd, $J = 7.8, 1.8$ Hz, 3H), 4.63 (s, 6H), 4.09 (t, $J = 4.2$ Hz, 6H), 3.80 (t, $J = 4.2$ Hz, 6H), 1.12–1.07 (m, 21H); ^{13}C NMR (151 MHz, CDCl_3) δ 158.3, 154.5, 154.3, 150.1, 148.5, 146.5, 139.4, 136.3, 133.9, 128.7, 122.2, 122.1, 121.0, 120.6, 115.7, 113.3, 113.1, 85.8, 70.6, 69.0, 67.3, 56.8, 18.8, 11.4; HRMS (ESI): m/z calcd for $\text{C}_{69}\text{H}_{70}\text{Br}_3\text{N}_6\text{O}_6\text{Si}^+$ ($[\mathbf{2a}\cdot\text{H}]^+$): 1343.2671; found: 1343.2703.

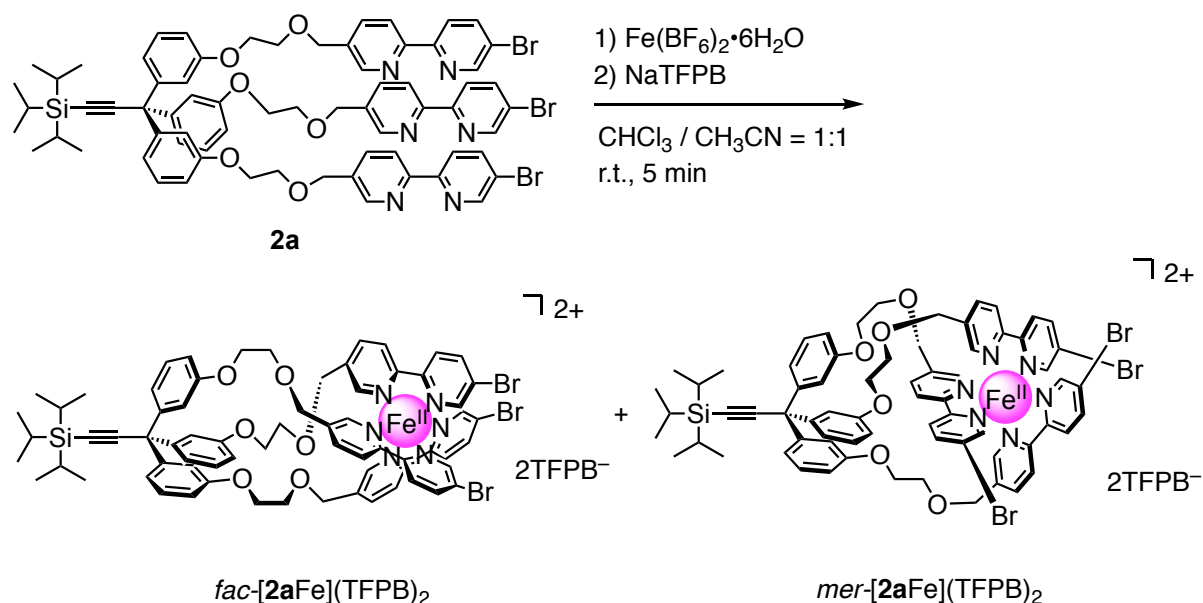
Synthesis of **2b**



A solution of **2a** (0.686 g, 0.510 mmol), 4-ethynylbenzaldehyde^[S7] (0.390 g, 3.00 mmol), Pd(PPh₃)₄ (0.200 g, 0.17 mmol), and CuI (68.0 mg, 0.350 mmol) in a mixed solvent of dry THF (50 mL) and Et₃N (50 mL) was refluxed under an argon atmosphere. After 20 h, the mixture was concentrated *in vacuo*. The residue was suspended in a solution of EDTA•4Na•4H₂O (2.32 g, 5.13 mmol) in H₂O (200 mL) and extracted with CHCl₃ (50 mL × 3). The combined organic layer was dried over Na₂SO₄, filtered, and concentrated *in vacuo*. The crude product was purified by GPC (using CHCl₃ as eluent) to give **2b** as a pale brown solid (0.602 g, 0.403 mmol, 79%).

2b: pale brown solid; ¹H NMR (600 MHz, CDCl₃) δ 10.02 (s, 3H), 8.82 (d, *J* = 1.8 Hz, 3H), 8.64 (d, *J* = 1.8 Hz, 3H), 8.42 (d, *J* = 8.4 Hz, 3H), 8.40 (d, *J* = 8.4 Hz, 3H), 7.94 (dd, *J* = 8.4, 1.8 Hz, 3H), 7.88 (d, *J* = 8.4 Hz, 6H), 7.82 (dd, *J* = 8.4, 1.8 Hz, 3H), 7.70 (d, *J* = 8.4 Hz, 6H), 7.18 (dd, *J* = 7.8, 7.8 Hz, 3H), 6.95 (br s, 3H), 6.87 (br d, *J* = 7.8 Hz, 3H), 6.82 (dd, *J* = 7.8, 1.8 Hz, 3H), 4.67 (s, 6H), 4.10 (t, *J* = 4.8 Hz, 6H), 3.83 (t, *J* = 4.8 Hz, 6H), 1.09–1.80 (m, 21H); ¹³C NMR (151 MHz, CDCl₃) δ 191.4, 158.5, 155.4, 154.9, 151.9, 148.8, 146.7, 139.6, 136.5, 135.9, 134.2, 132.3, 129.7, 128.9, 122.8, 122.3, 121.3, 120.5, 119.6, 115.8, 113.4, 113.2, 92.6, 90.4, 86.0, 70.8, 69.1, 67.4, 56.9, 18.9, 11.6; HRMS (ESI): *m/z* calcd for C₉₆H₈₅N₆O₉Si⁺ ([**2b**•H]⁺): 1493.6142; found: 1493.6138.

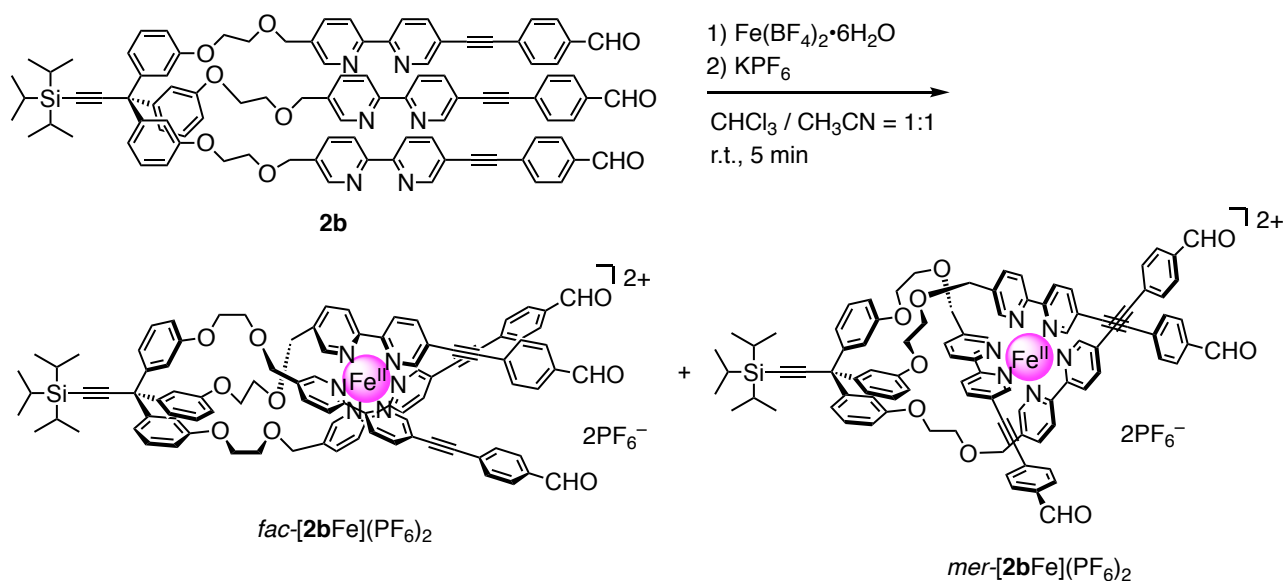
Synthesis of $[2\mathbf{a}Fe](TFPB)_2$



A solution of **2a** (0.108 g, 80.2 μ mol) and $Fe(BF_4)_2 \cdot 6H_2O$ (32.1 mg, 95.1 μ mol) in a mixed solvent of $CH_3CN/CHCl_3 = 1/1$ (30 mL) was sonicated for 5 min. A solution of NaTFPB (0.408 g, 456 μ mol) in H_2O (100 mL) was added to the reaction mixture, and the mixture was extracted with a mixed solvent of $CH_3CN/CHCl_3 = 1/2$ (30 mL \times 3). The combined organic layer was dried over Na_2SO_4 , filtered, and concentrated *in vacuo*. The crude product was purified by column chromatography on silica gel ($CH_3CN/CHCl_3 = 1/4$) to give $[2\mathbf{a}Fe](TFPB)_2$ as a red solid (0.123 g, 39.3 mmol, 49%).

$[2\mathbf{a}Fe](TFPB)_2$: red solid; 1H NMR (600 MHz, CD_3CN , the signals for the *fac*-isomer are shown) δ 8.49 (d, $J = 8.4$ Hz, 3H), 8.37 (d, $J = 8.4$ Hz, 3H), 8.28 (dd, $J = 8.4, 1.8$ Hz, 3H), 8.13 (dd, $J = 8.4, 1.2$ Hz, 3H), 7.69 (br s, 16H), 7.66 (s, 8H), 7.45 (d, $J = 1.8$ Hz, 3H), 7.42 (dd, $J = 7.8, 1.8$ Hz, 3H), 7.34 (dd, $J = 7.8, 7.8$ Hz, 3H), 7.14 (d, $J = 1.2$ Hz, 3H), 6.83 (dd, $J = 7.8, 1.8$ Hz, 3H), 6.07 (dd, $J = 1.8, 1.8$ Hz, 3H), 4.31 (dd, $J = 41.4, 12.0$ Hz, 6H), 4.13–4.08 (m, 3H), 3.97–3.92 (m, 3H), 3.92–3.87 (m, 3H), 3.72–3.67 (m, 3H), 1.12–1.08 (m, 21H); ^{13}C NMR (151 MHz, CD_3CN , the signals for the *fac*-isomer are shown) δ 162.6 (q, $^1J_{C-B} = 49.7$ Hz), 159.0, 158.9, 158.6, 156.4, 153.4, 147.3, 142.9, 140.1, 139.6, 135.7 (br s), 130.9, 130.0 (qq, $^2J_{C-F} = 31.9$ Hz, $^3J_{C-F} = 3.8$ Hz), 125.7, 125.5, 125.5 (q, $^1J_{C-F} = 272$ Hz), 123.9, 122.7, 118.7 (septet, $^3J_{C-F} = 3.8$ Hz), 117.7, 113.6, 111.4, 87.0, 70.8, 70.1, 68.6, 57.1, 19.1, 12.3; ^{11}B NMR (192 MHz, CD_3CN) δ -6.65; ^{19}F NMR (376 MHz, CD_3CN) δ -63.2; HRMS (ESI): m/z calcd for $C_{69}H_{70}Br_3FeN_6O_6Si^+$ ($[2\mathbf{a}Fe]^{2+}$): 698.6031; found: 698.6010.

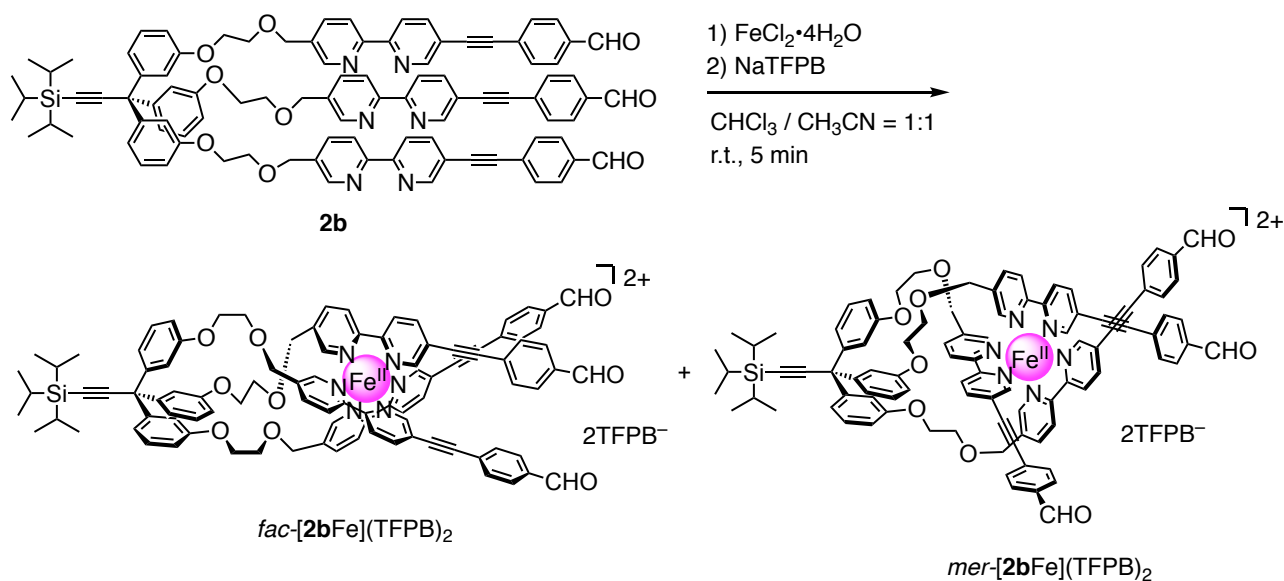
Synthesis of [2bFe](PF₆)₂



A solution of **2b** (0.337 g, 0.226 mmol) and Fe(BF₄)₂·6H₂O (50.7 mg, 0.254 mmol) in a mixed solvent of CH₃CN/CHCl₃ = 1/1 (30 mL) was sonicated for 5 min. A solution of KPF₆ (0.1898 g, 10.4 mmol) in H₂O (100 mL) was added to the reaction mixture, and the mixture was extracted with a mixed solvent of CH₃CN/CHCl₃ = 1/2 (30 mL × 3). The combined organic layer was dried over Na₂SO₄, filtered, and concentrated *in vacuo*. The crude product was purified by column chromatography on silica gel (CH₃CN/CHCl₃ = 1/4) to give [2bFe](PF₆)₂ as a purple solid (0.100 g, 54.4 μmol, 24%).

[2bFe](PF₆)₂: purple solid; ¹H NMR (600 MHz, CD₃CN, the signals for the *fac*-isomer are shown) δ 10.00 (s, 3H), 8.55 (d, *J* = 8.4 Hz, 3H), 8.54 (d, *J* = 8.4 Hz, 3H), 8.25 (dd, *J* = 8.4, 2.4 Hz, 3H), 8.16 (dd, *J* = 8.4, 1.2 Hz, 3H), 7.90 (d, *J* = 8.4 Hz, 6H), 7.66–7.63 (m, 9H), 7.43 (dd, *J* = 7.8, 1.8 Hz, 3H), 7.34 (dd, *J* = 7.8, 7.8 Hz, 3H), 7.22 (d, *J* = 1.2 Hz, 3H), 6.84 (dd, *J* = 7.8, 1.8 Hz, 3H), 6.08 (dd, *J* = 1.8, 1.8 Hz, 3H), 4.34 (dd, *J* = 30.6, 12.6 Hz, 6H) 4.15–4.10 (m, 3H), 3.98–3.89 (m, 6H), 3.74–3.69 (m, 3H) 1.12–1.09 (m, 21H); ¹³C NMR (151 MHz, CD₃CN, the signals for the *fac*-isomer are shown) δ 192.8, 159.5, 159.1, 158.9, 157.4, 153.7, 147.4, 142.3, 140.2, 139.6, 137.9, 133.4, 130.9, 130.6, 128.2, 125.8, 124.9, 124.1, 122.8, 117.8, 113.8, 111.7, 96.2, 88.3, 88.0, 70.8, 70.2, 68.7, 57.3, 19.2, 12.4; ¹⁹F NMR (376 MHz, CD₃CN) δ –72.6 (d, ¹*J*_{F-P} = 706 Hz); ³¹P NMR (243 MHz, CD₃CN) δ –144.6 (septet, ¹*J*_{P-F} = 706 Hz); HRMS (ESI): *m/z* calcd for C₉₆H₈₄FeN₆O₉Si²⁺ ([2bFe]²⁺): 773.2727; found: 773.2722.

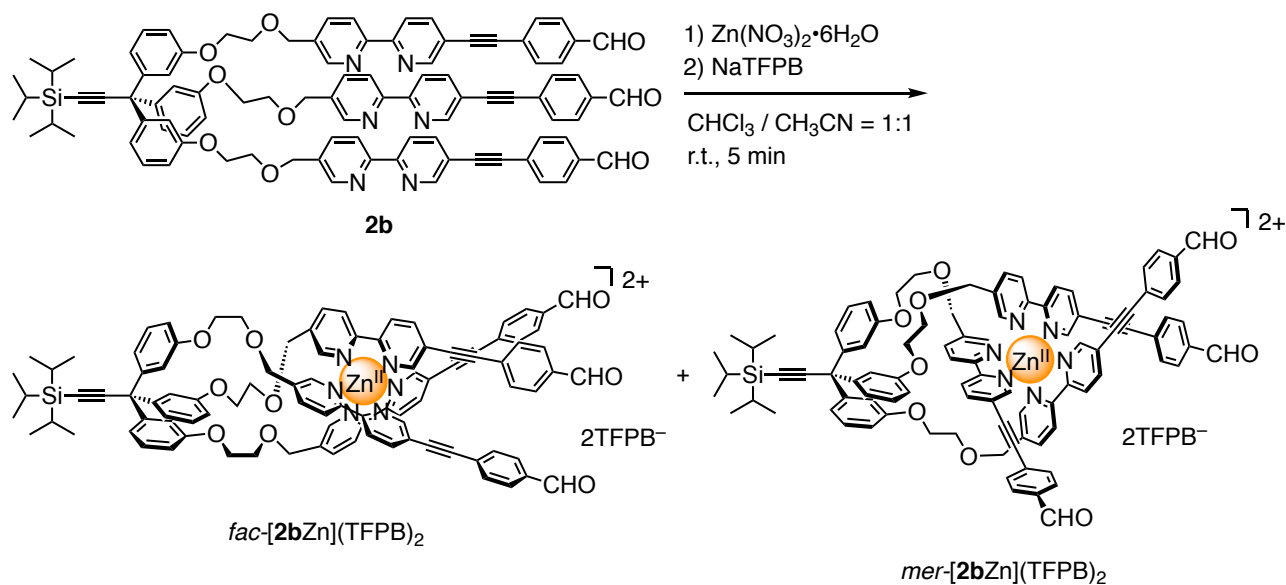
Synthesis of $[\mathbf{2bFe}](\text{TFPB})_2$



A solution of **2b** (0.167 g, 0.100 mmol) and $\text{FeCl}_2 \cdot 4\text{H}_2\text{O}$ (36.0 mg, 0.181 mmol) in a mixed solvent of $\text{CH}_3\text{CN}/\text{CHCl}_3 = 1/1$ (10 mL) was sonicated for 5 min. A solution of NaTFPB (0.8732 g, 0.985 mmol) in H_2O (100 mL) was added to the reaction mixture, and the mixture was extracted with a mixed solvent of $\text{CH}_3\text{CN}/\text{CHCl}_3 = 1/2$ (30 mL \times 3). The combined organic layer was dried over Na_2SO_4 , filtered, and concentrated *in vacuo*. The crude product was purified by column chromatography on silica gel ($\text{CH}_3\text{CN}/\text{CHCl}_3 = 1/4$) to give $[\mathbf{2bFe}](\text{TFPB})_2$ as a purple solid (0.241 g, 73.7 μmol , 74%).

$[\mathbf{2bFe}](\text{TFPB})_2$: purple solid; ^1H NMR (600 MHz, CD_3CN , the signals for the *fac*-isomer are shown) δ 9.98 (s, 3H), 8.57 (d, $J = 8.4$ Hz, 3H), 8.55 (d, $J = 8.4$ Hz, 3H), 8.25 (dd, $J = 8.4, 2.4$ Hz, 3H), 8.18 (dd, $J = 8.4, 1.2$ Hz, 3H), 7.87 (d, $J = 7.8$ Hz, 6H), 7.74 (br s, 16H), 7.71 (d, $J = 2.4$ Hz, 3H), 7.66 (br s, 8H), 7.63 (d, $J = 7.8$ Hz, 6H), 7.47 (dd, $J = 7.8, 2.4$ Hz, 3H), 7.36 (dd, $J = 7.8, 7.8$ Hz, 3H), 7.28 (d, $J = 1.2$ Hz, 3H), 6.85 (dd, $J = 7.8, 2.4$ Hz, 3H), 6.14 (dd, $J = 2.4, 2.4$ Hz, 3H), 4.38 (dd, $J = 29.4, 12.6$ Hz, 6H), 4.18–4.11 (m, 3H), 4.00–3.92 (m, 6H), 3.75–3.70 (m, 3H), 1.14–1.08 (m, 21H); ^{13}C NMR (151 MHz, CD_3CN , the signals for the *fac*-isomer are shown) δ 192.7, 162.7 (q, $^1J_{\text{C-B}} = 49.7$ Hz), 159.4, 159.0, 158.9, 157.4, 153.7, 147.3, 142.2, 140.2, 139.6, 137.8, 135.8 (br s), 133.3, 130.9, 130.6, 130.0 (qq, $^2J_{\text{C-F}} = 31.9$ Hz, $^3J_{\text{C-F}} = 3.8$ Hz), 128.1, 125.7, 125.4 (q, $^1J_{\text{C-F}} = 272$ Hz), 124.9, 124.1, 122.9, 122.8, 118.7 (septet, $^3J_{\text{C-F}} = 3.8$ Hz), 117.8, 113.7, 111.4, 96.1, 88.2, 87.0, 70.8, 70.2, 68.6, 57.2, 19.1, 12.3; ^{11}B NMR (192 MHz, CD_3CN) δ -6.63; ^{19}F NMR (376 MHz, CD_3CN) δ -63.2; HRMS (ESI): m/z calcd for $\text{C}_{96}\text{H}_{84}\text{FeN}_6\text{O}_9\text{Si}^{2+}$ ($[\mathbf{2bFe}]^{2+}$): 773.2727; found: 773.2747.

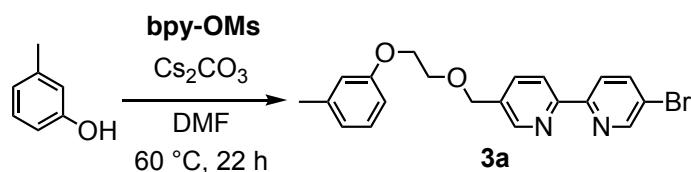
Synthesis of [2bZn](TFPB)₂



A solution of **2b** (75.0 mg, 50.0 μmol) and $\text{Zn}(\text{NO}_3)_2 \cdot 6\text{H}_2\text{O}$ (16.2 mg, 52.2 μmol) in a mixed solvent of $\text{CH}_3\text{CN}/\text{CHCl}_3 = 1/1$ (10 mL) was sonicated for 5 min. A solution of NaTFPB (0.2248 g, 251 μmol) in H_2O (20 mL) was added to the reaction mixture, and the mixture was extracted with a mixed solvent of $\text{CH}_3\text{CN}/\text{CHCl}_3 = 1/2$ (20 mL \times 3). The combined organic layer was dried over Na_2SO_4 , filtered, and concentrated *in vacuo* to give [2bZn](TFPB)₂ as a brown solid (0.1763 g, quant.).

[2bZn](TFPB)₂: brown solid; ¹H NMR (600 MHz, CD_3CN , the signals for the *fac*-isomer are shown) δ 10.00 (s, 3H), 8.51 (d, $J = 8.4$ Hz, 3H), 8.51 (d, $J = 8.4$ Hz, 3H), 8.35 (dd, $J = 8.4, 1.8$ Hz, 3H), 8.26 (dd, $J = 8.4, 1.8$ Hz, 3H), 8.21 (d, $J = 1.8$ Hz, 6H), 7.90 (d, $J = 7.8$ Hz, 6H), 7.84 (d, $J = 1.8$ Hz, 3H), 7.69 (br s, 16H), 7.66 (s, 8H), 7.42 (d, $J = 7.8$ Hz, 3H), 7.34 (dd, $J = 7.8, 7.8$ Hz, 3H), 6.84 (dd, $J = 7.8, 1.8$ Hz, 3H), 6.10 (s, 3H), 4.42 (dd, $J = 52.2, 11.4$ Hz, 6H), 4.14–4.09 (m, 3H), 3.99–3.89 (m, 6H), 3.78–3.72 (m, 3H), 1.12–1.08 (m, 21H); ¹³C NMR (151 MHz, CD_3CN , the signals for the *fac*-isomer are shown) δ 192.7, 162.6 (q, $^1J_{\text{C-B}} = 49.8$ Hz), 158.9, 151.4, 149.4, 149.1, 147.9, 147.3, 144.9, 142.5, 139.9, 135.7 (br s), 133.2, 130.8, 130.5, 130.0 (qq, $^2J_{\text{C-F}} = 31.9$ Hz, $^3J_{\text{C-F}} = 3.8$ Hz), 128.1, 125.4 (q, $^1J_{\text{C-F}} = 272$ Hz), 125.0, 124.4, 124.2, 122.8, 118.7 (septet, $^3J_{\text{C-F}} = 3.8$ Hz), 117.6, 113.8, 111.3, 96.0, 88.2, 86.8, 70.8, 70.1, 68.5, 57.2, 19.1, 12.2; ¹¹B NMR (192 MHz, CD_3CN) δ -6.64; ¹⁹F NMR (376 MHz, CD_3CN) δ -63.2; HRMS (ESI): m/z calcd for $\text{C}_{96}\text{H}_{85}\text{ZnN}_6\text{O}_9\text{Si}^{2+}$ ([2bZn]²⁺): 778.7714; found: 778.7730.

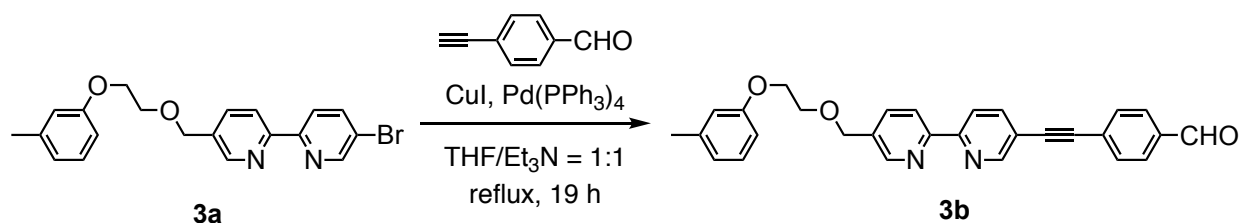
Synthesis of **3a**



A suspension of *m*-cresol (0.51 mL, 3.0 mmol) and Cs₂CO₃ (0.983 g, 3.02 mmol) in dry DMF (10 mL) was stirred at 60 °C under an argon atmosphere. After 30 min, a solution of **bpy-OMs** (1.16 g, 3.00 mmol) in DMF (17 mL) was added to the reaction mixture, and the reaction mixture was further stirred at 60 °C for 22 h. H₂O (100 mL) was added, and the mixture was extracted with a mixed solvent of EtOAc/hexane = 1/1 (50 mL × 2). The combined organic layer was washed with H₂O (100 mL), dried over MgSO₄, filtered, and concentrated *in vacuo*. The crude product was purified by GPC (using CHCl₃ as an eluent) to give **3a** as a colorless solid (1.00 g, 2.51 mmol, 84%).

3a: colorless solid; ¹H NMR (600 MHz, CDCl₃) δ 8.71 (d, *J* = 1.8 Hz, 3H), 8.64 (d, *J* = 1.8 Hz, 1H), 8.36 (d, *J* = 8.4 Hz, 1H), 8.31 (d, *J* = 8.4 Hz, 1H), 7.92 (dd, *J* = 8.4, 1.8 Hz, 1H), 7.83 (dd, *J* = 8.4, 1.8 Hz, 1H), 7.16 (dd, *J* = 7.8, 7.8 Hz, 1H), 6.78–6.75 (m, 2H), 6.73 (dd, *J* = 7.8, 1.8 Hz, 1H), 4.70 (s, 2H), 4.18–4.14 (m, 2H), 3.89–3.86 (m, 2H), 2.32 (s, 3H); ¹³C NMR (151 MHz, CDCl₃) δ 158.8, 154.8, 154.6, 150.3, 148.7, 139.6, 139.6, 136.6, 134.1, 129.3, 122.5, 122.0, 121.2, 120.8, 115.6, 111.6, 70.8, 69.2, 67.4, 21.6; HRMS (ESI): *m/z* calcd for C₂₀H₂₀BrN₂O₂⁺ ([**3a**•H]⁺): 399.0703; found: 399.0686.

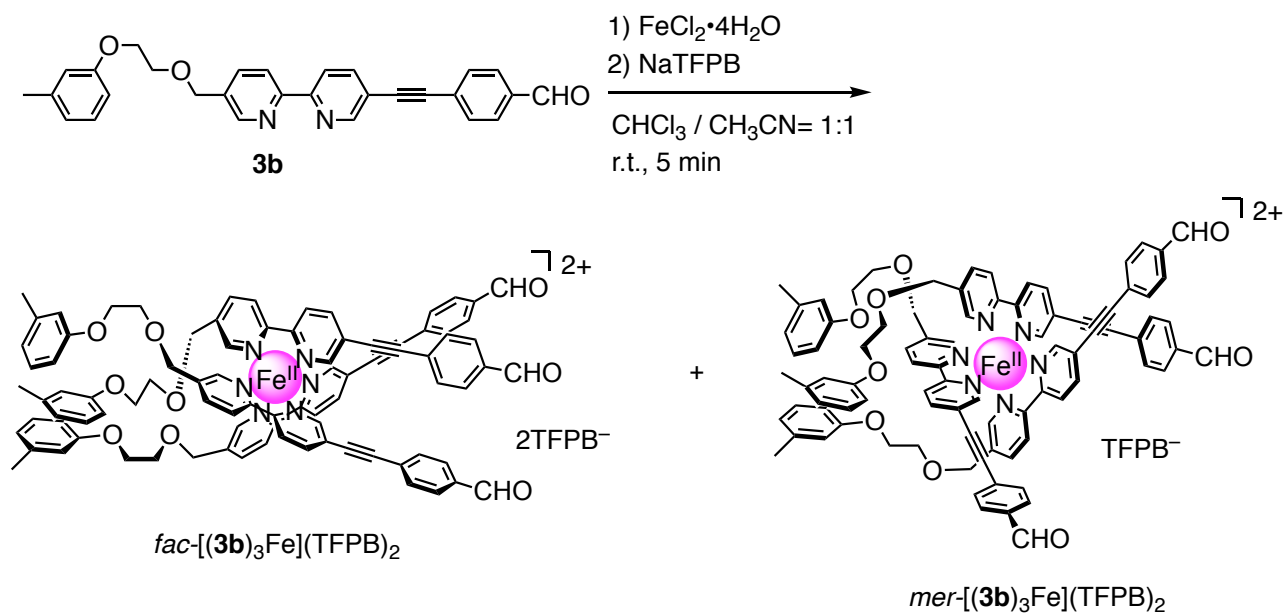
Synthesis of **3b**



A solution of **3a** (0.576 g, 1.44 mmol), 4-ethynylbenzaldehyde^[S71] (0.375 g, 2.88 mmol), Pd(PPh₃)₄ (0.168 g, 0.140 mmol), and CuI (62.3 mg, 0.330 mmol) in a mixed solvent of dry THF (50 mL) and Et₃N (50 mL) was refluxed under an argon atmosphere. After 19 h, the mixture was concentrated *in vacuo*. The residue was suspended in a solution of EDTA•4Na (2.32 g, 5.12 mmol) in H₂O (200 mL) and extracted with CHCl₃ (50 mL × 3). The combined organic layer was dried over Na₂SO₄, filtered, and concentrated *in vacuo*. The crude product was purified by GPC (using CHCl₃ as an eluent) to give **3b** as a pale brown solid (0.137 g, 0.305 mmol, 21%).

3b: pale brown solid; ¹H NMR (600 MHz, CDCl₃) δ 10.04 (s, 1H), 8.67 (d, *J* = 1.8 Hz, 1H), 8.68 (d, *J* = 1.8 Hz, 1H), 8.42 (d, *J* = 8.4 Hz, 1H), 8.40 (d, *J* = 8.4 Hz, 1H), 7.96 (dd, *J* = 8.4, 1.8 Hz, 1H), 7.90 (d, *J* = 8.4 Hz, 2H), 7.86 (dd, *J* = 8.4, 1.8 Hz, 1H), 7.72 (d, *J* = 8.4 Hz, 1H), 7.16 (dd, *J* = 7.8, 7.8 Hz, 3H), 6.79–6.76 (m, 2H), 6.74 (dd, *J* = 7.8, 2.4 Hz, 1H), 4.73 (s, 2H), 4.19–4.16 (m, 2H), 3.91–3.87 (m, 2H), 2.33 (s, 3H); ¹³C NMR (151 MHz, CDCl₃) δ 191.4, 158.8, 155.4, 154.9, 151.9, 148.8, 139.6, 136.5, 135.9, 134.3, 132.3, 129.7, 129.3, 128.9, 121.9, 121.3, 120.5, 119.6, 115.6, 111.6, 92.5, 90.4, 70.8, 69.2, 67.4, 21.6; HRMS (ESI): *m/z* calcd for C₂₉H₂₅N₂O₃⁺ ([**3b**•H]⁺): 449.1859; found: 449.1855.

Synthesis of $[(\mathbf{3b})_3\text{Fe}](\text{TFPB})_2$



A solution of **3b** (338.5 mg, 85.8 μmol) and $\text{FeCl}_2 \cdot 4\text{H}_2\text{O}$ (5.68 mg, 28.6 μmol) in a mixed solvent of $\text{CH}_3\text{CN}/\text{CHCl}_3 = 1/1$ (6.0 mL) was sonicated for 5 min. A solution of NaTFPB (0.253 g, 0.286 mmol) in H_2O (10.0 mL) was added to the reaction mixture, and the mixture was extracted with a mixed solvent of $\text{CH}_3\text{CN}/\text{CHCl}_3 = 1/2$ (5.0 mL \times 3). The combined organic layer dried over Na_2SO_4 , filtered, and concentrated *in vacuo*. The crude product was purified by column chromatography on silica gel ($\text{CH}_3\text{CN}/\text{CHCl}_3 = 1/4$) to give $[(\mathbf{3b})_3\text{Fe}](\text{TFPB})_2$ as a purple solid (56.5 mg, 24.9 μmol , 89%).

$[(\mathbf{3b})_3\text{Fe}](\text{TFPB})_2$: purple solid; ^{11}B NMR (192 MHz, CD_3CN) δ -6.65; ^{19}F NMR (376 MHz, CD_3CN) δ -63.2; HRMS (ESI): m/z calcd for $\text{C}_{87}\text{H}_{72}\text{FeN}_6\text{O}_9^+$ ($[(\mathbf{3b})_3\text{Fe}]^{2+}$): 699.2373; found: 699.2387.

^1H NMR (600 MHz, CD_3CN) and ^{13}C NMR (151 MHz, CD_3CN) spectra was shown in **Fig. S61** and **S62**.

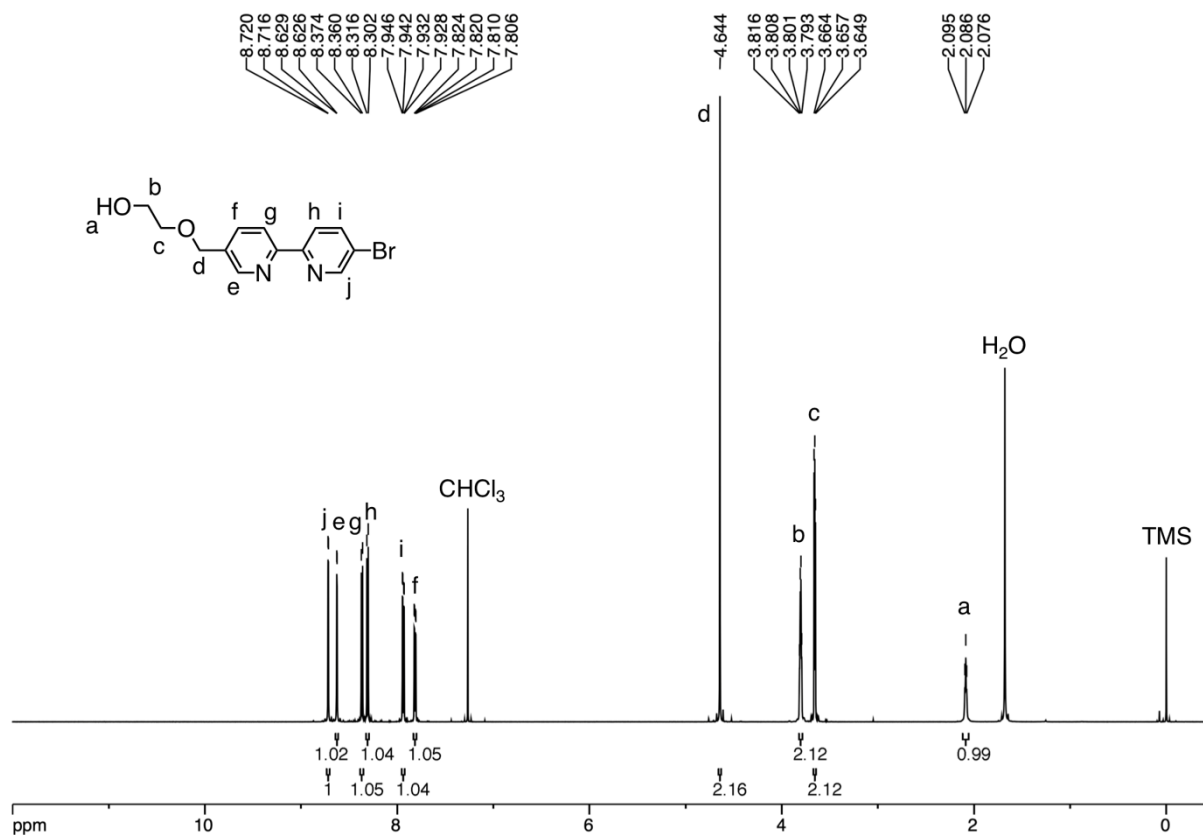


Figure S1. ¹H NMR spectrum of **bpy-OH** (600 MHz, CDCl₃).

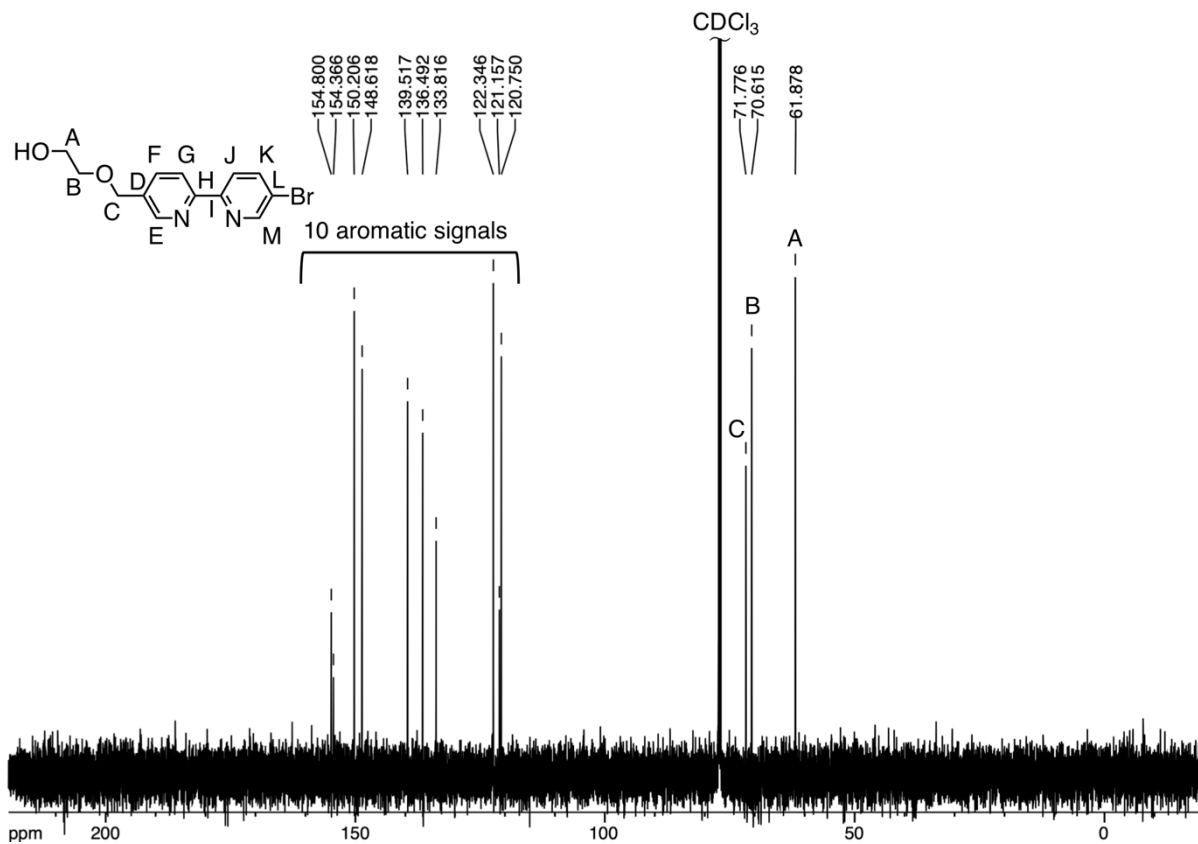


Figure S2. ¹³C NMR spectrum of **bpy-OH** (151 MHz, CDCl₃).

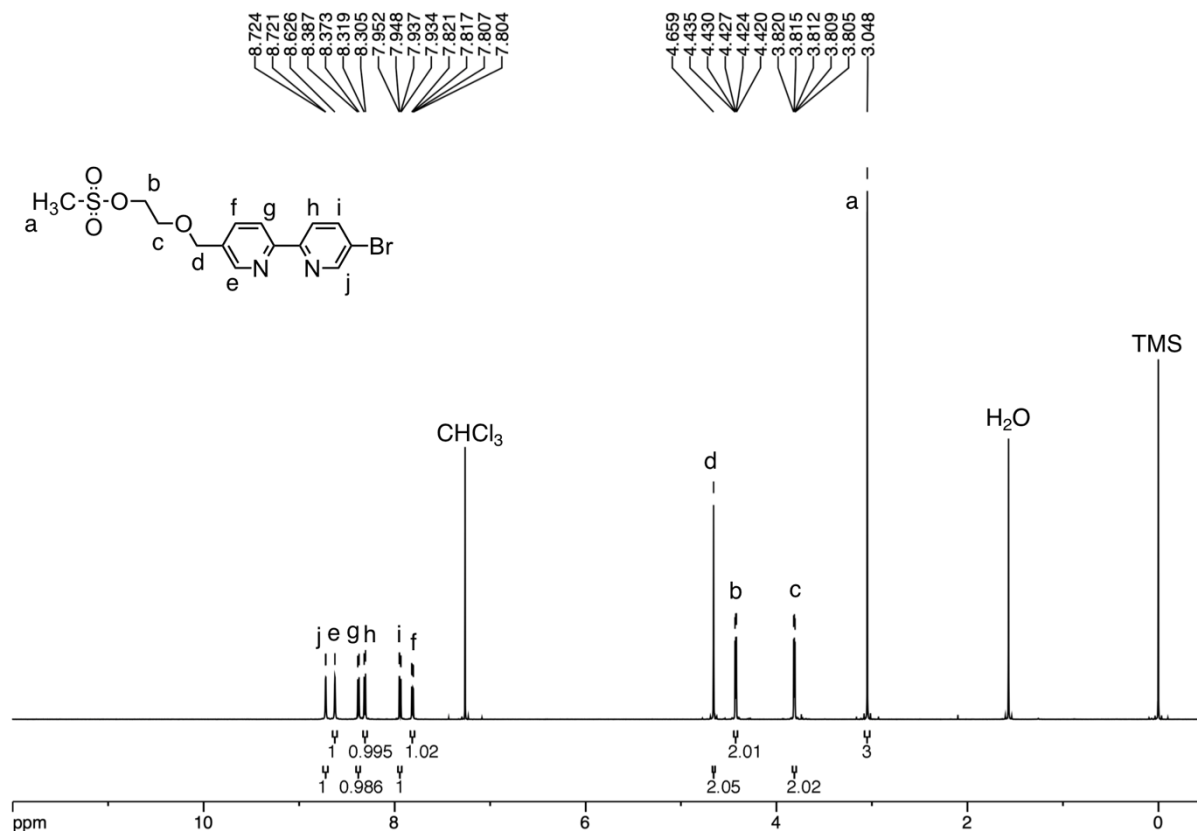


Figure S3. ¹H NMR spectrum of **bpy-OMs** (600 MHz, CDCl₃).

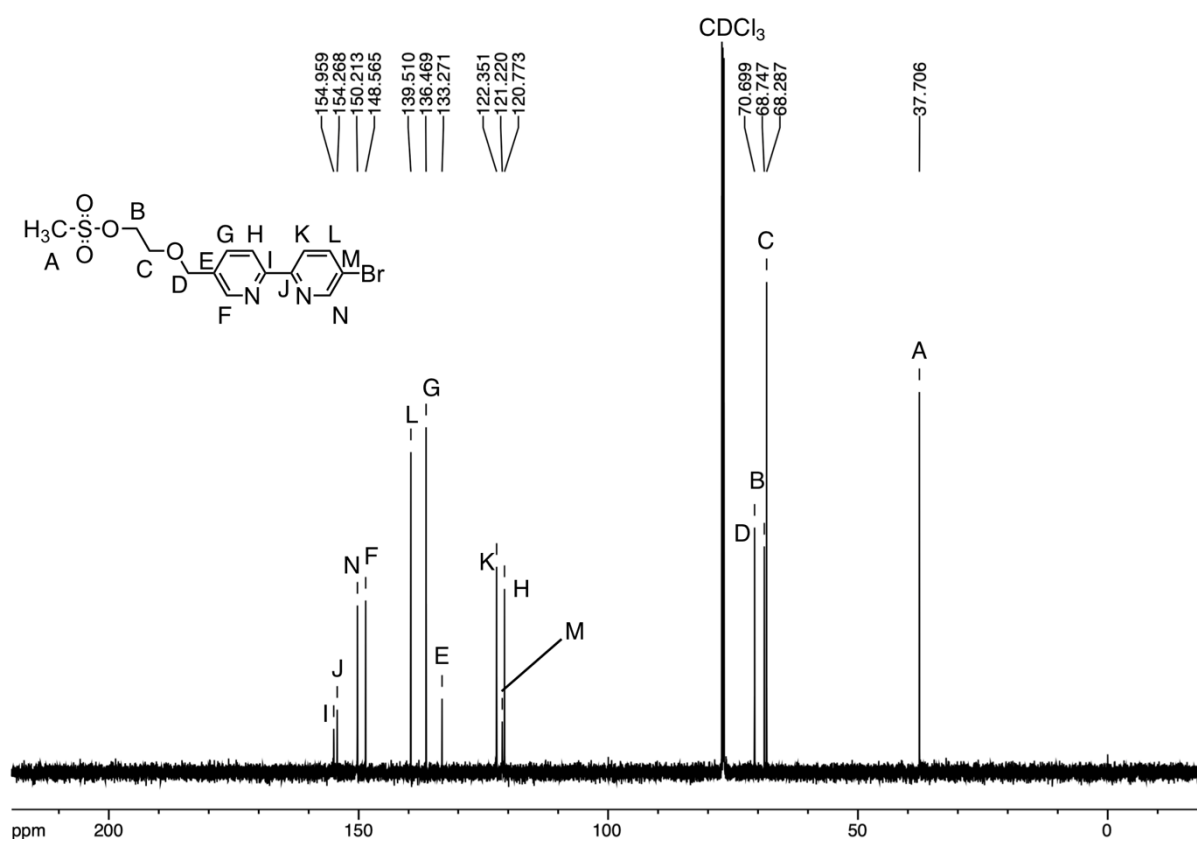


Figure S4. ¹³C NMR spectrum of **bpy-OMs** (151 MHz, CDCl₃).

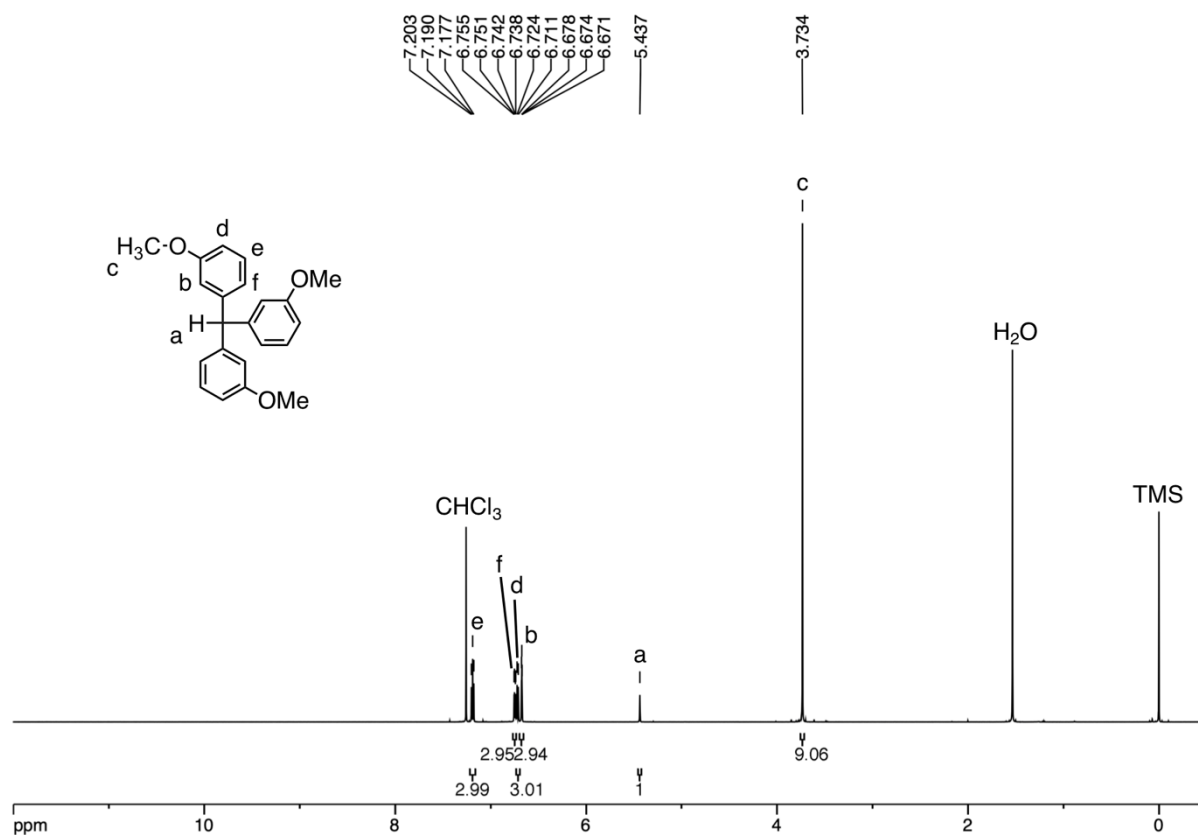


Figure S5. ¹H NMR spectrum of 4-H (600 MHz, CDCl₃).

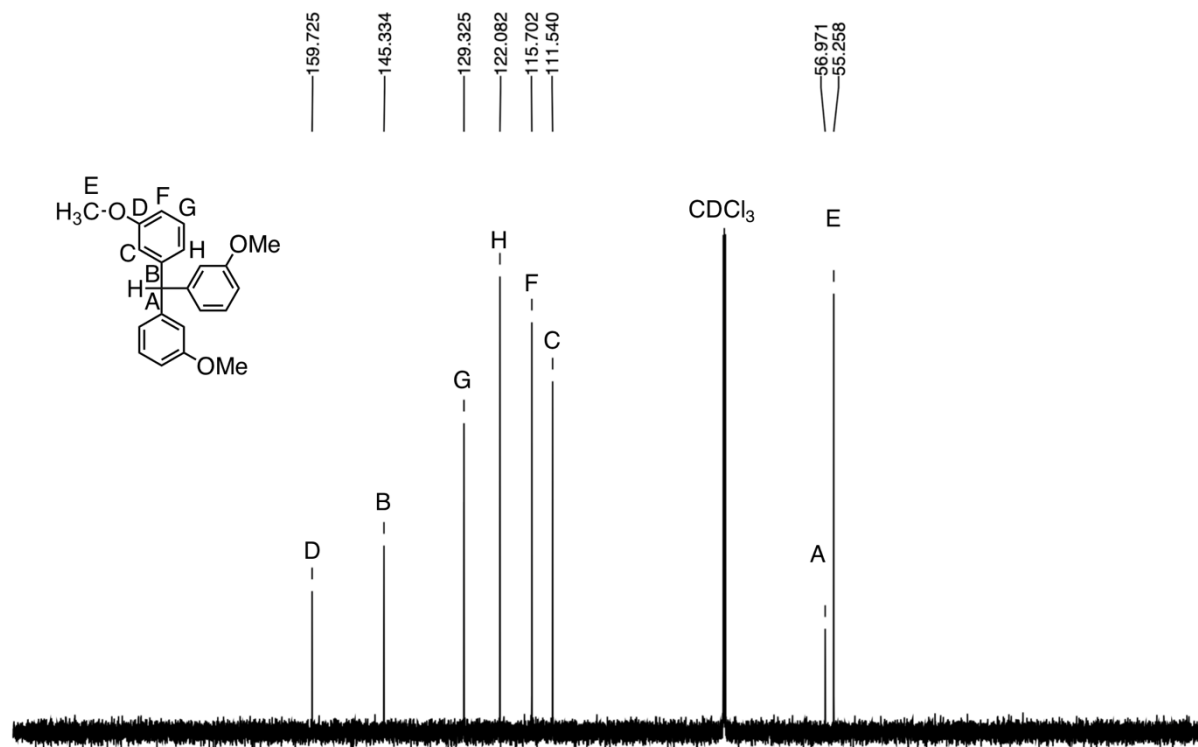


Figure S6. ¹³C NMR spectrum of 4-H (151 MHz, CDCl₃).

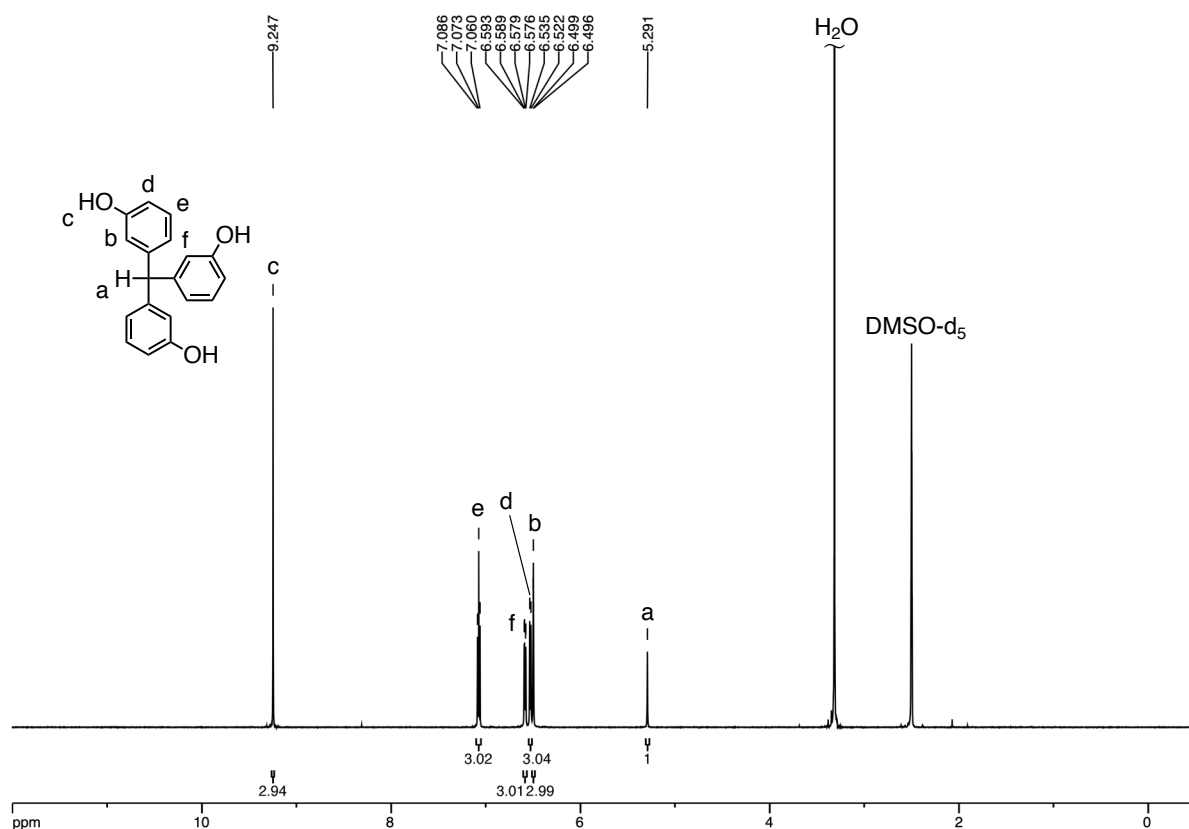


Figure S7. ^1H NMR spectrum of **5-H** (600 MHz, $\text{DMSO-}d_6$).

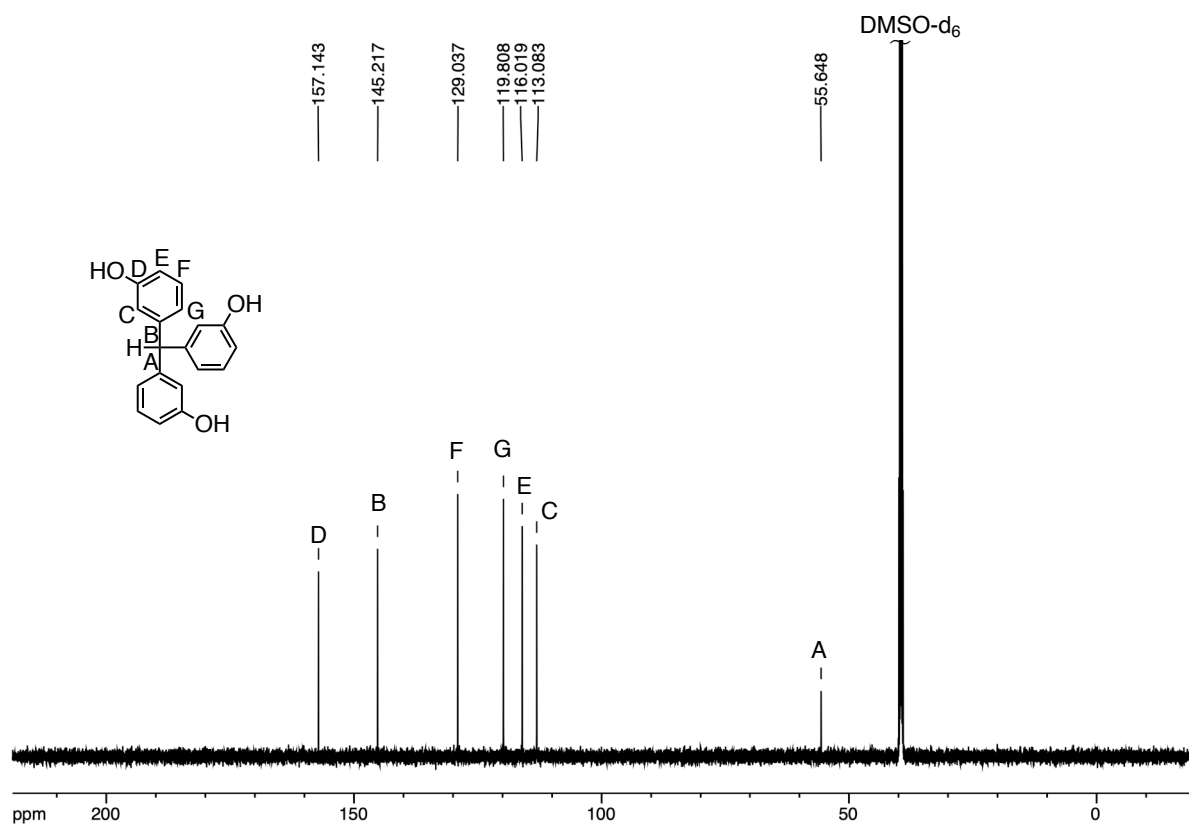


Figure S8. ^{13}C NMR spectrum of **5-H** (151 MHz, $\text{DMSO-}d_6$).

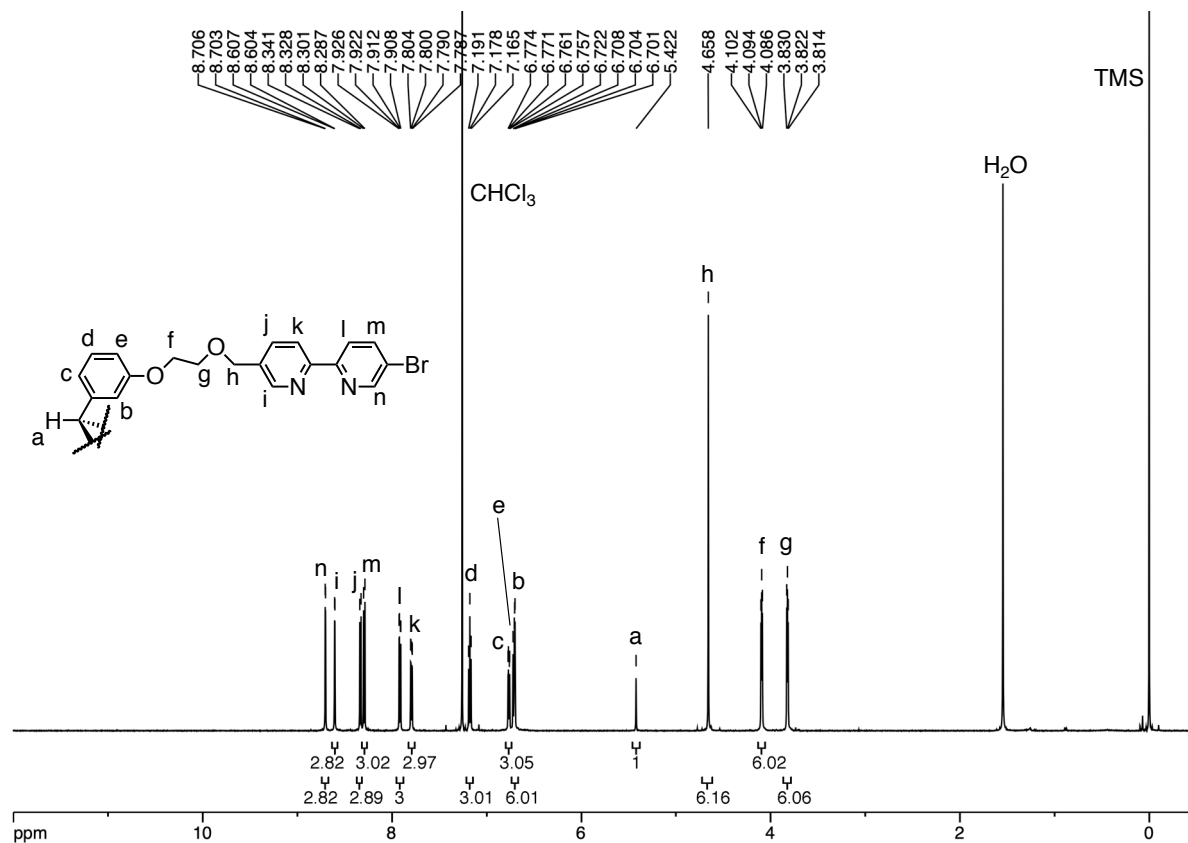


Figure S9. ¹H NMR spectrum of **1a** (600 MHz, CDCl₃).

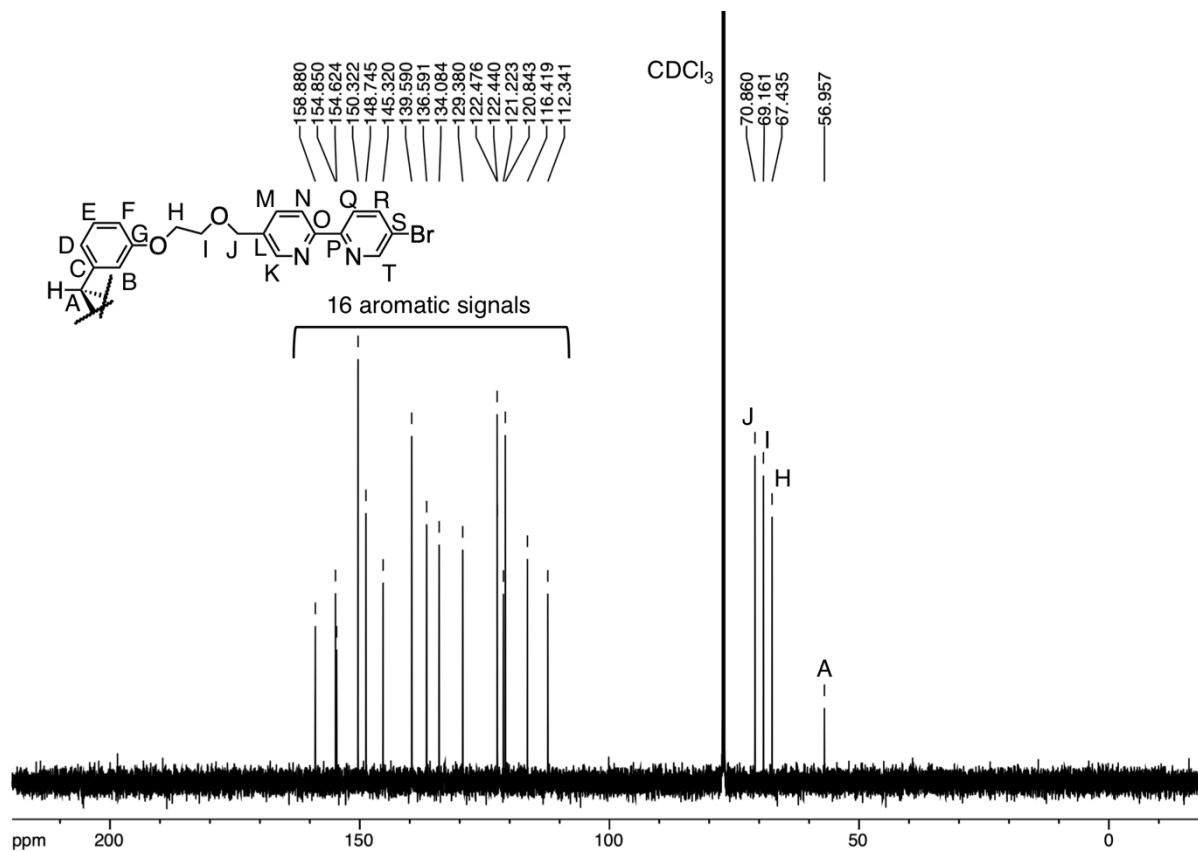


Figure S10. ¹³C NMR spectrum of **1a** (151 MHz, CDCl₃).

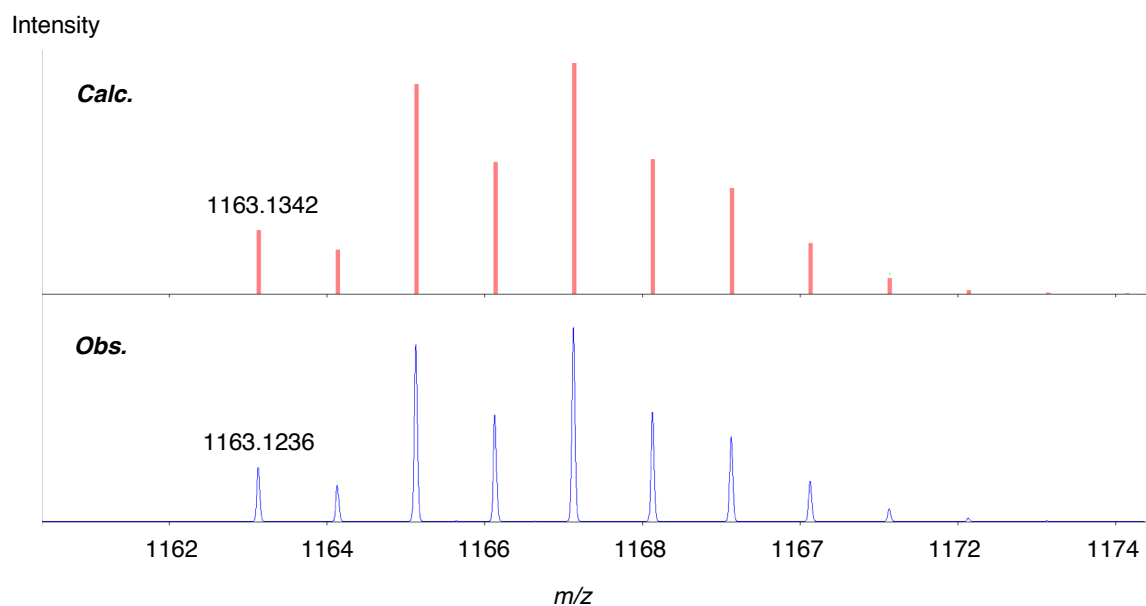


Figure S11. Simulated and observed isotopic pattern of $[1\mathbf{a}\cdot\mathbf{H}]^+$ (ESI-MS, positive).

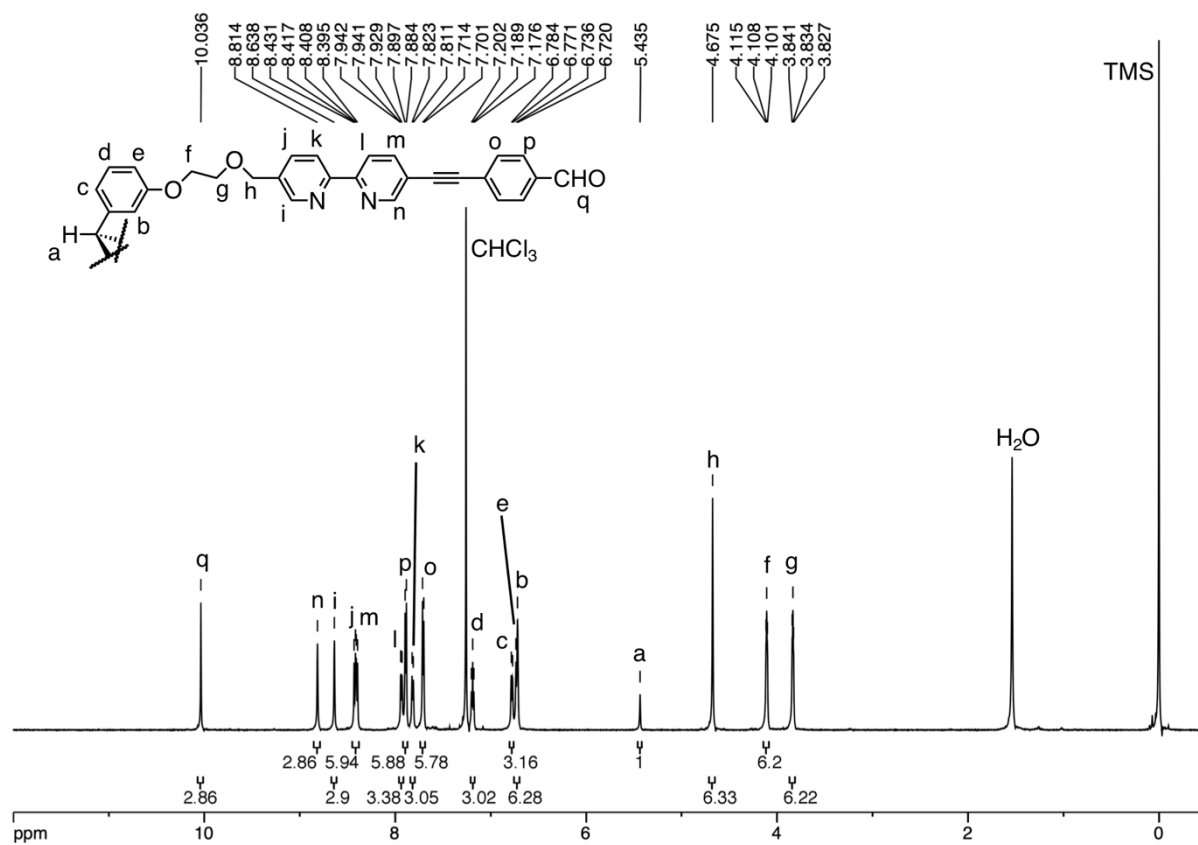


Figure S12. ^1H NMR spectrum of $\mathbf{1b}$ (600 MHz, CDCl_3).

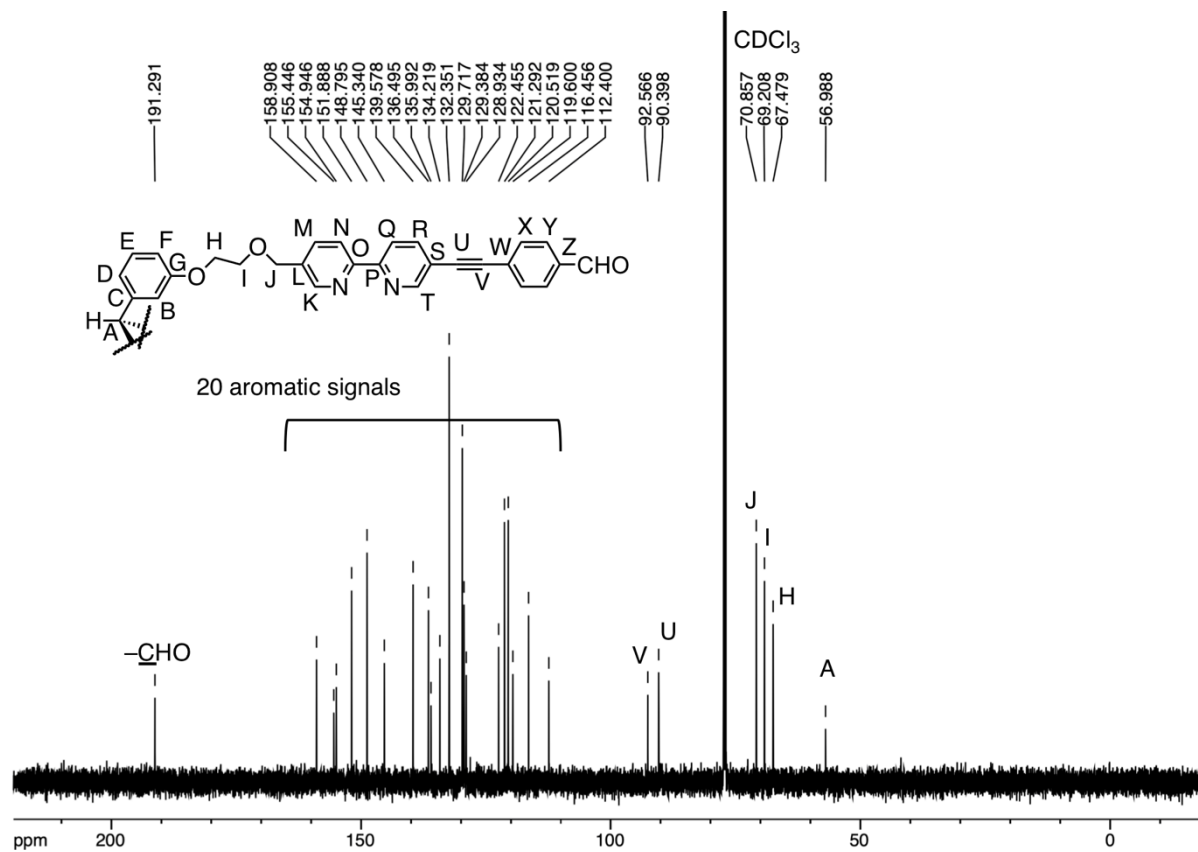


Figure S13. ^{13}C NMR spectrum of **1b** (151 MHz, CDCl_3).

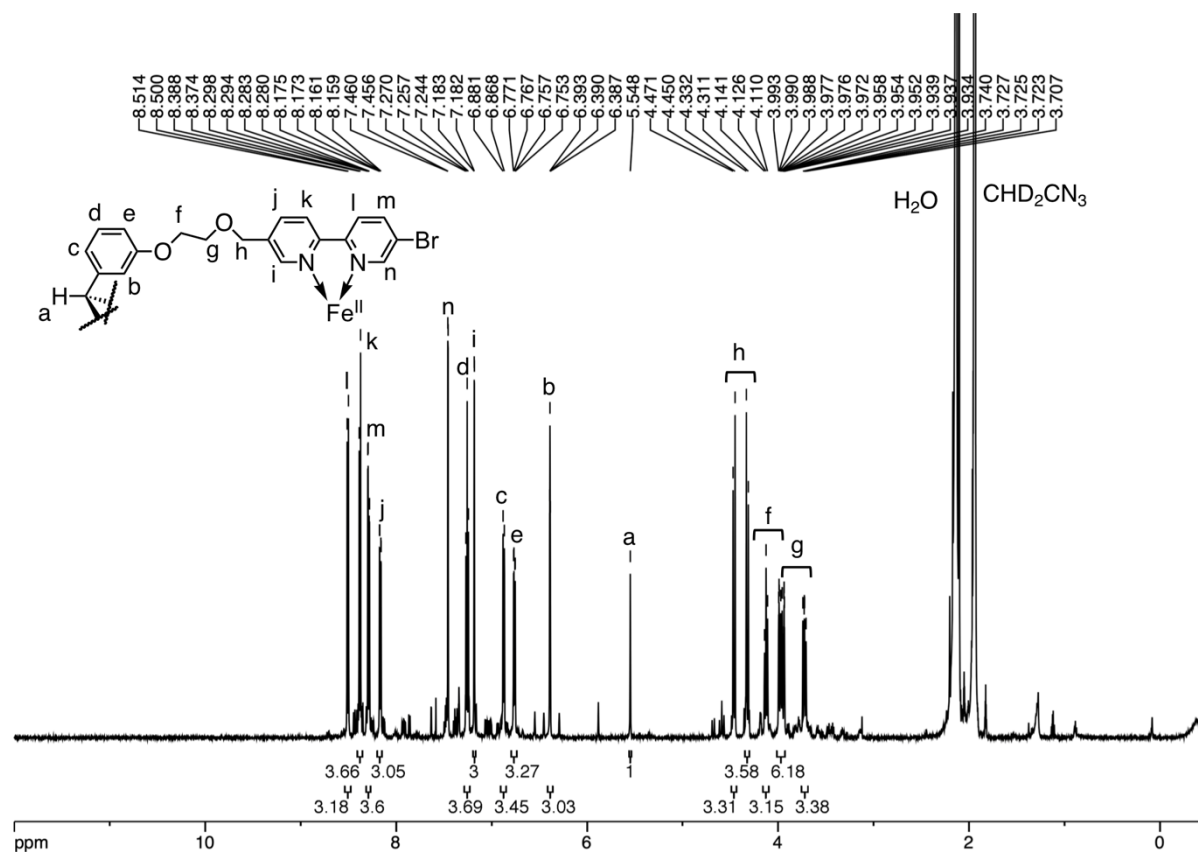


Figure S14. ^1H NMR spectrum of $[\mathbf{1aFe}](\text{PF}_6)_2$ (600 MHz, CD_3CN).

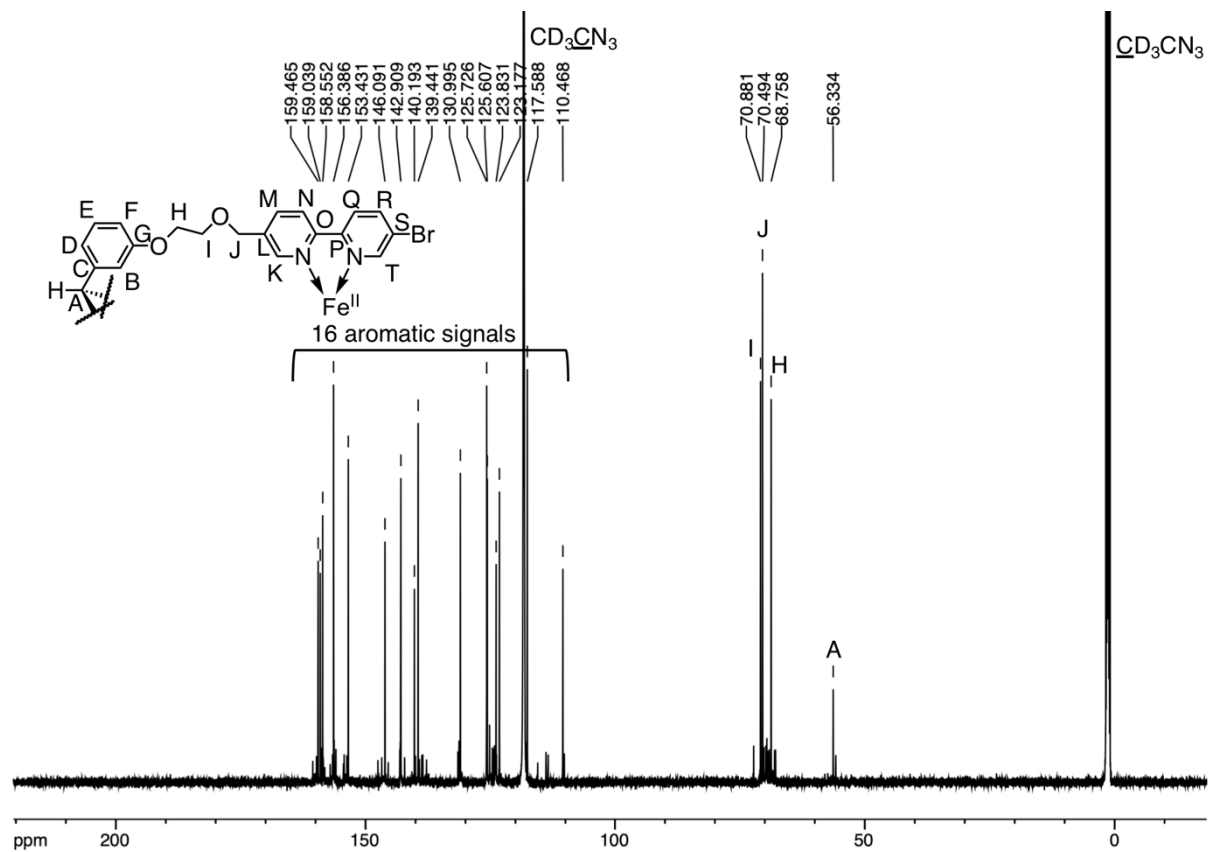


Figure S15. ¹³C NMR spectrum of [1aFe](PF₆)₂ (151 MHz, CD₃CN).

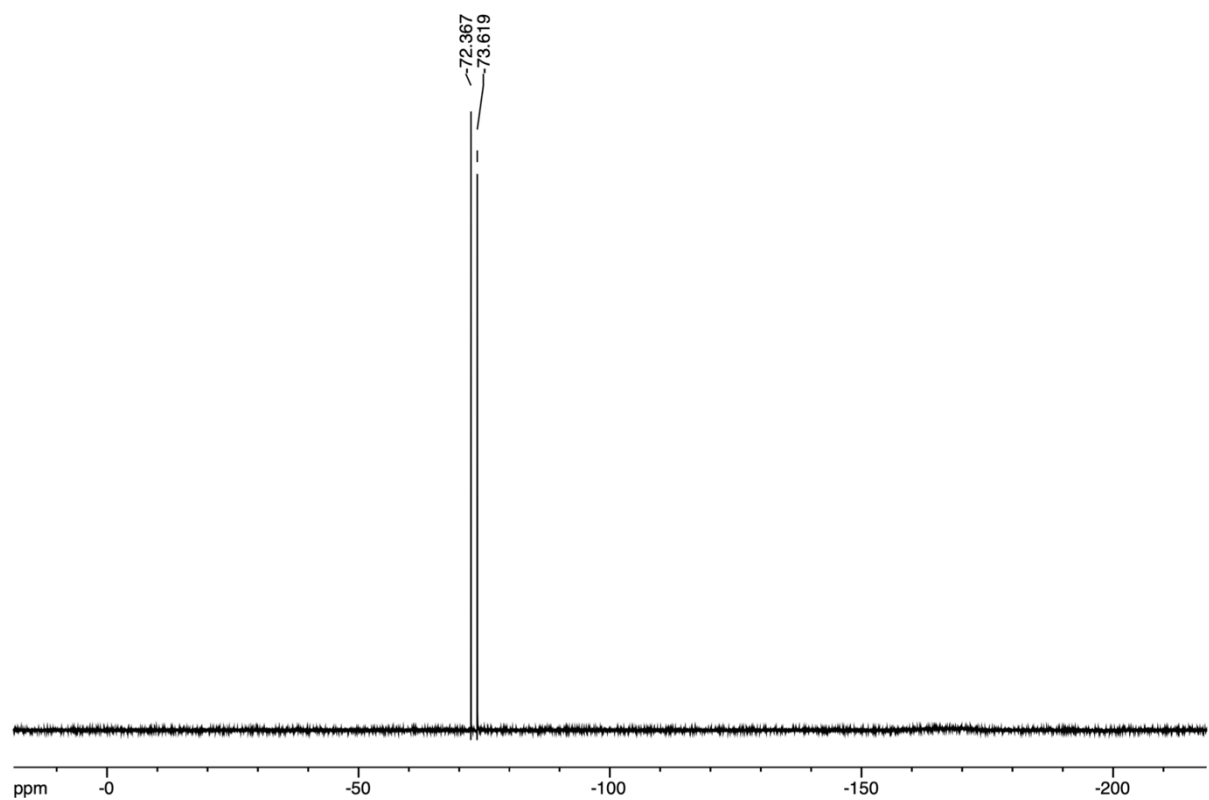


Figure S16. ¹⁹F NMR spectrum of [1aFe](PF₆)₂ (376 MHz, CD₃CN).

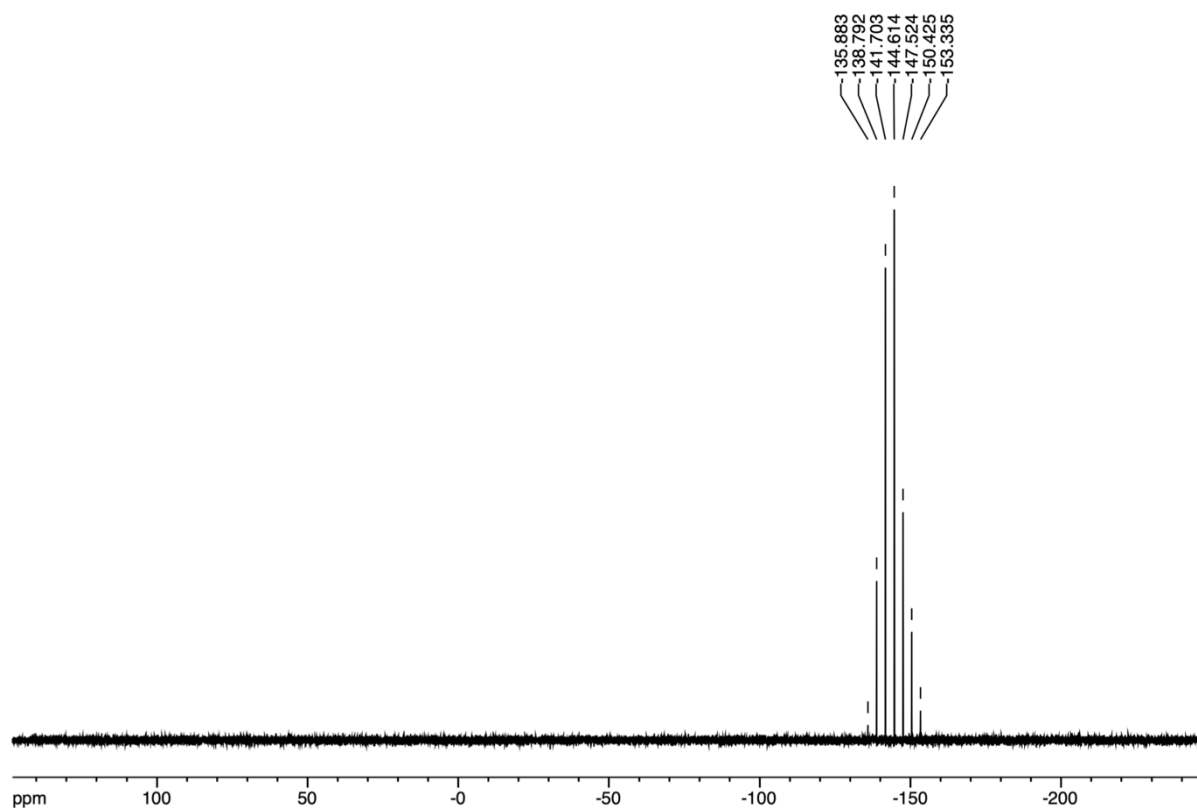


Figure S17. ^{31}P NMR spectrum of $[\mathbf{1aFe}](\text{PF}_6)_2$ (243 MHz, CD_3CN).

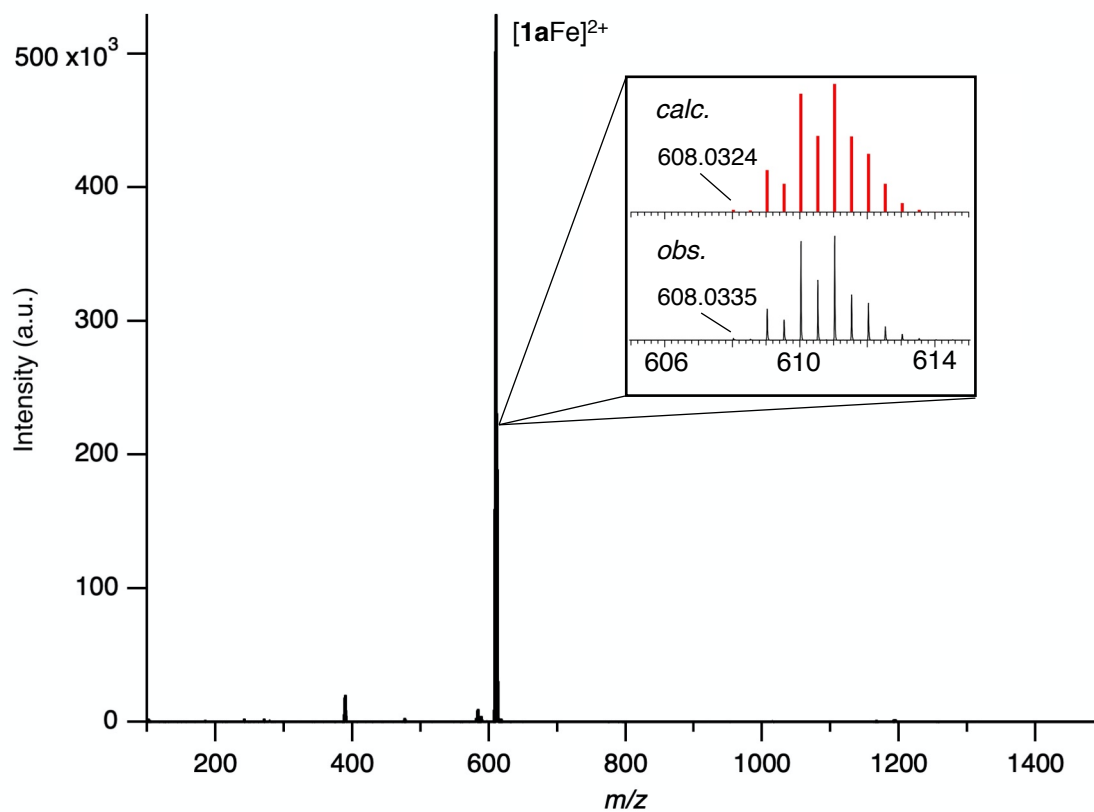


Figure S18. ESI mass spectrum of $[\mathbf{1aFe}](\text{PF}_6)_2$ (solv. CD_3CN).

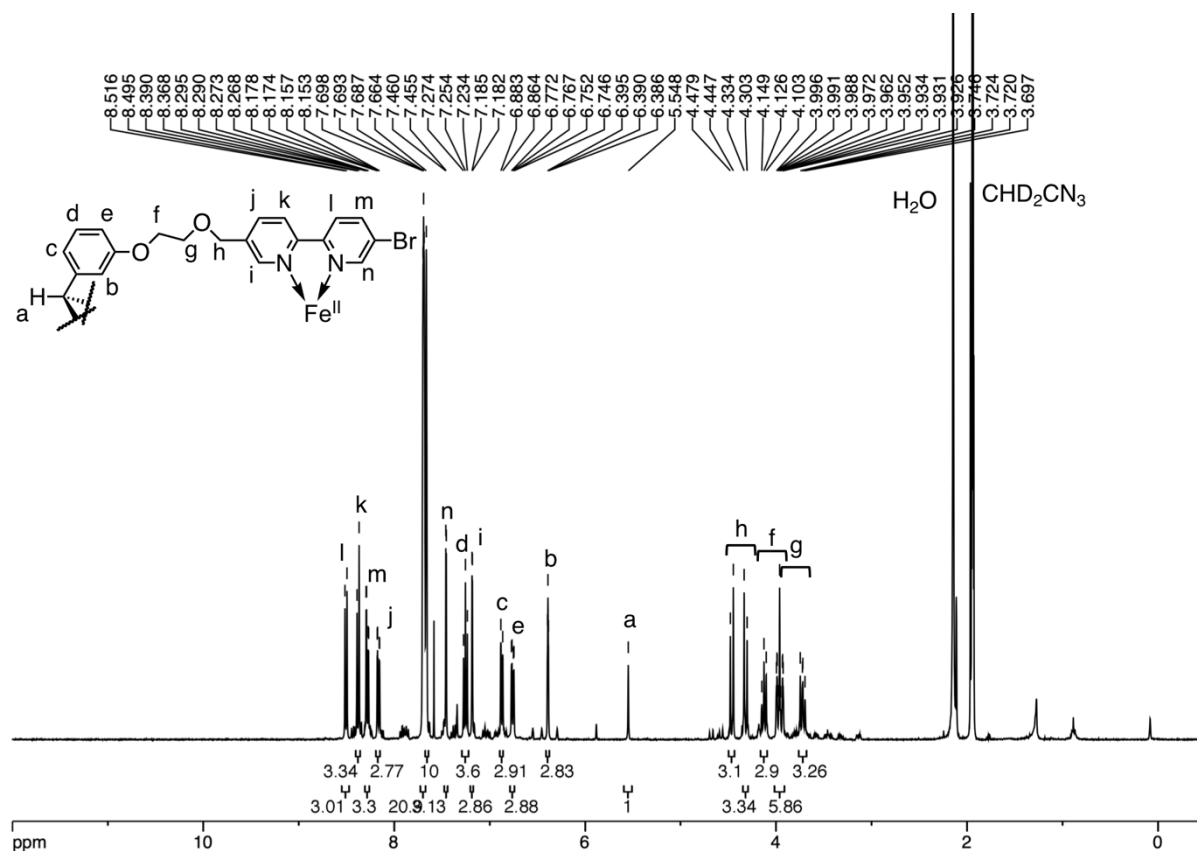


Figure S19. 1H NMR spectrum of $[1aFe](TFPB)_2$ (600 MHz, CD_3CN).

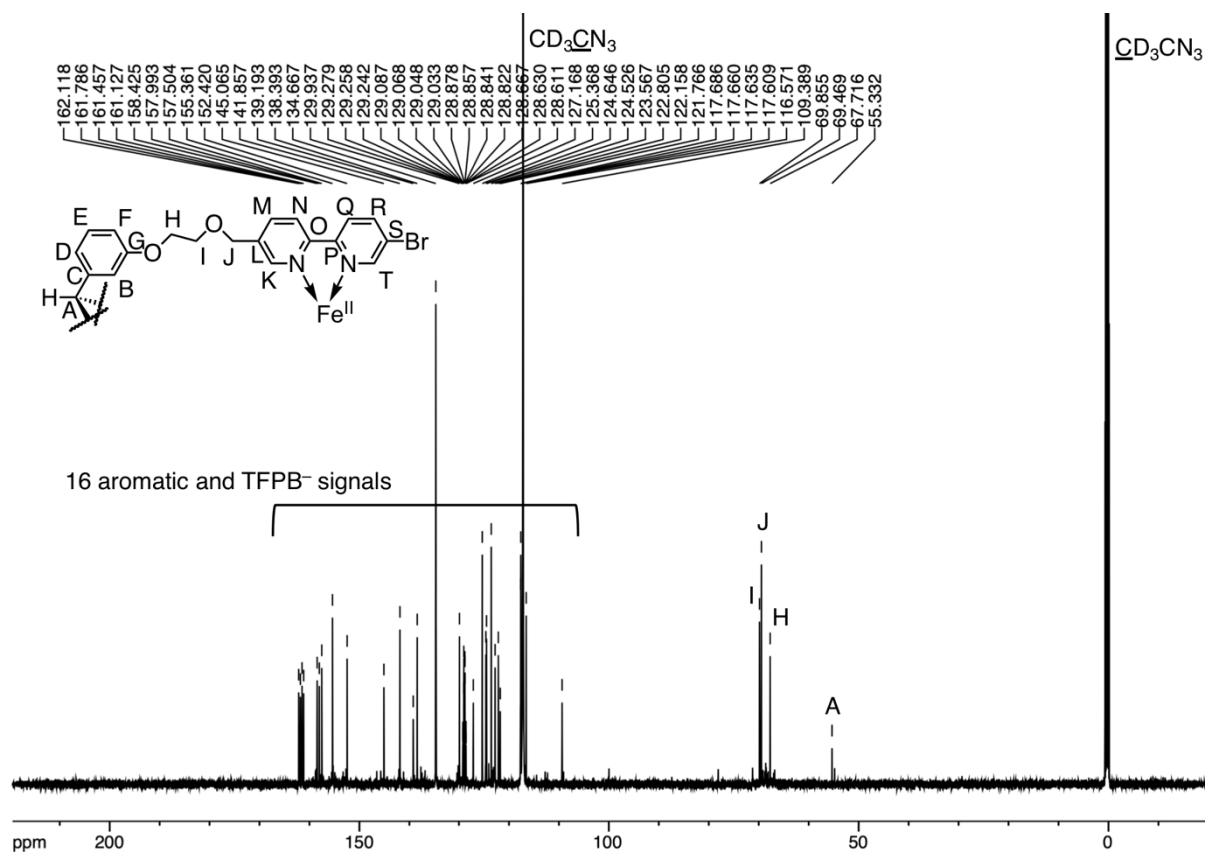


Figure S20. ^{13}C NMR spectrum of $[1aFe](TFPB)_2$ (151 MHz, CD_3CN).

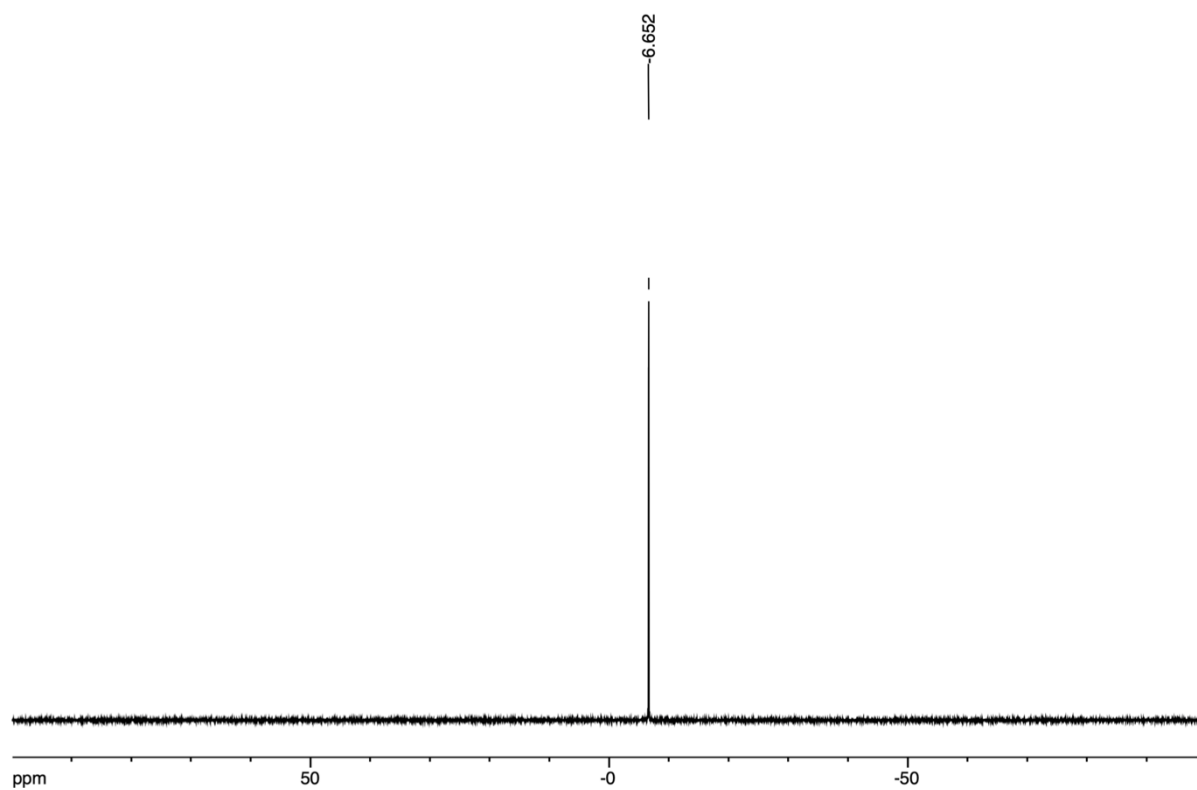


Figure S21. ^{11}B NMR spectrum of $[\mathbf{1aFe}](\text{TFPB})_2$ (192 MHz, CD_3CN).

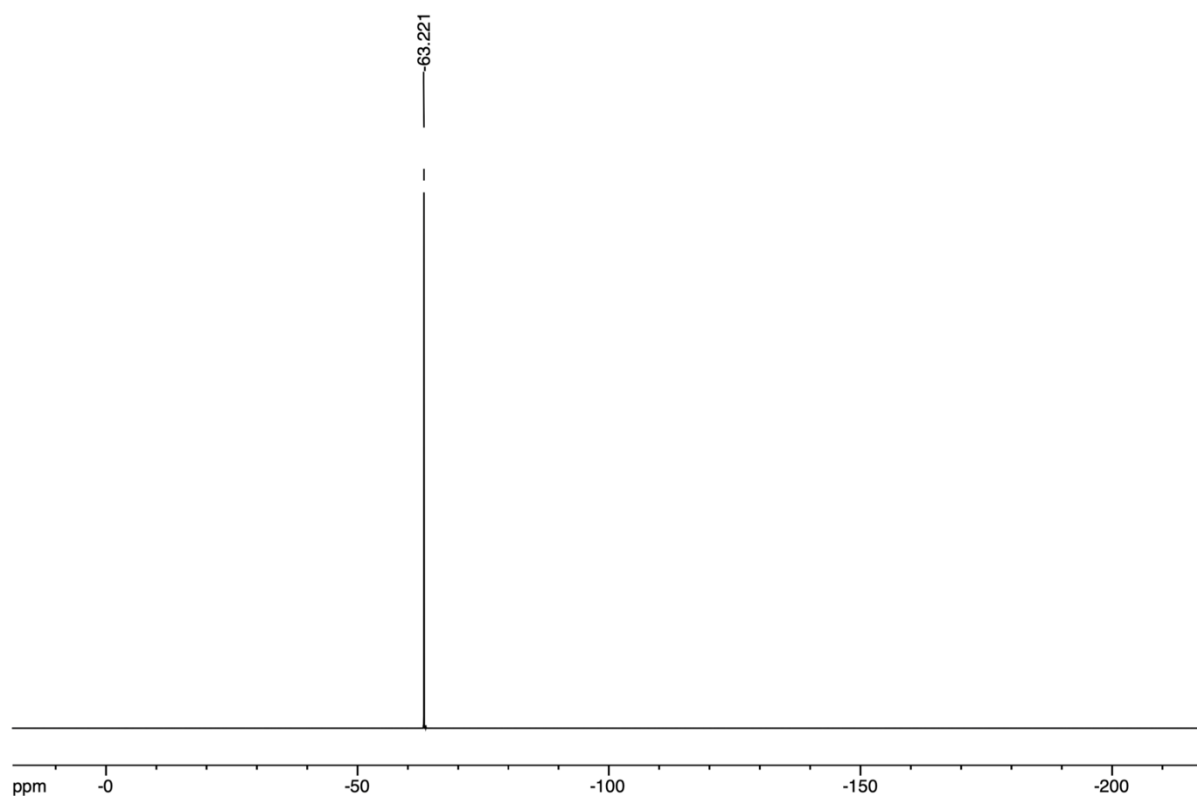


Figure S22. ^{19}F NMR spectrum of $[\mathbf{1aFe}](\text{TFPB})_2$ (376 MHz, CD_3CN).

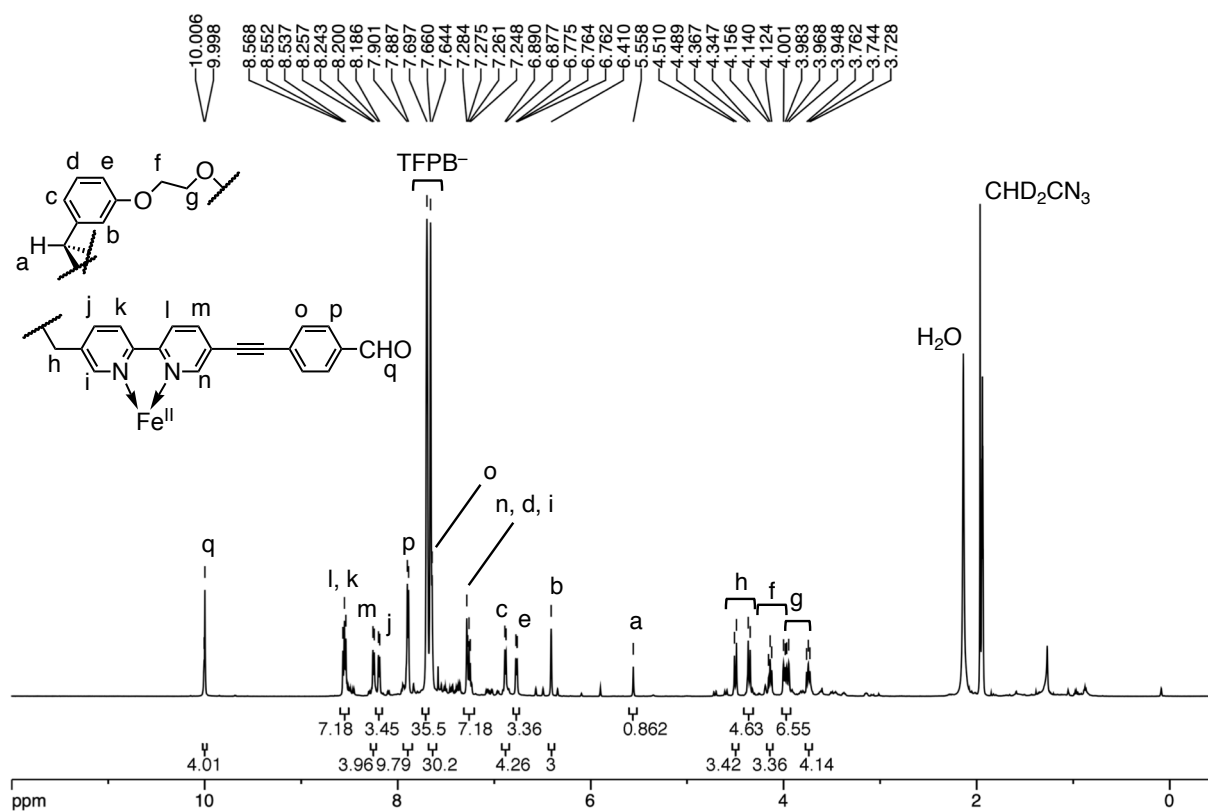


Figure S23. 1H NMR spectrum of $[1bFe](TFPB)_2$ (600 MHz, CD_3CN).

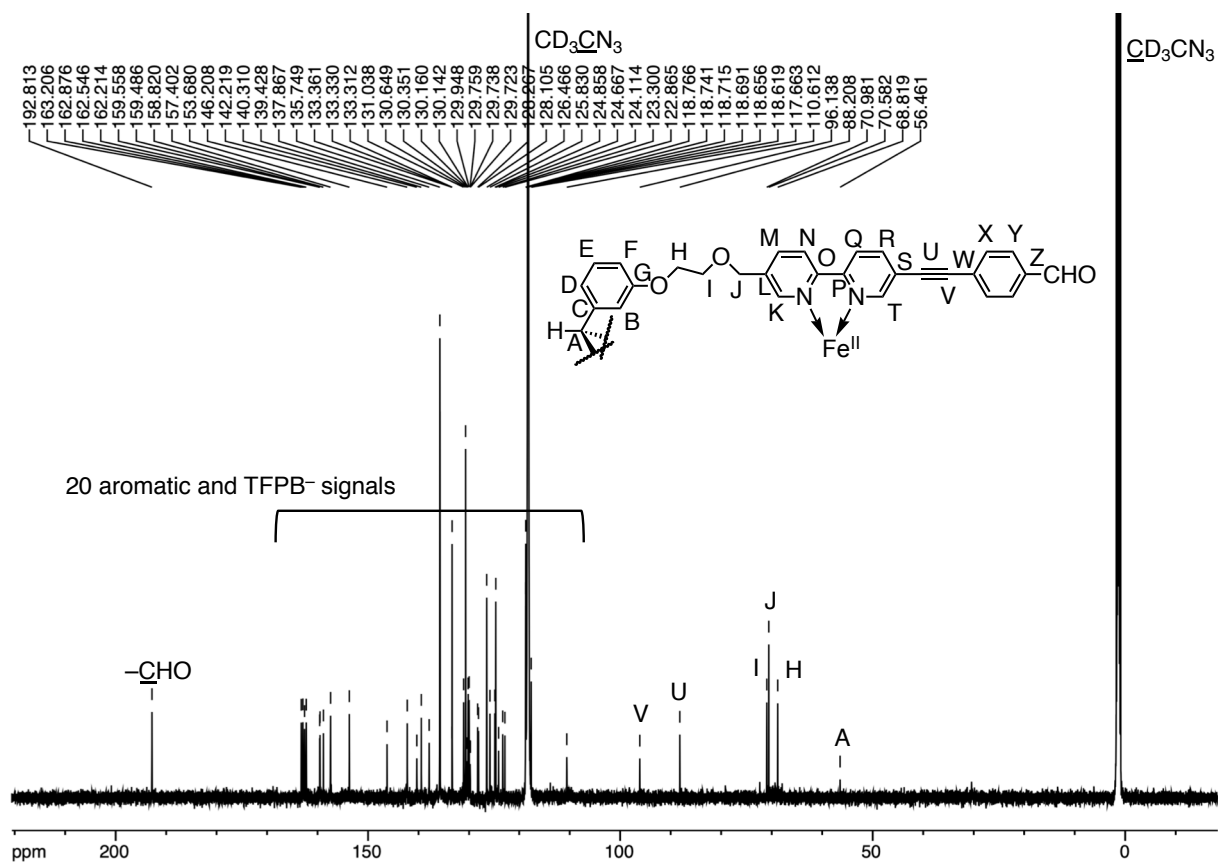


Figure S24. ^{13}C NMR spectrum of $[1bFe](TFPB)_2$ (151 MHz, CD_3CN).

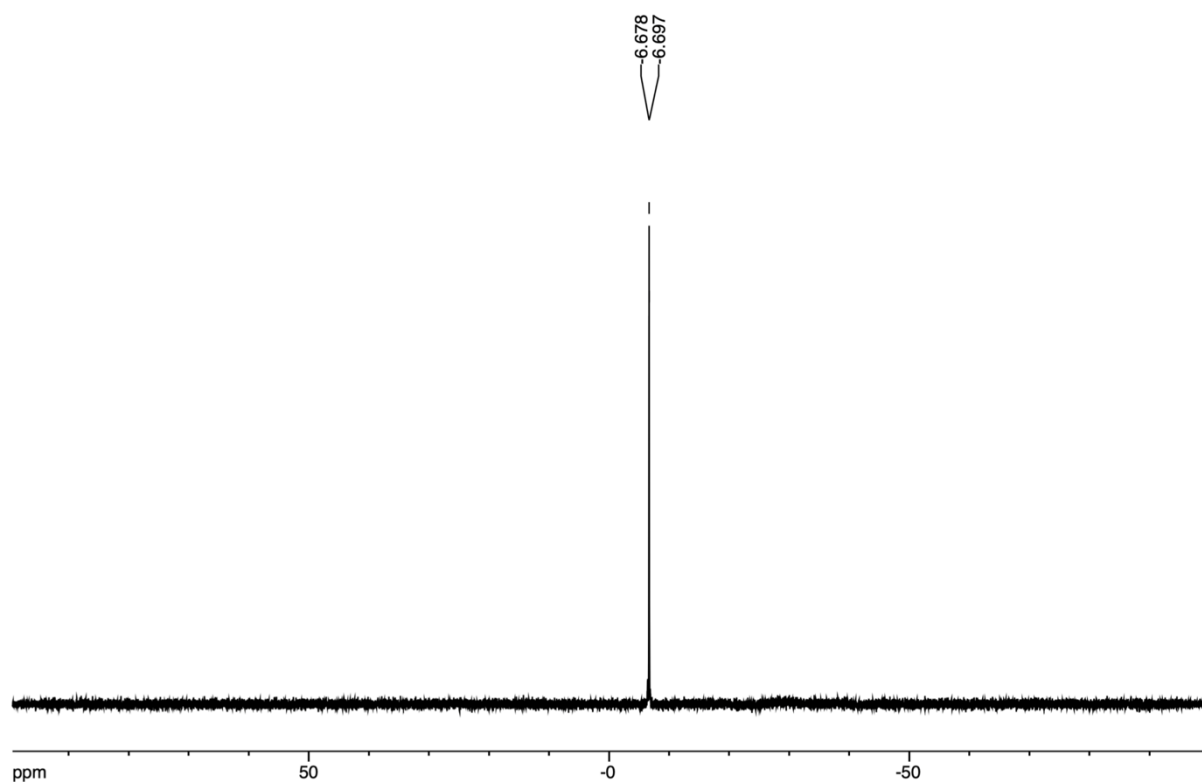


Figure S25. ^{11}B NMR spectrum of $[\mathbf{1bFe}](\text{TFPB})_2$ (192 MHz, CD_3CN).

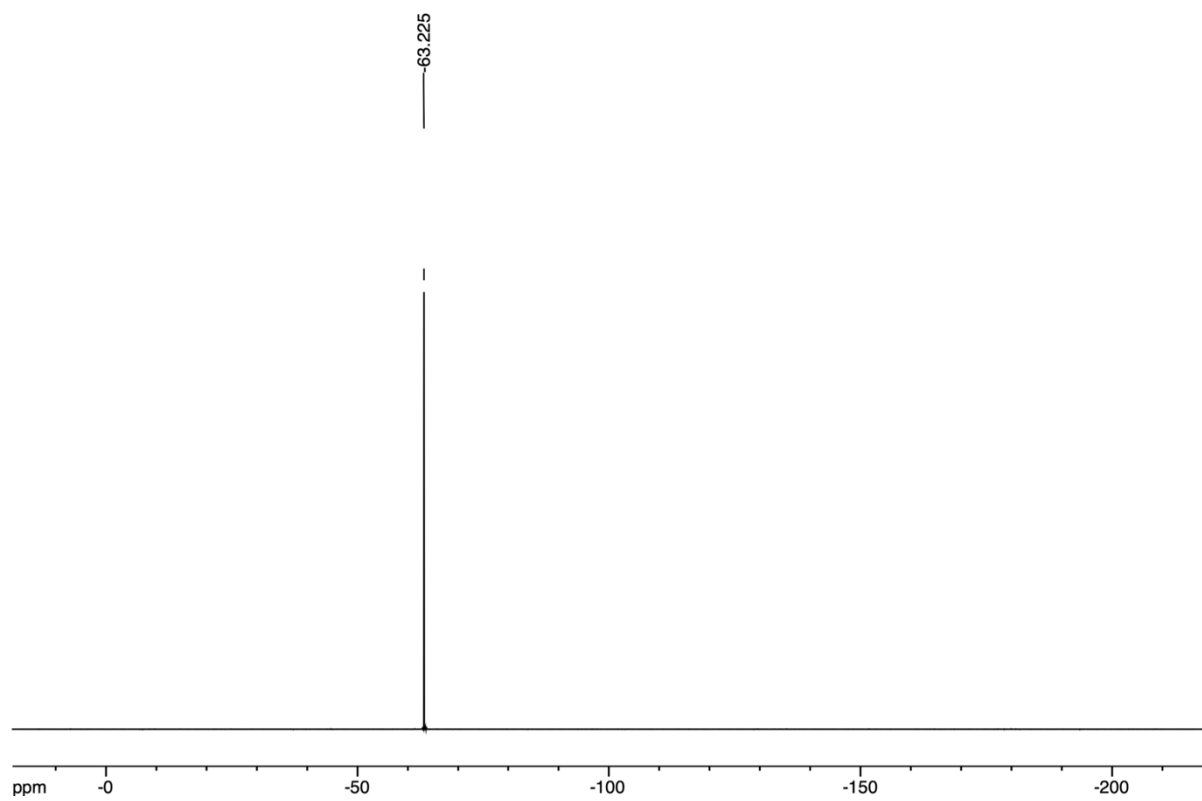


Figure S26. ^{19}F NMR spectrum of $[\mathbf{1bFe}](\text{TFPB})_2$ (376 MHz, CD_3CN).

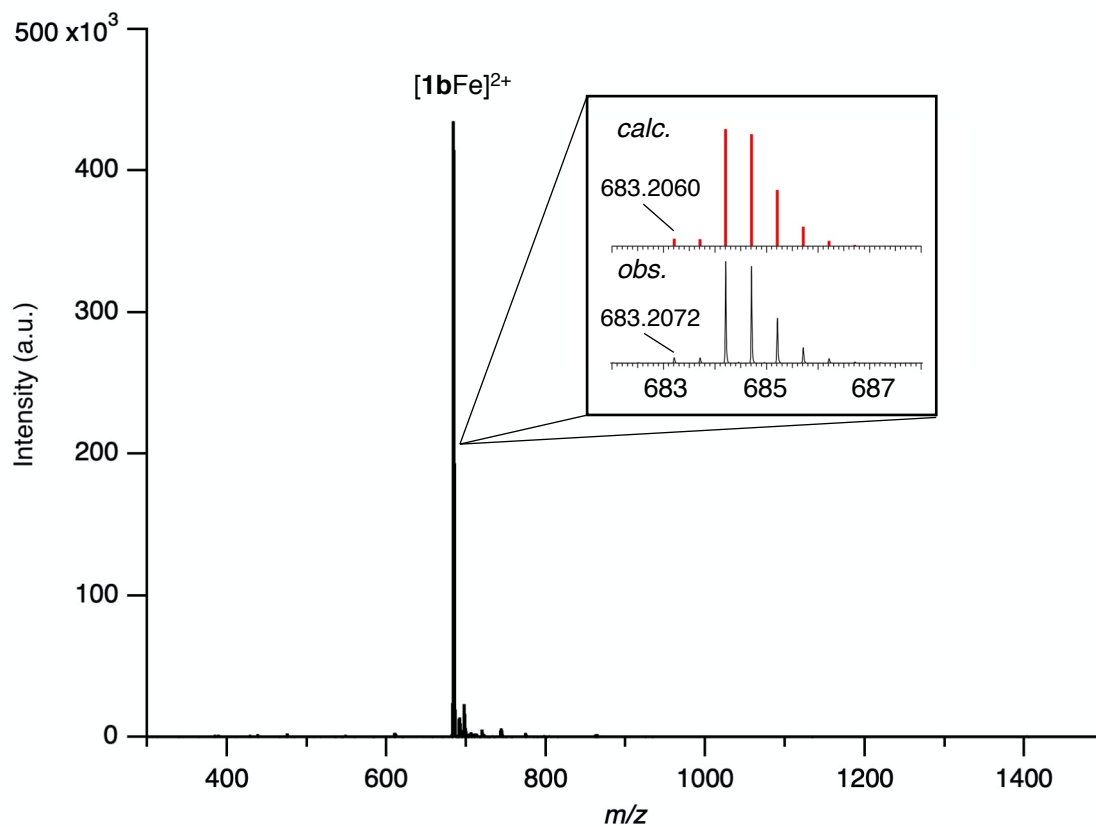


Figure S27. ESI mass spectrum of $[1bFe](TFPB)_2$ (solv. CD_3CN).

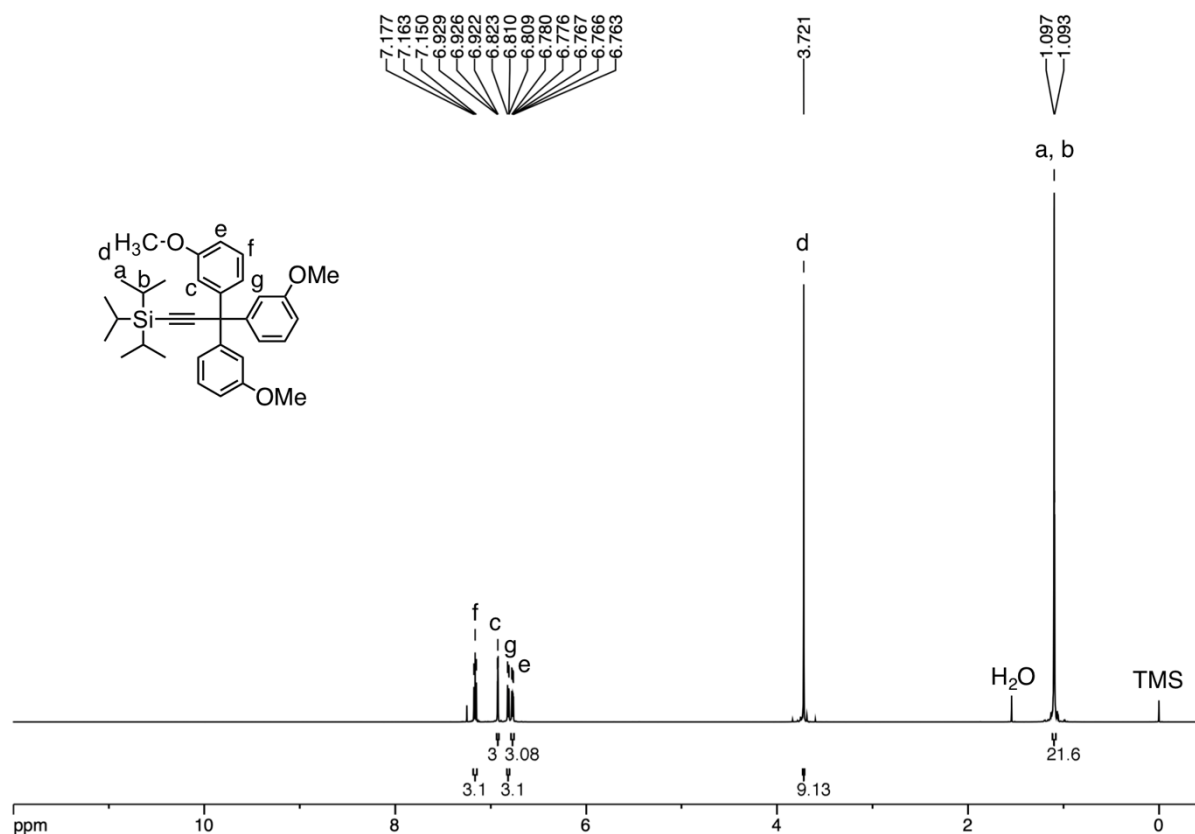


Figure S28. 1H NMR spectrum of **4-TE** (600 MHz, $CDCl_3$).

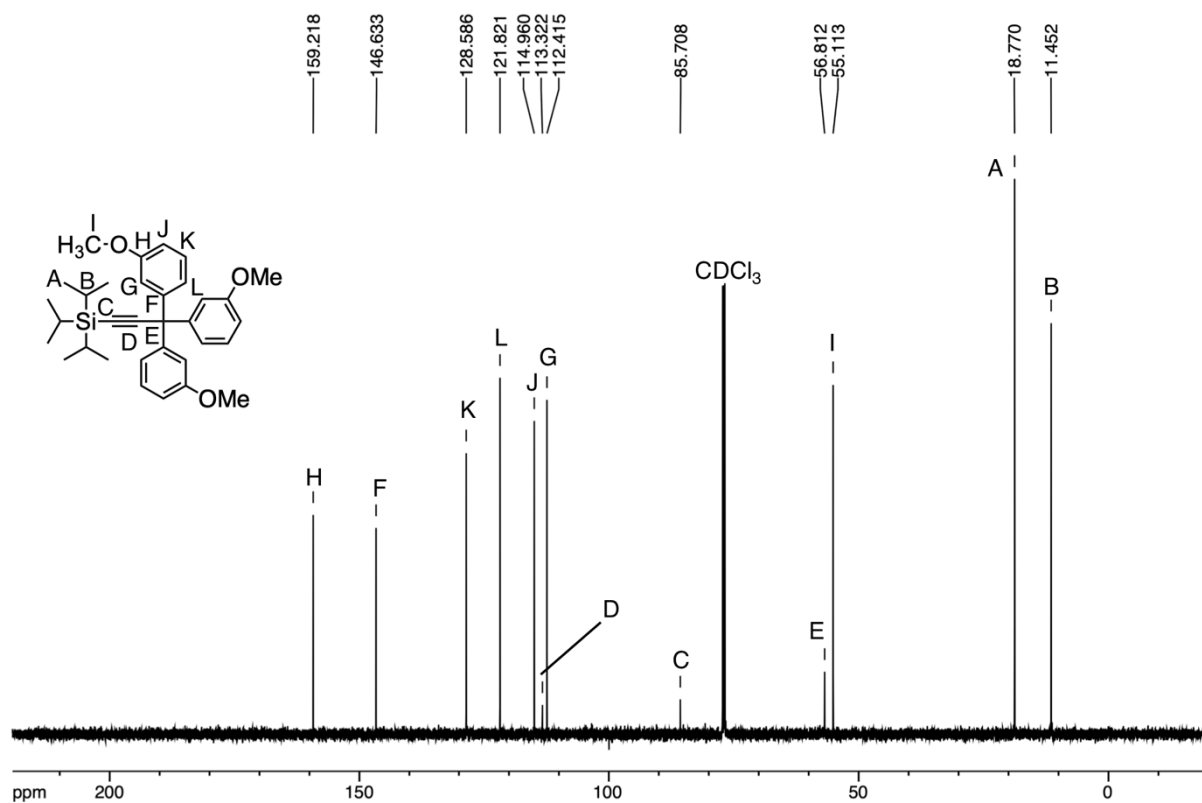


Figure S29. ¹³C NMR spectrum of 4-TE (151 MHz, CDCl₃).

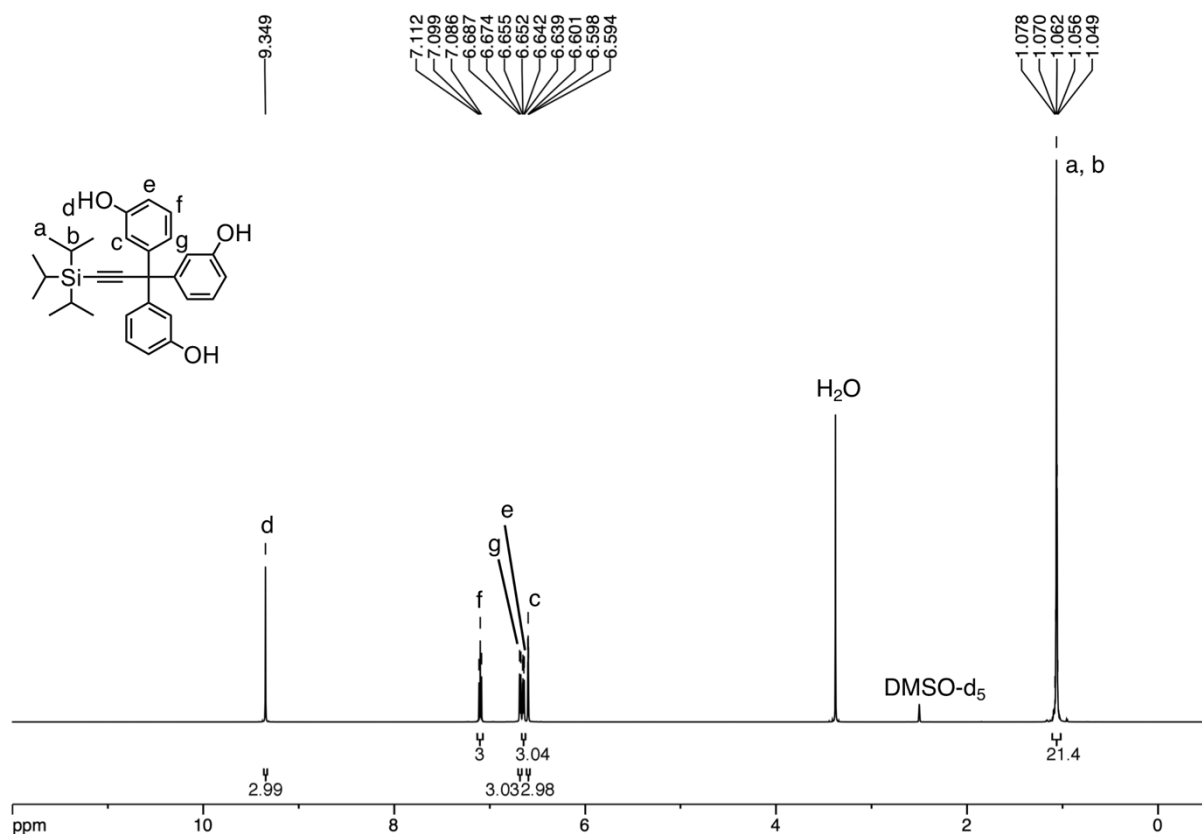


Figure S30. ¹H NMR spectrum of 5-TE (600 MHz, DMSO-d₆).

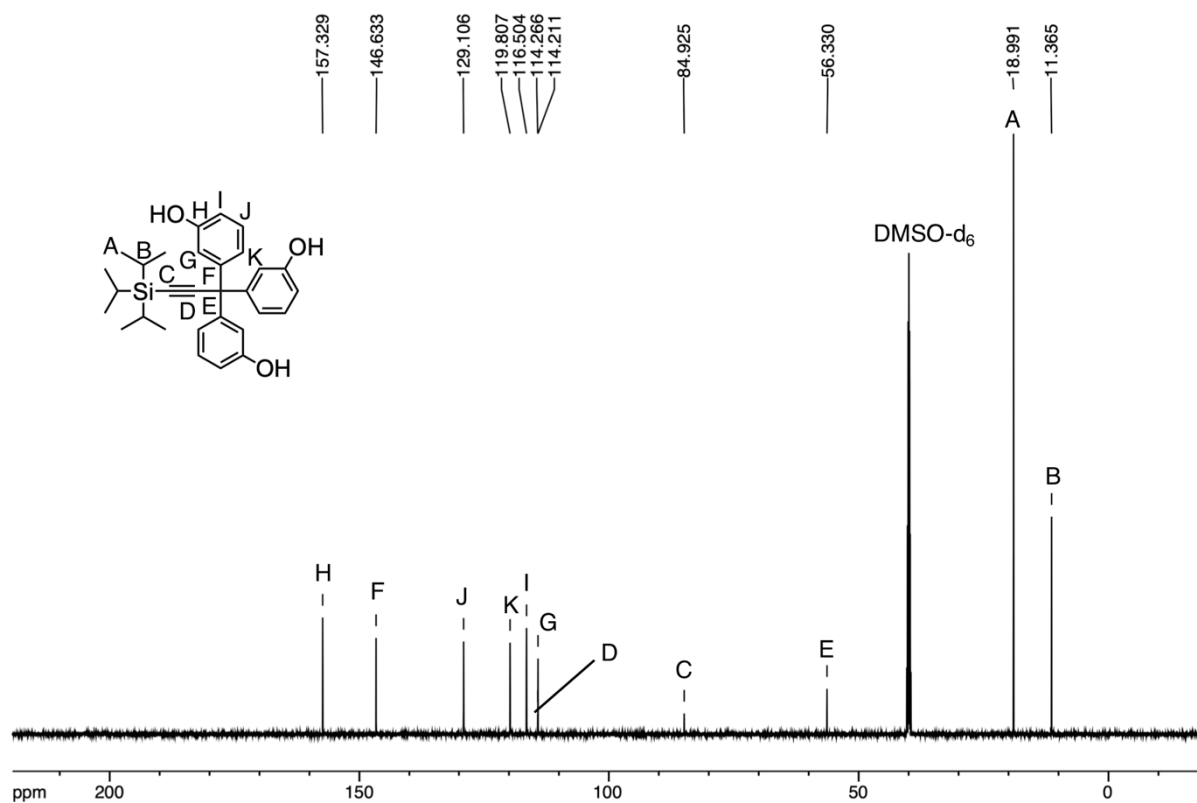


Figure S31. ¹³C NMR spectrum of **5-TE** (151 MHz, DMSO-*d*₆).

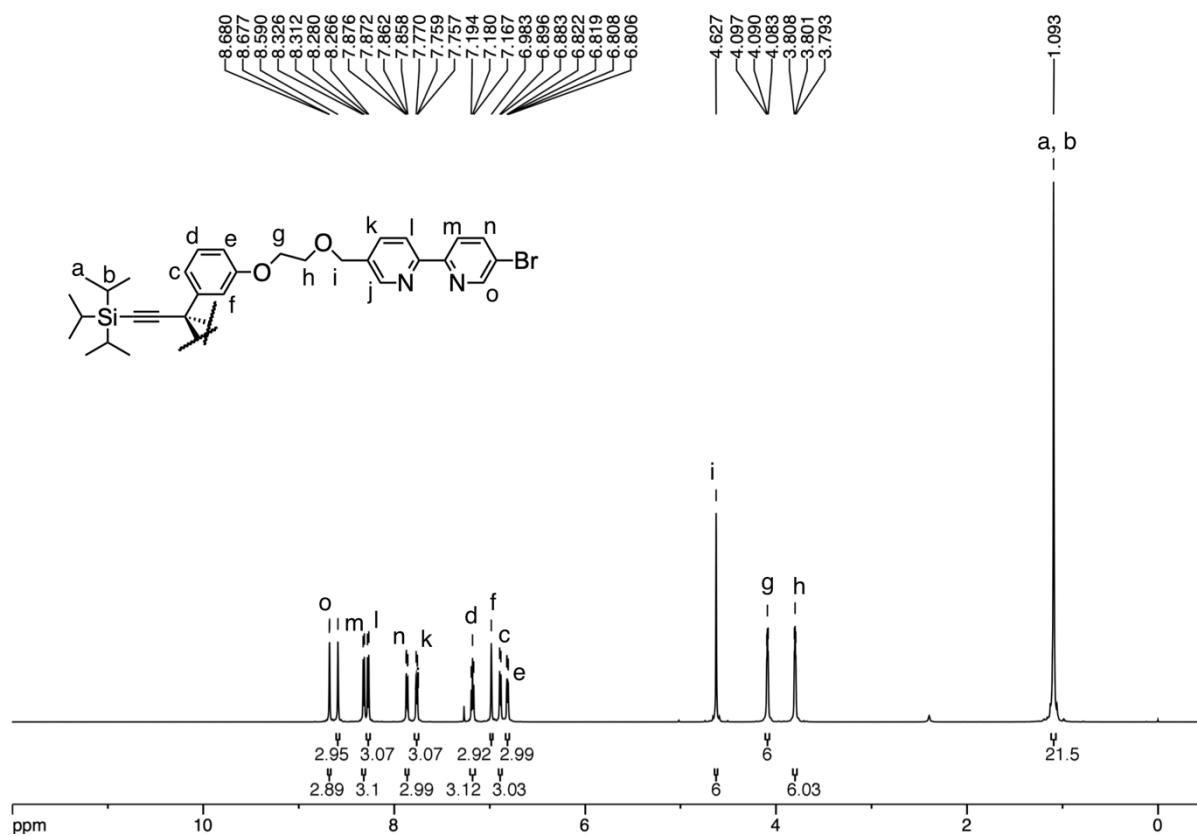


Figure S32. ¹H NMR spectrum of **2a** (600 MHz, CDCl₃).

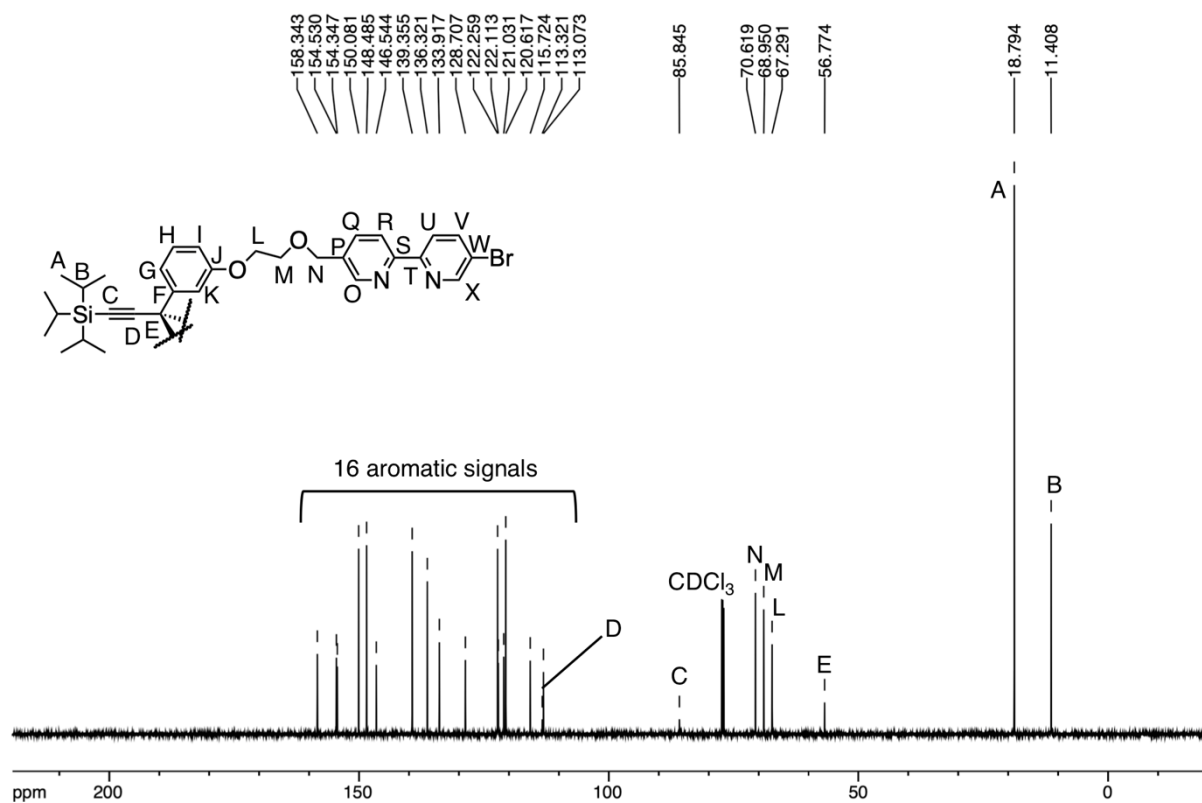


Figure S33. ^{13}C NMR spectrum of **2a** (151 MHz, CDCl_3).

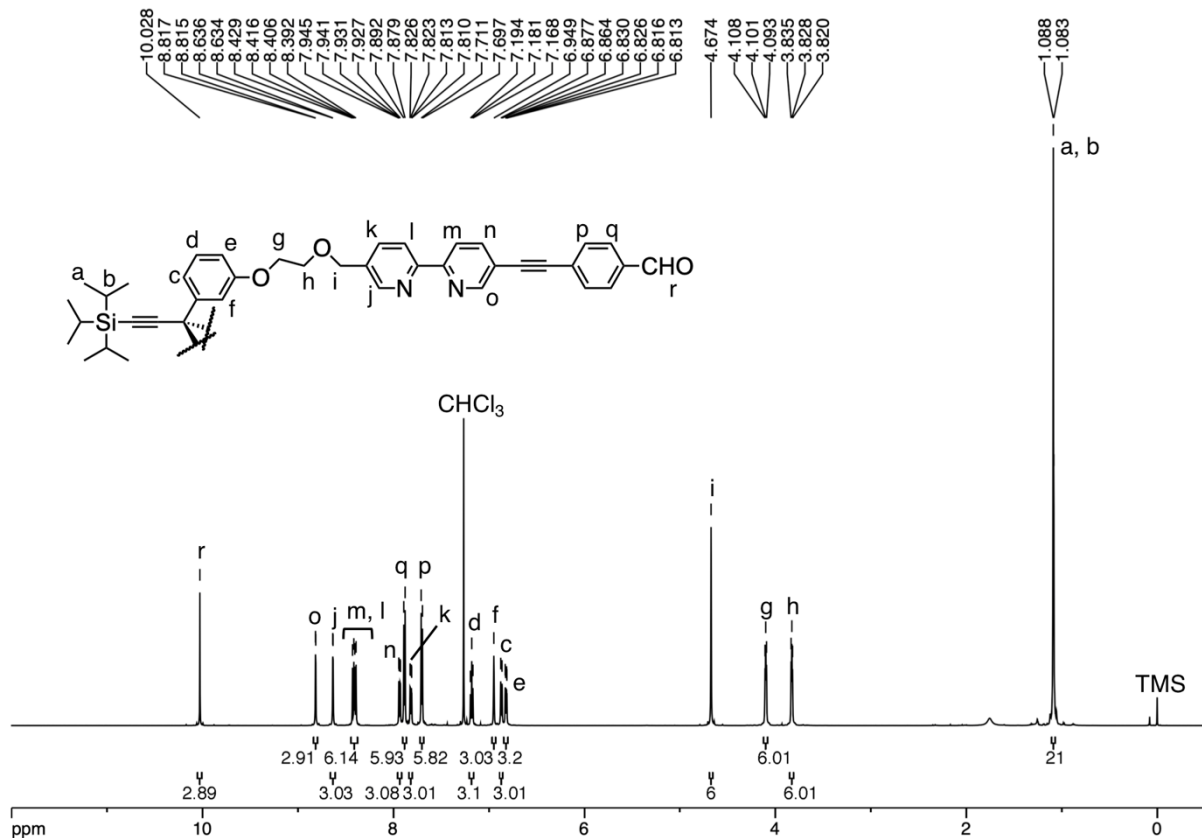


Figure S34. ^1H NMR spectrum of **2b** (600 MHz, CD_3CN).

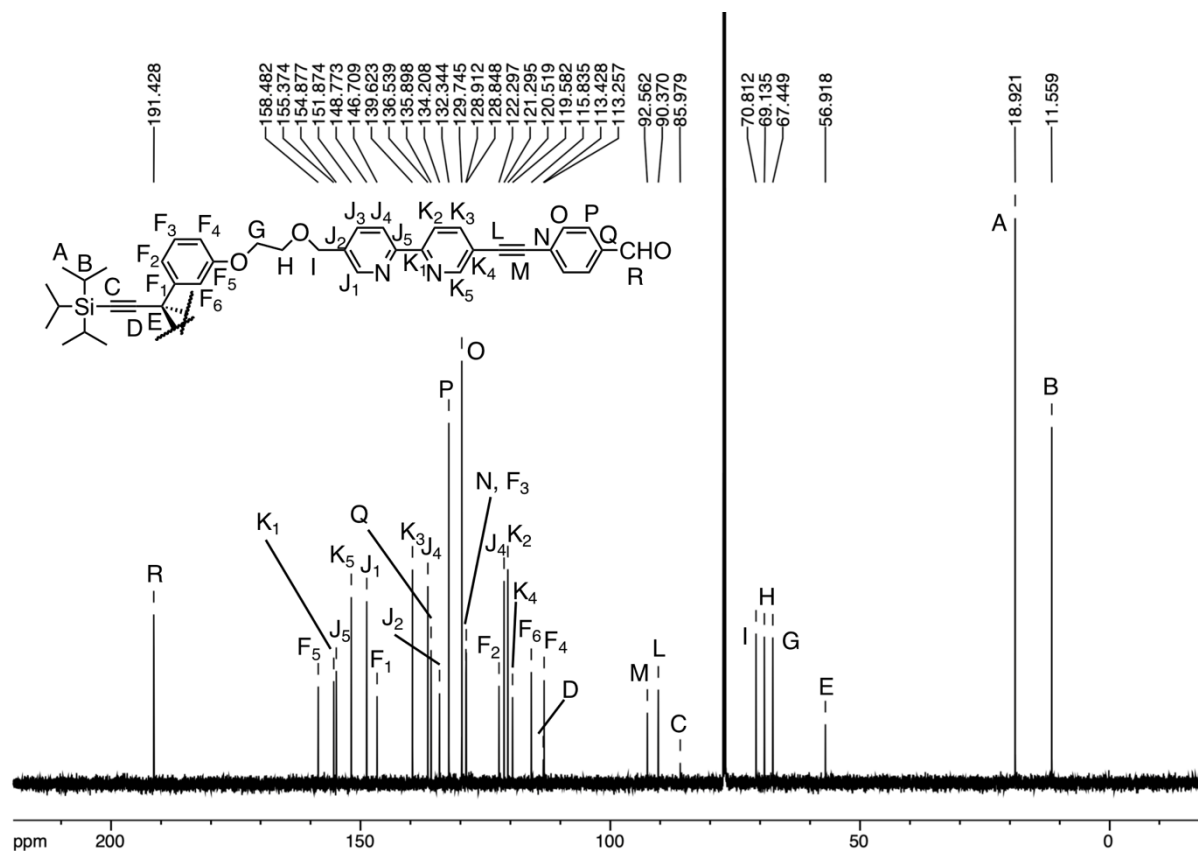


Figure S35. ^{13}C NMR spectrum of **2b** (151 MHz, CD_3CN).

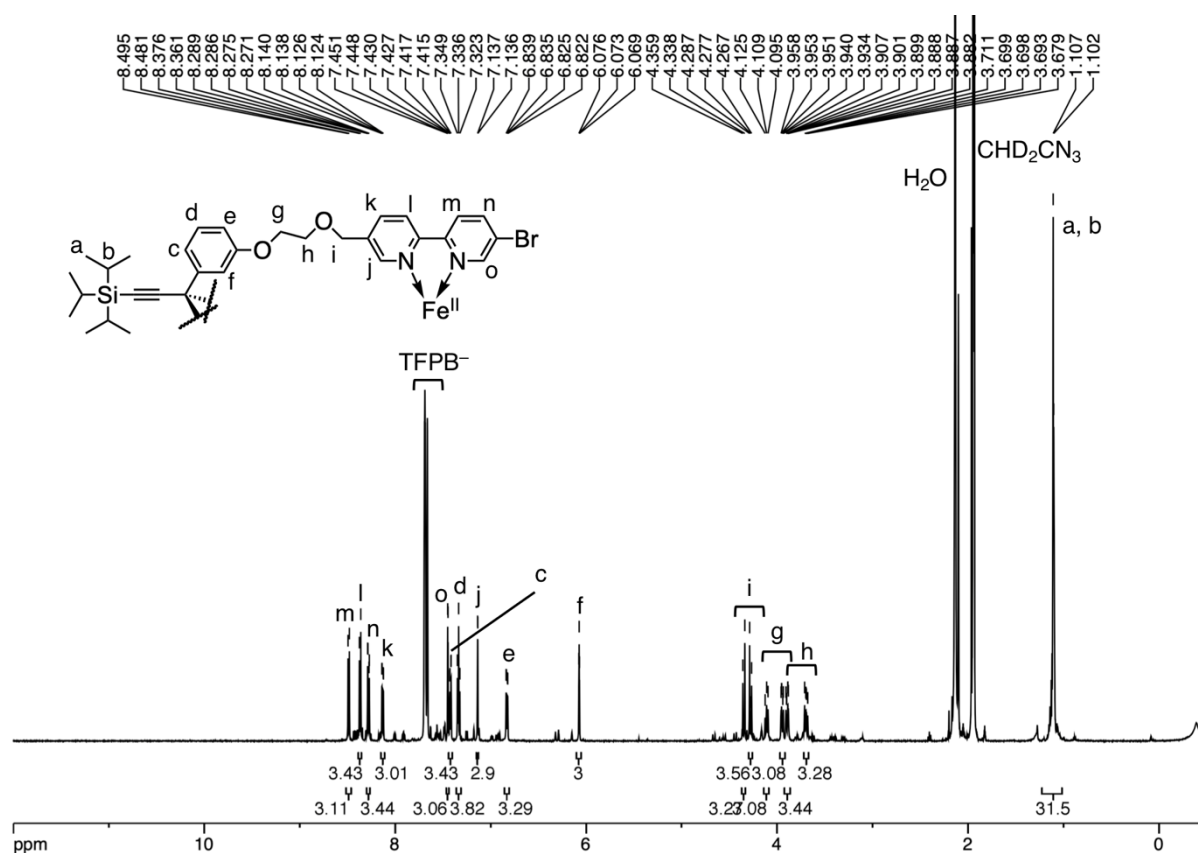


Figure S36. ^1H NMR spectrum of $[\mathbf{2aFe}](\text{TFPB})_2$ (600 MHz, CD_3CN).

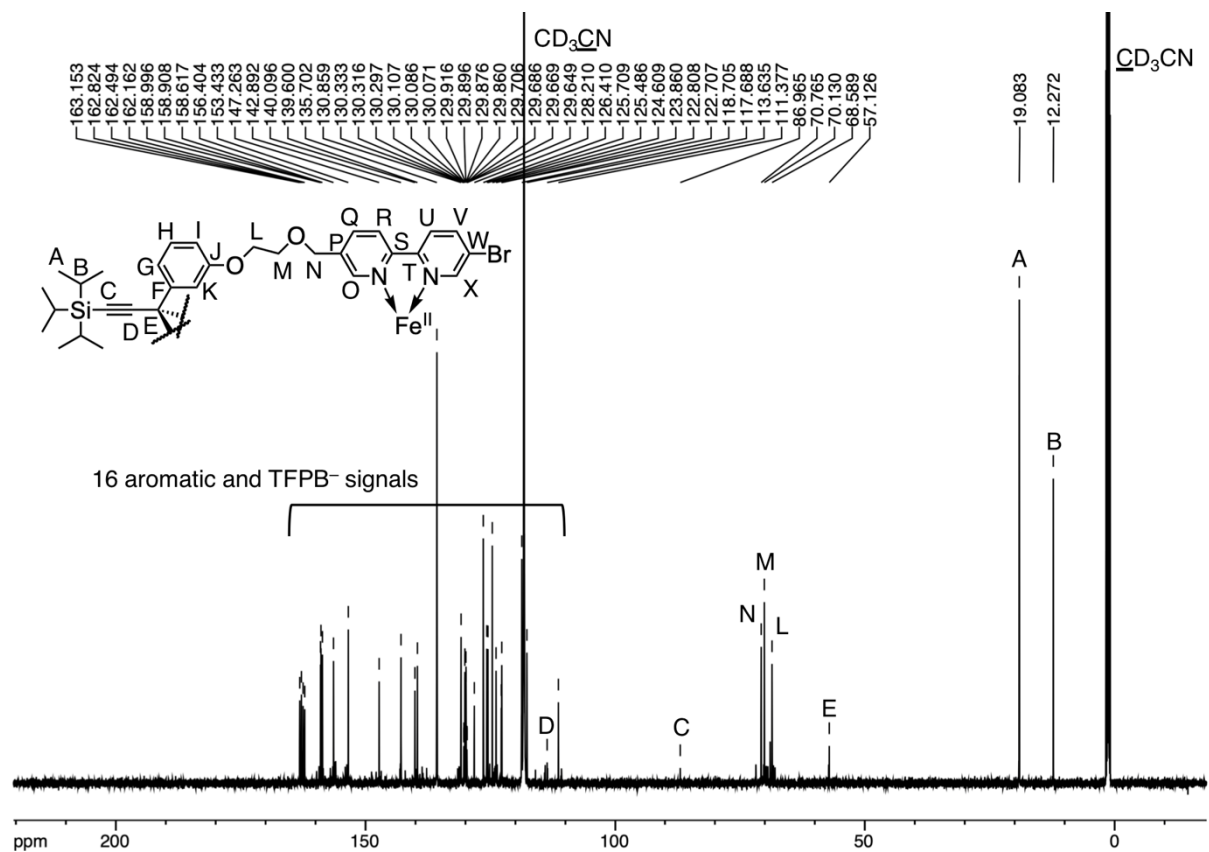


Figure S37. ¹³C NMR spectrum of [2aFe](TFPB)₂ (151 MHz, CD₃CN).

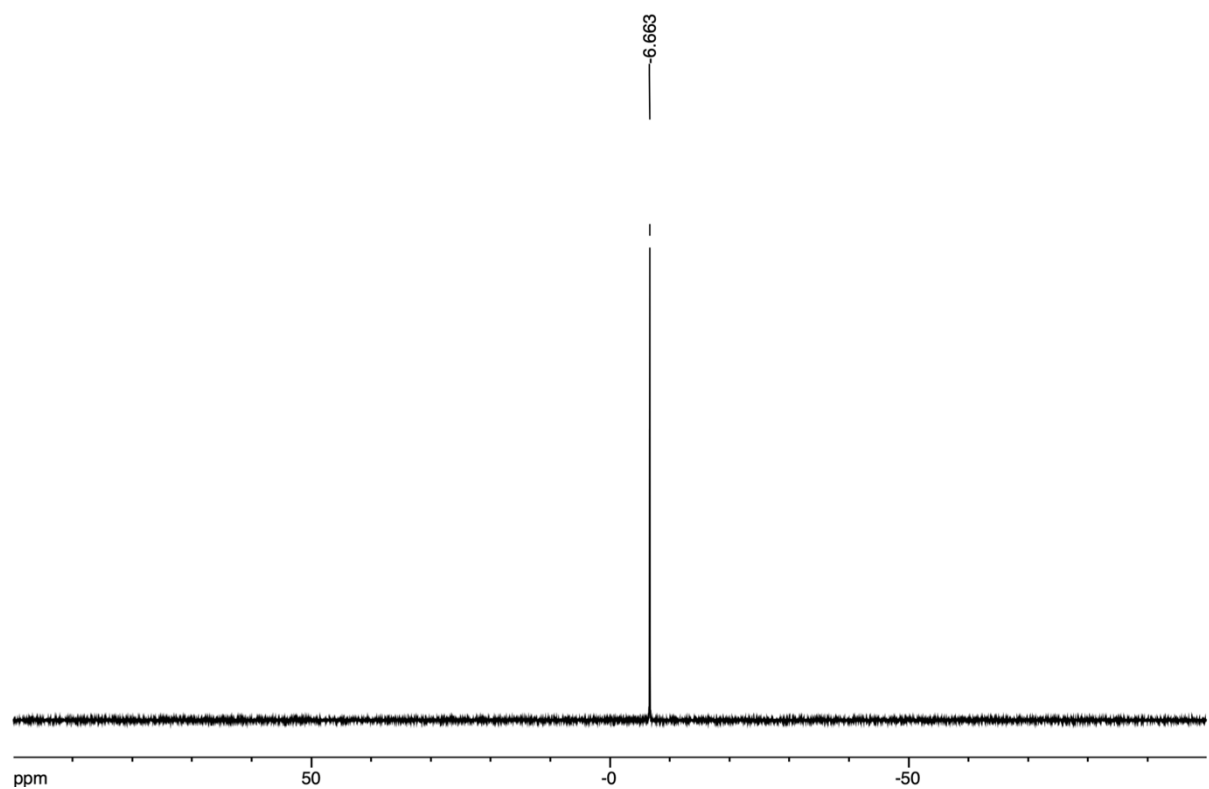


Figure S38. ¹¹B NMR spectrum of [2aFe](TFPB)₂ (192 MHz, CD₃CN).

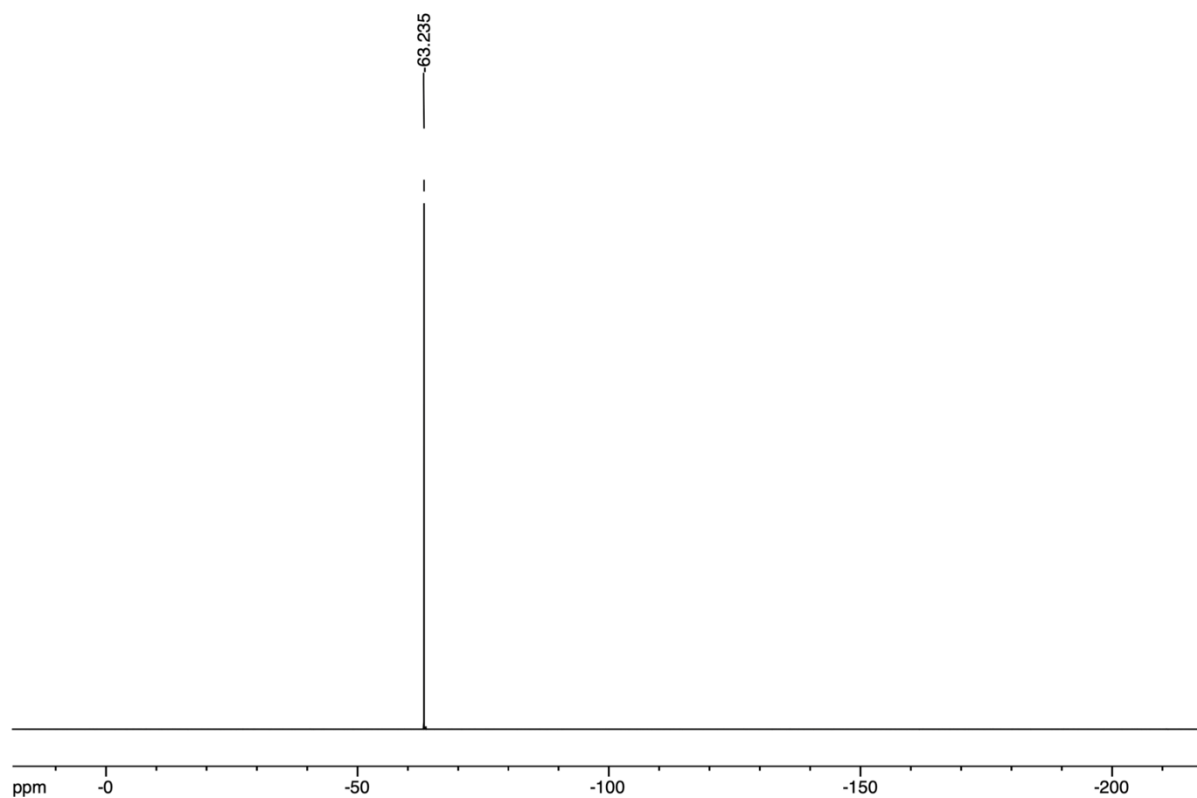


Figure S39. ^{19}F NMR spectrum of $[\mathbf{2aFe}](\text{TFPB})_2$ (376 MHz, CD_3CN).

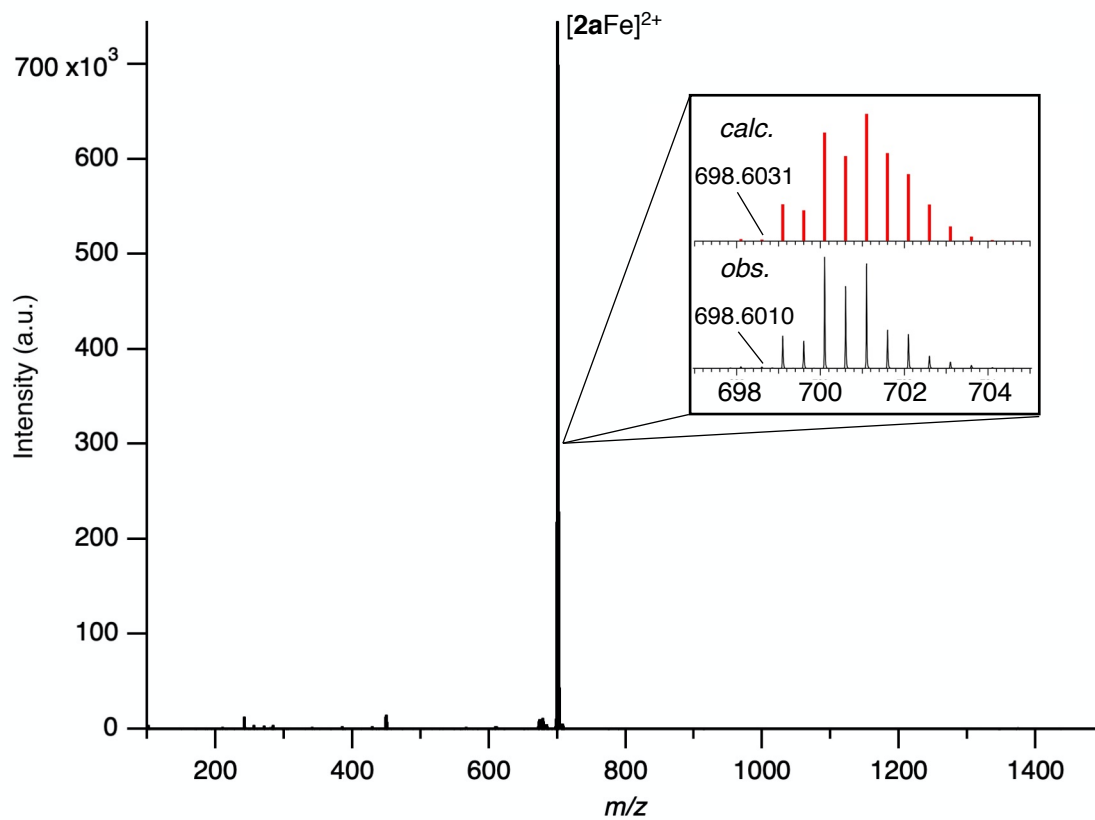


Figure S40. ESI mass spectrum of $[\mathbf{2aFe}](\text{TFPB})_2$ (solv. CH_3CN).

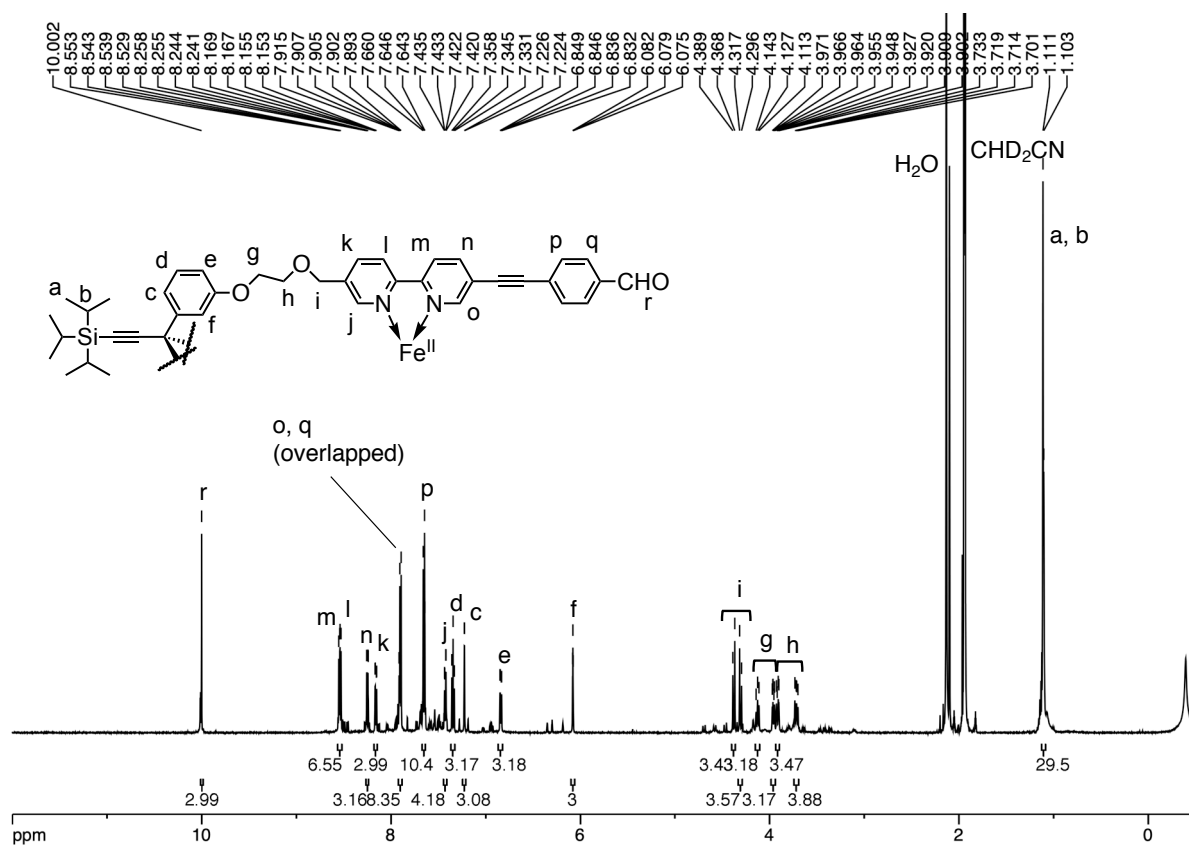


Figure S41. 1H NMR spectrum of $[2bFe](PF_6)_2$ (600 MHz, CD_3CN).

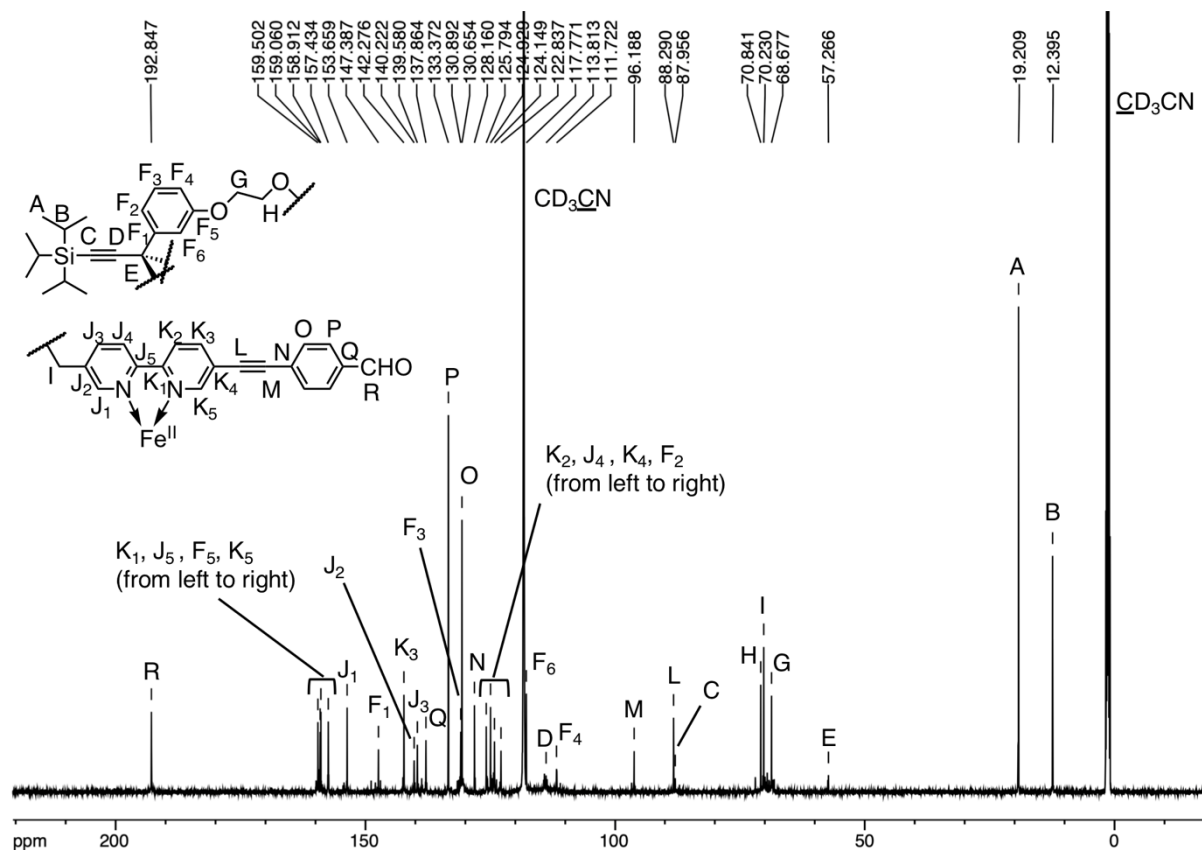


Figure S42. ^{13}C NMR spectrum of $[2bFe](PF_6)_2$ (151 MHz, CD_3CN).

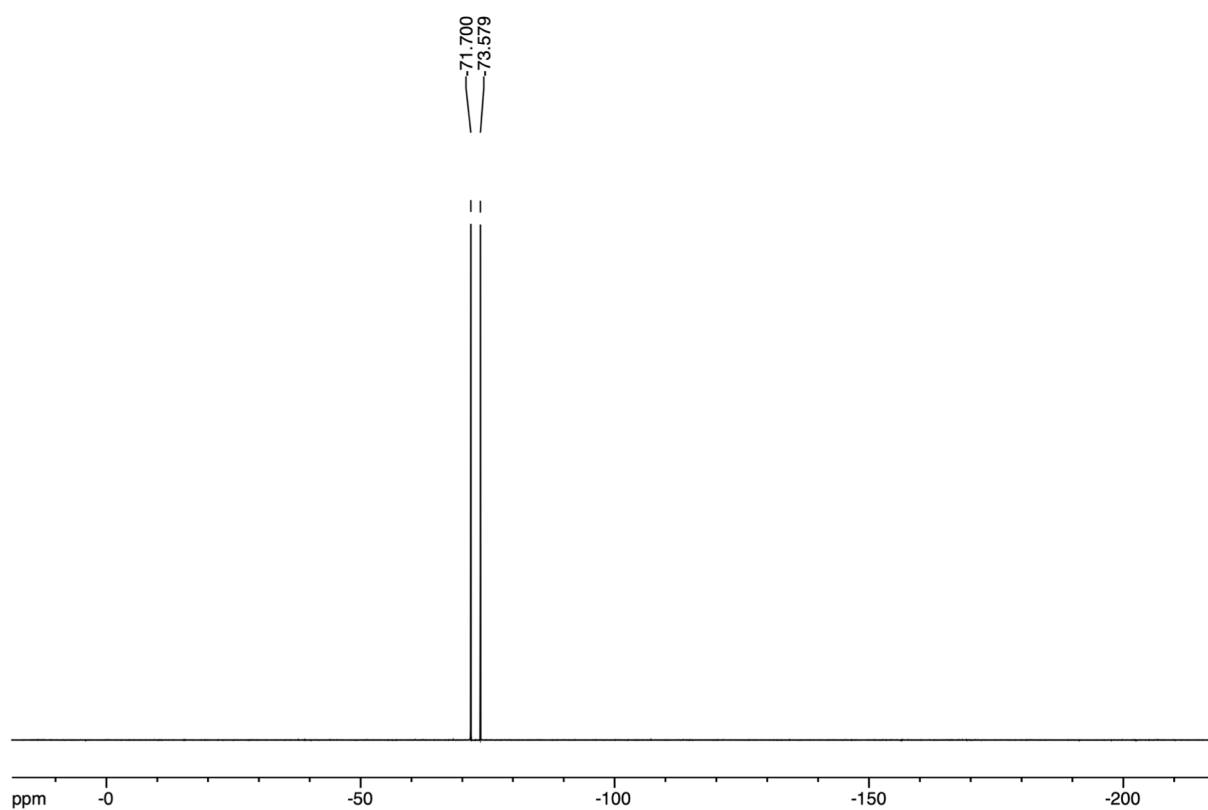


Figure S43. ^{19}F NMR spectrum of $[\mathbf{2bFe}](\text{PF}_6)_2$ (376 MHz, CD_3CN).

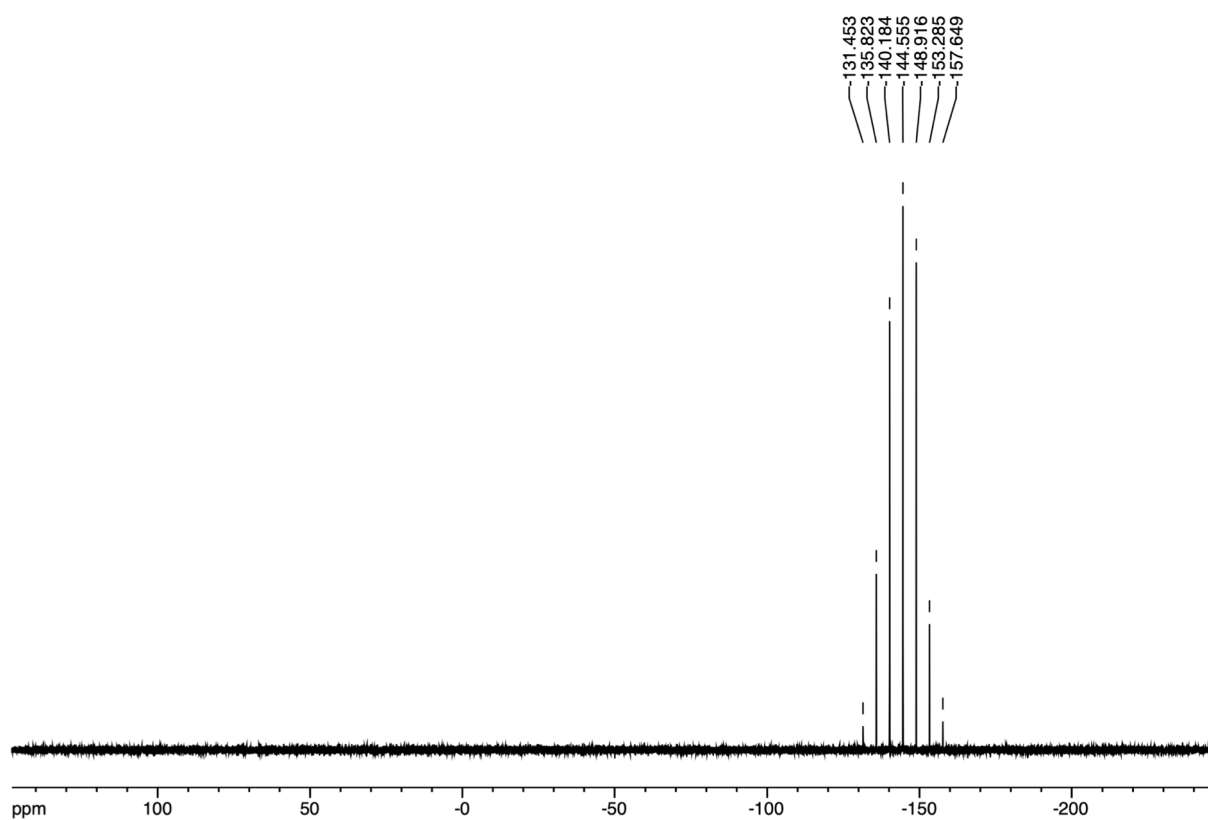


Figure S44. ^{31}P NMR spectrum of $[\mathbf{2bFe}](\text{PF}_6)_2$ (243 MHz, CD_3CN).

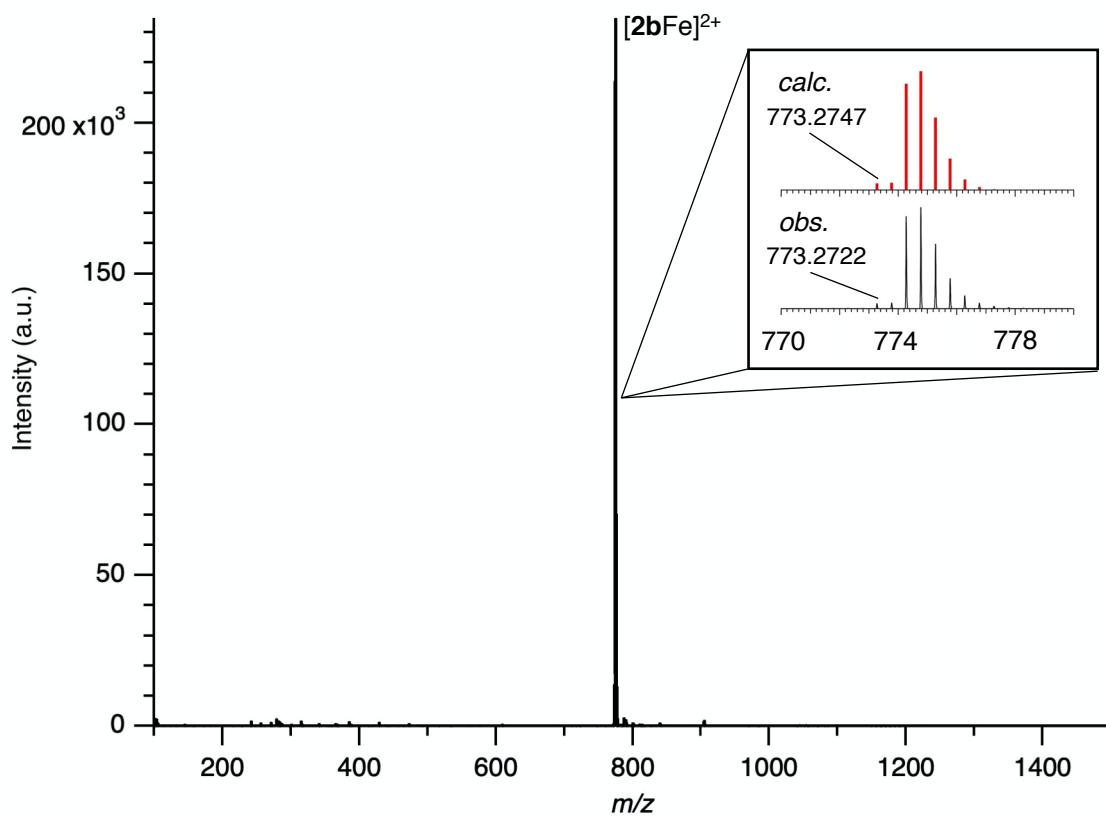


Figure S45. ESI mass spectrum of $[2bFe](PF_6)_2$ (solv. CH_3CN).

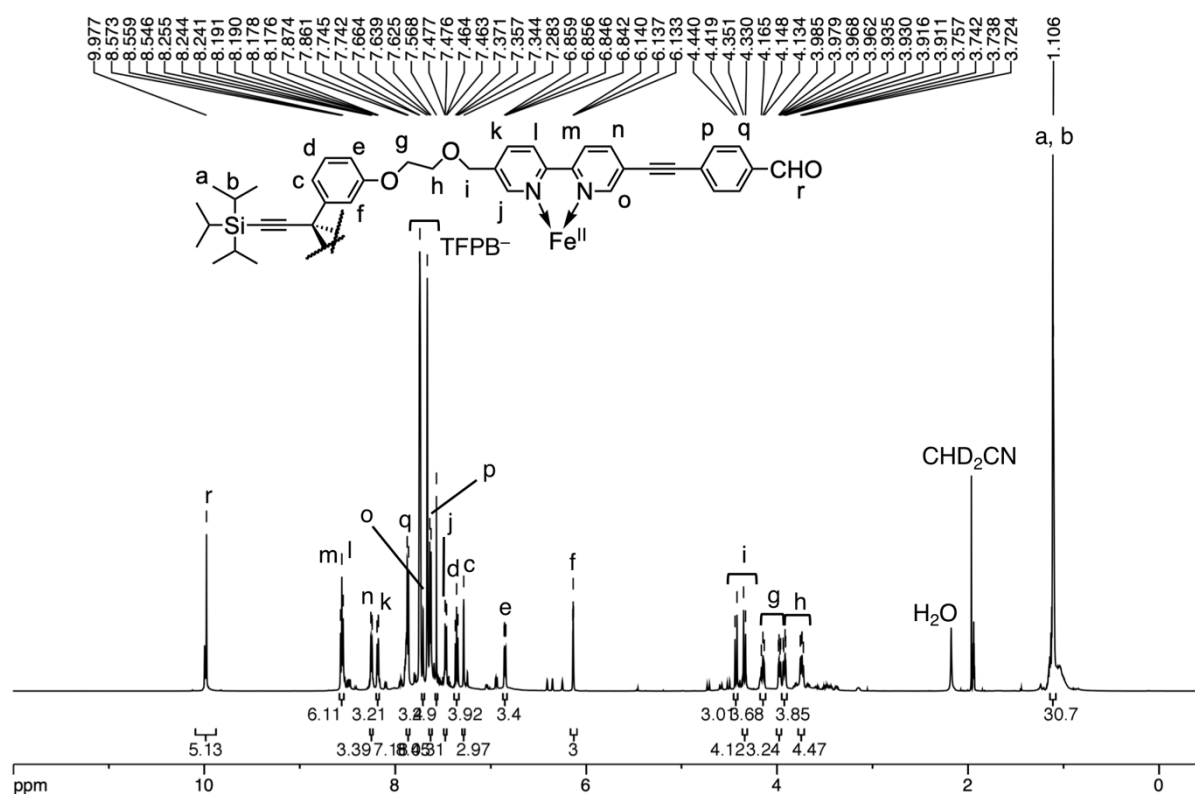


Figure S46. 1H NMR spectrum of $[2bFe](TFPB)_2$ (600 MHz, CD_3CN).

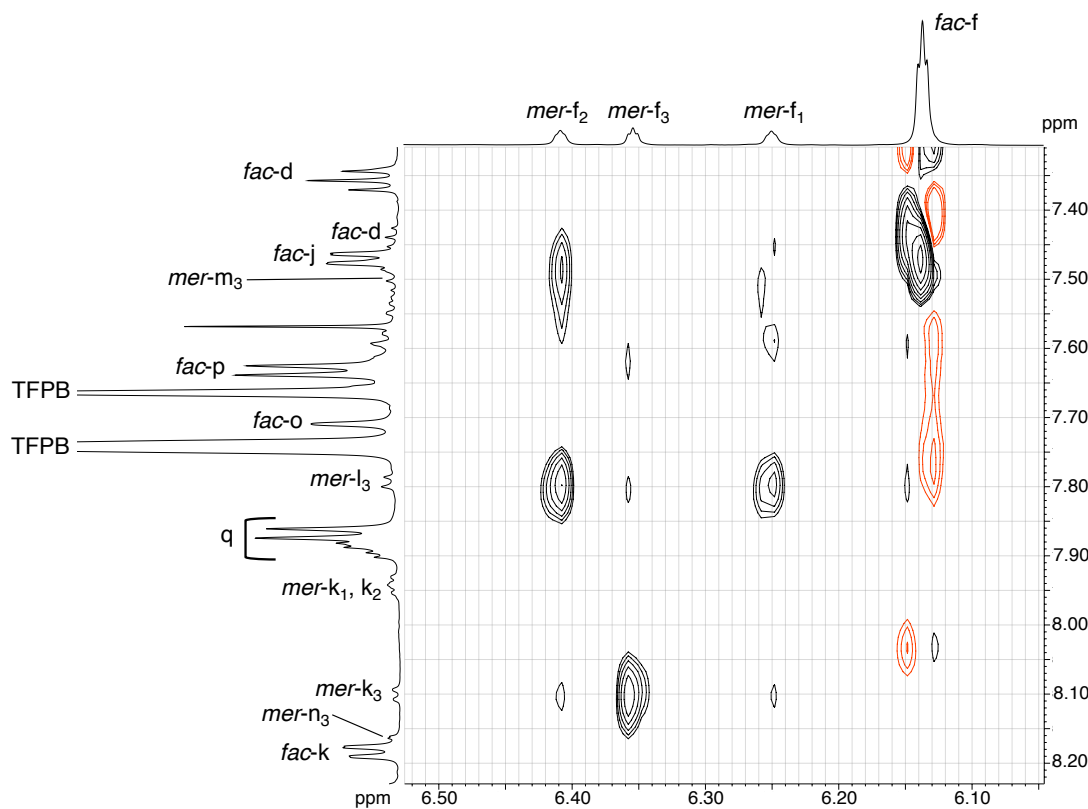


Figure S47. ^1H - ^1H ROESY spectrum of $[\mathbf{2bFe}](\text{TFPB})_2$ (600 MHz, CD_3CN . Signals of *mer*-isomer are numbered for each tripodal arm.).

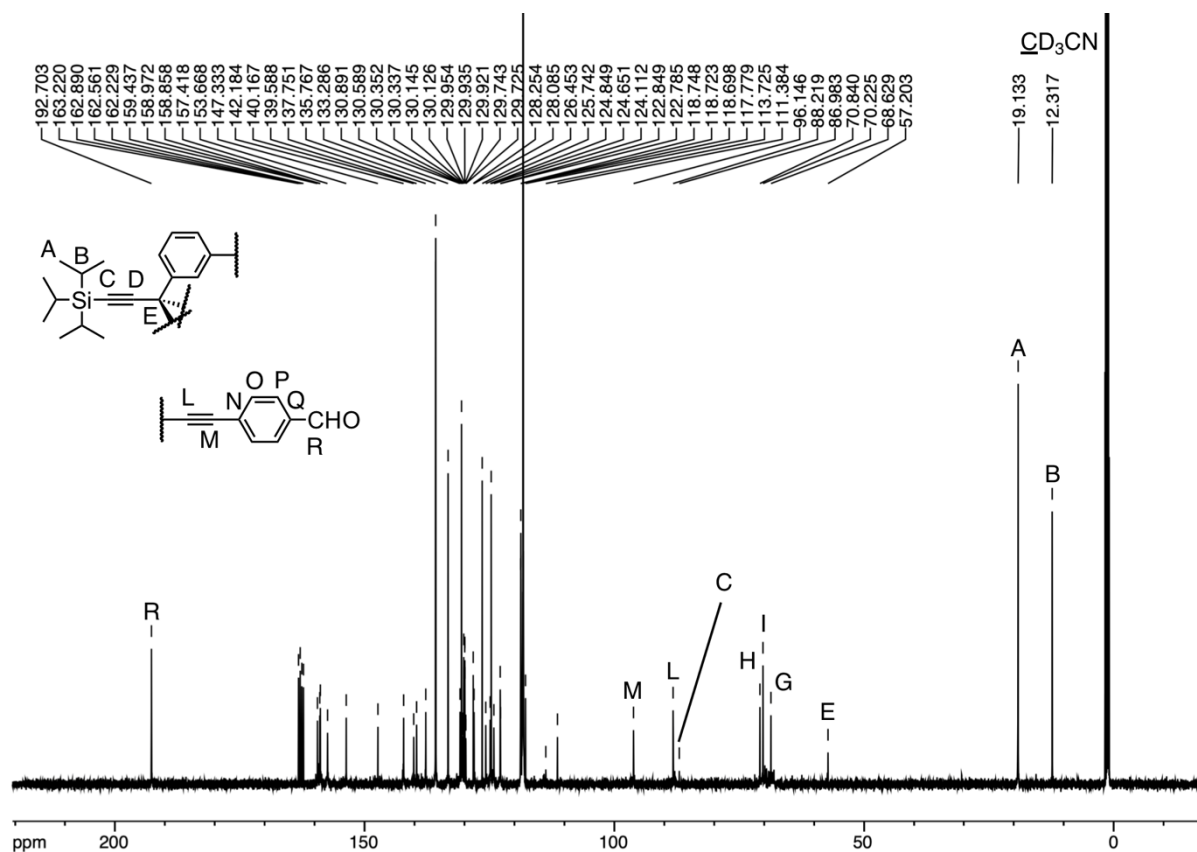
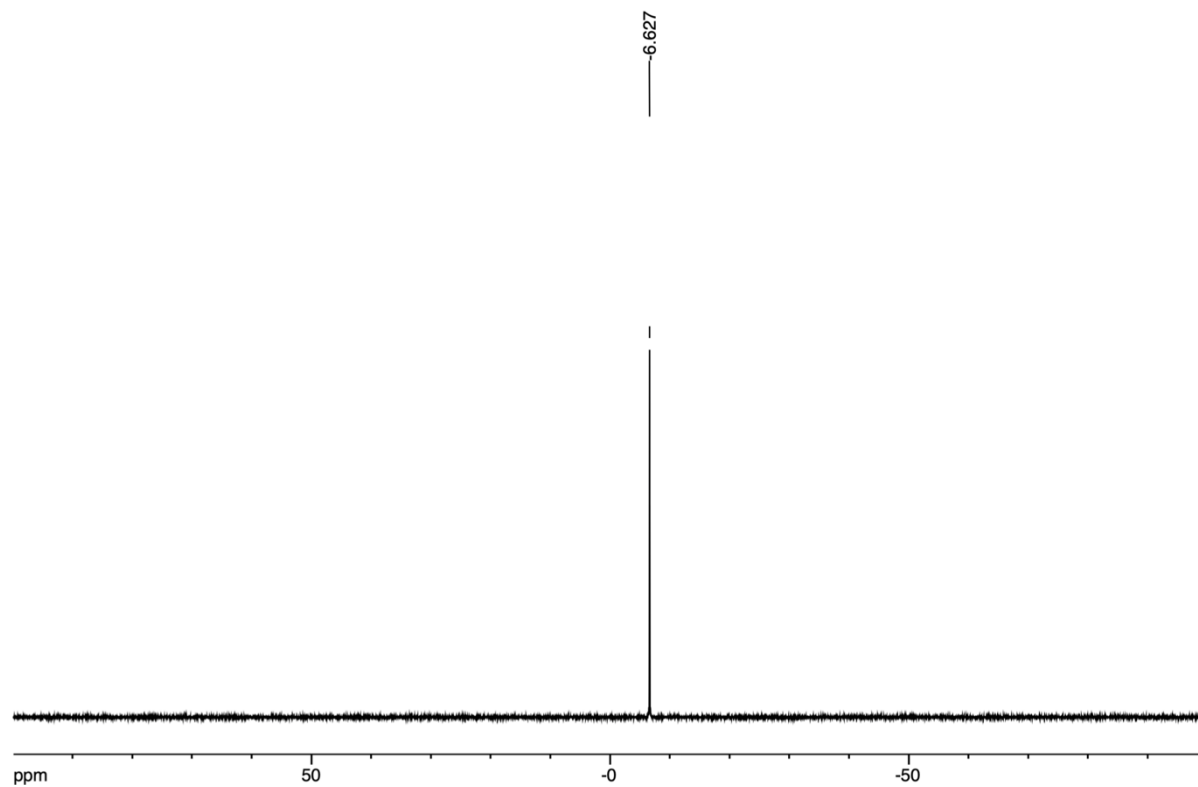
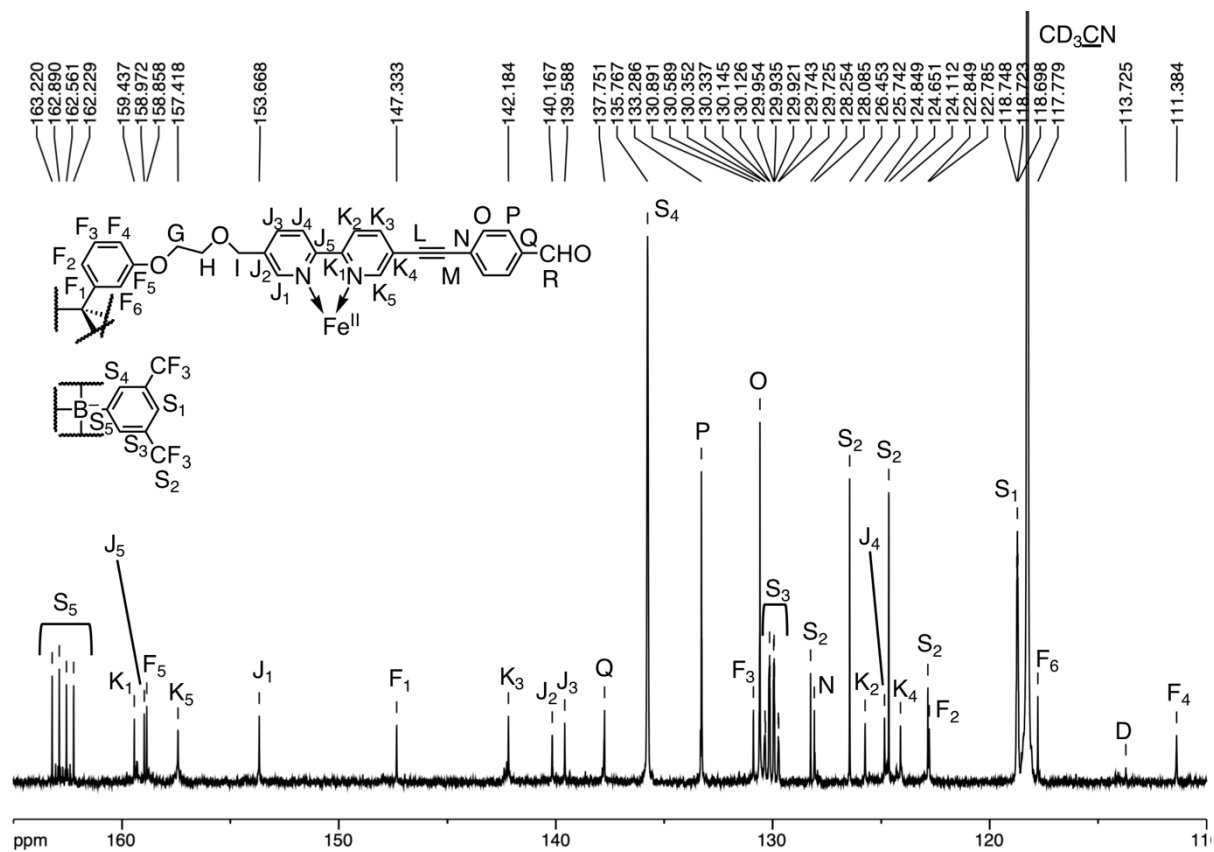


Figure S48. ^{13}C NMR spectrum of $[\mathbf{2bFe}](\text{TFPB})_2$ (151 MHz, CD_3CN).



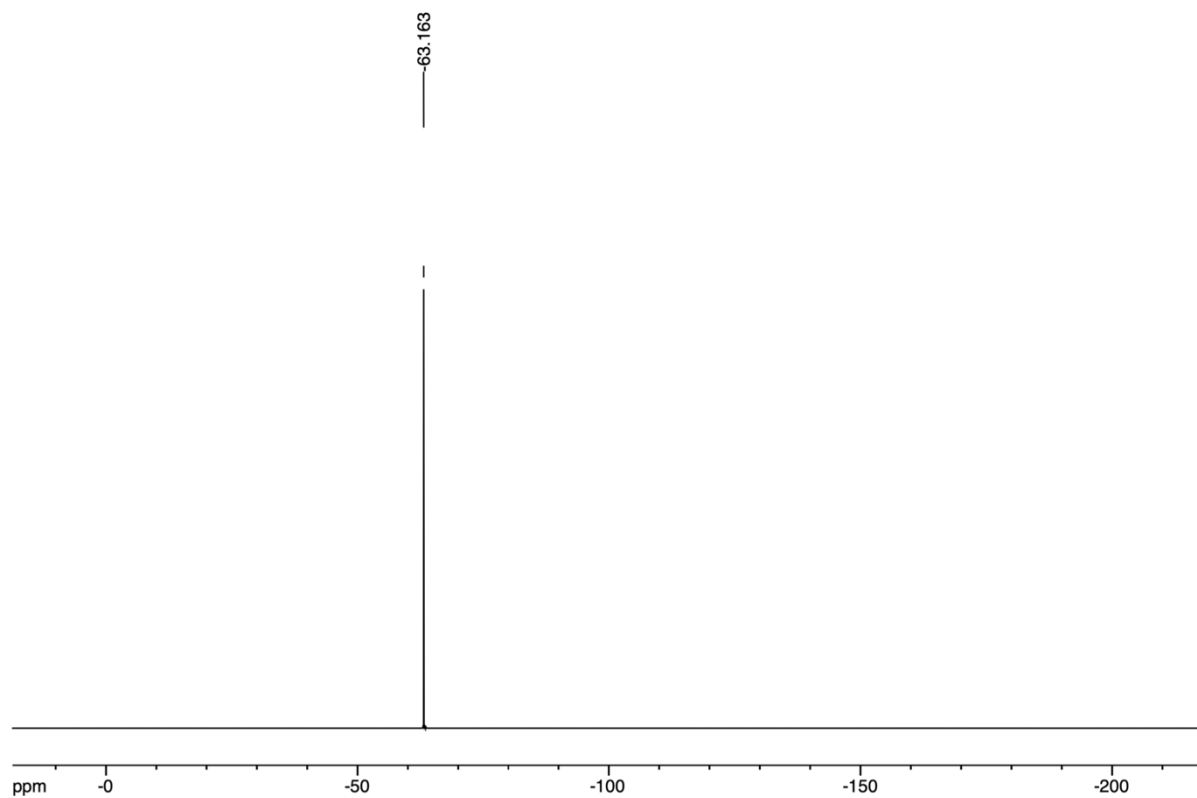


Figure S51. ^{19}F NMR spectrum of $[\mathbf{2bFe}](\text{TFPB})_2$ (376 MHz, CD_3CN).

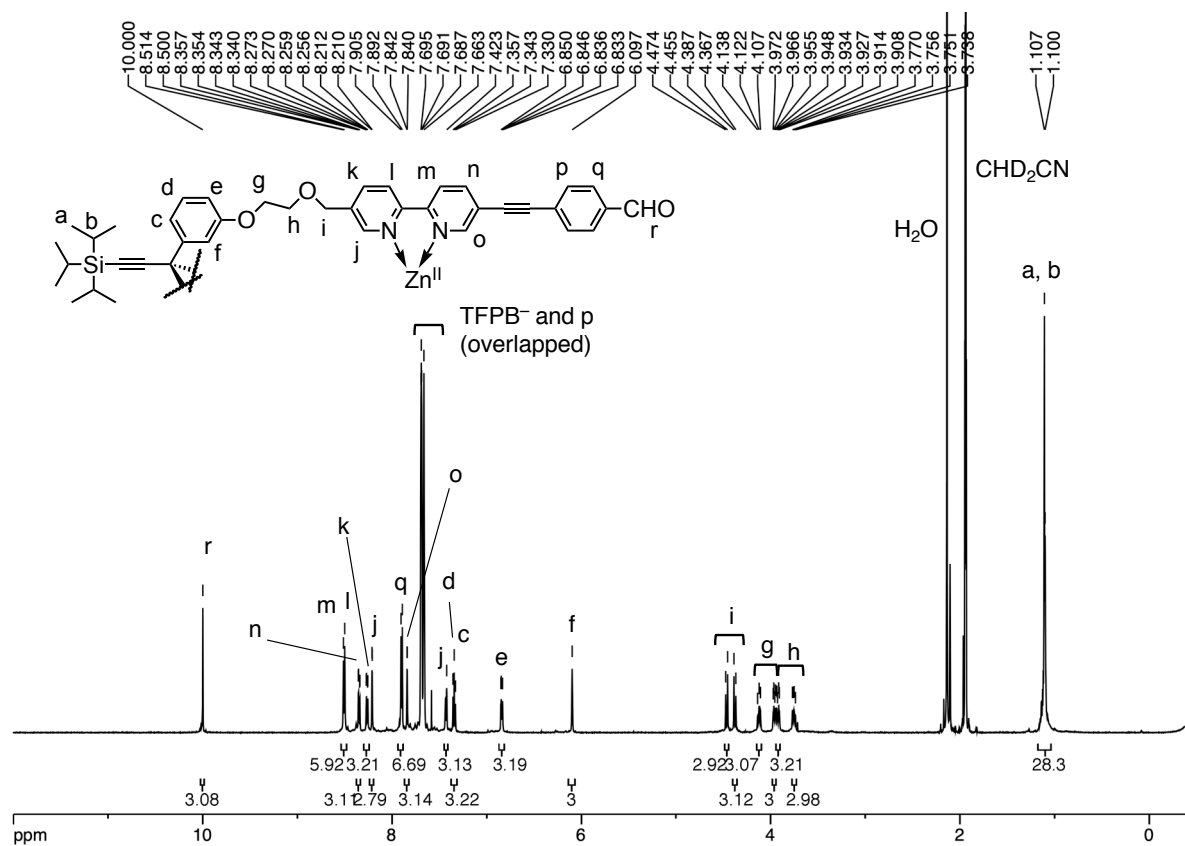


Figure S52. ^1H NMR spectrum of $[\mathbf{2bZn}](\text{TFPB})_2$ (600 MHz, CD_3CN).

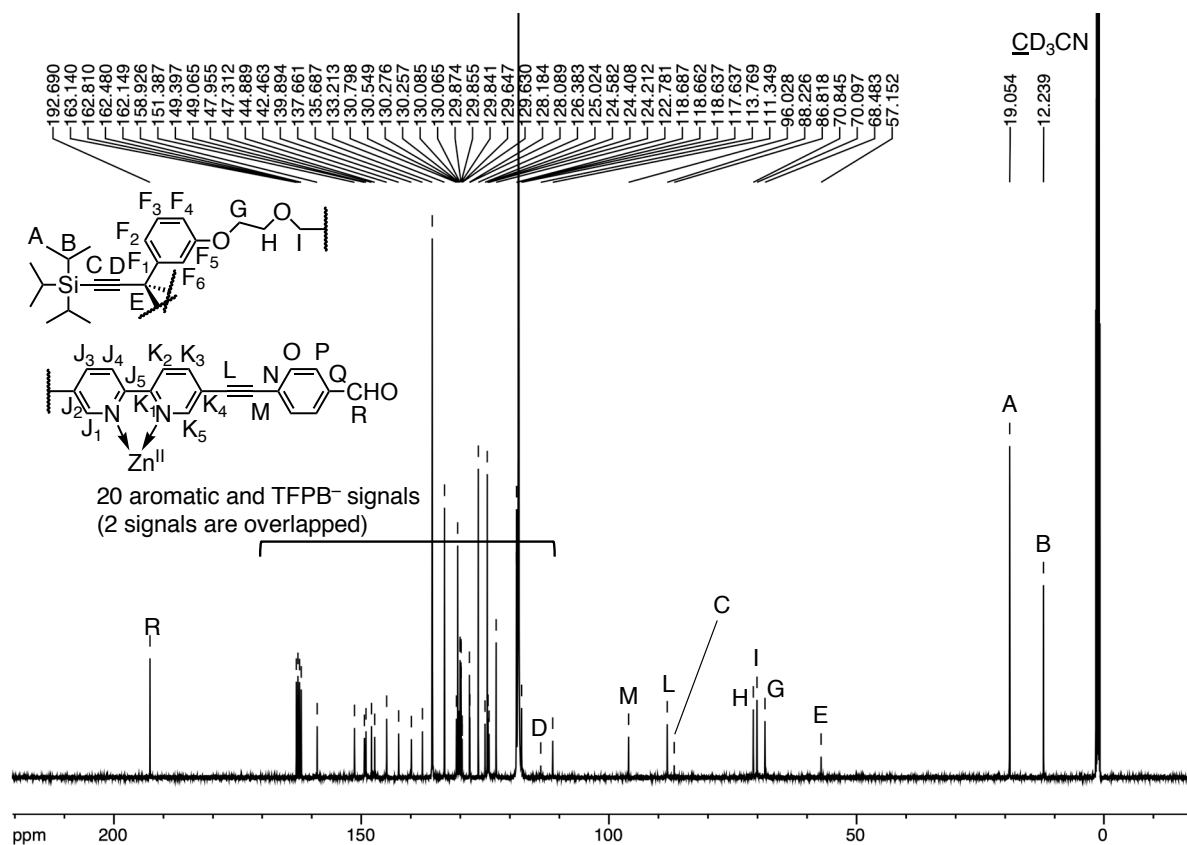


Figure S53. ¹³C NMR spectrum of [2bZn](TFPB)₂ (151 MHz, CD₃CN).

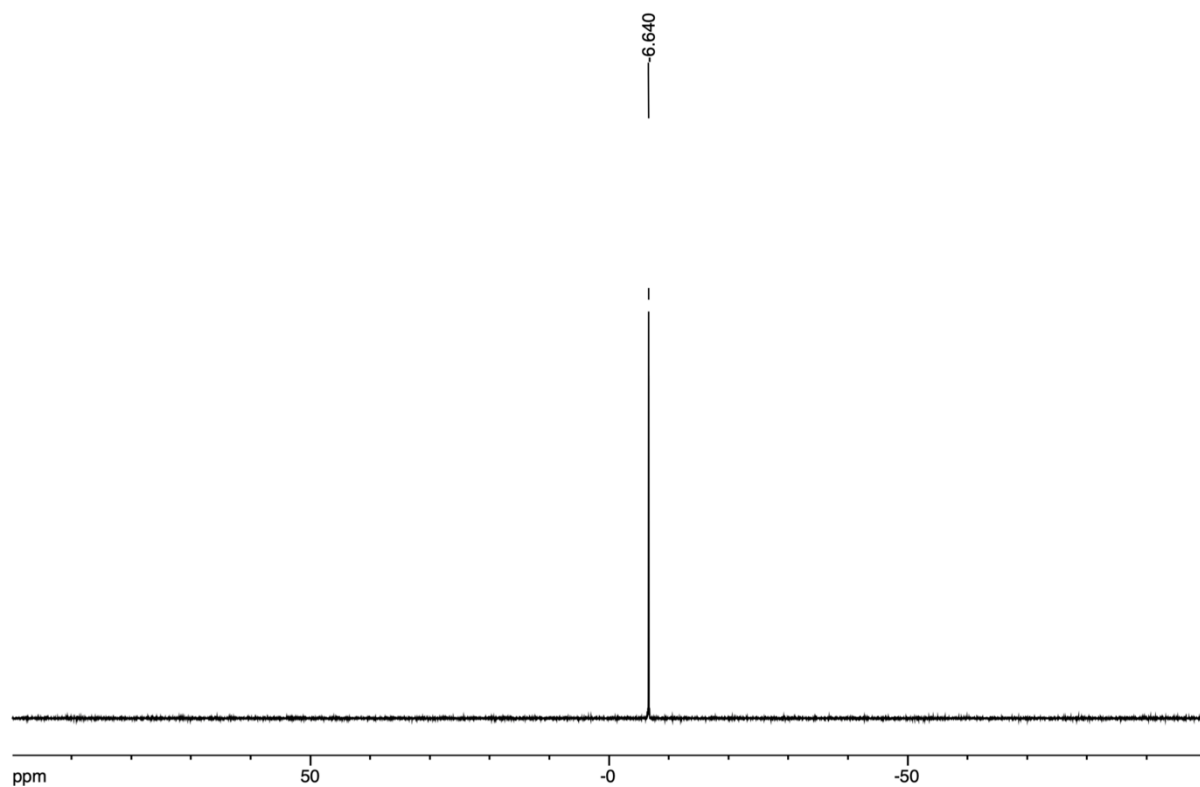


Figure S54. ¹¹B NMR spectrum of [2bZn](TFPB)₂ (192 MHz, CD₃CN).

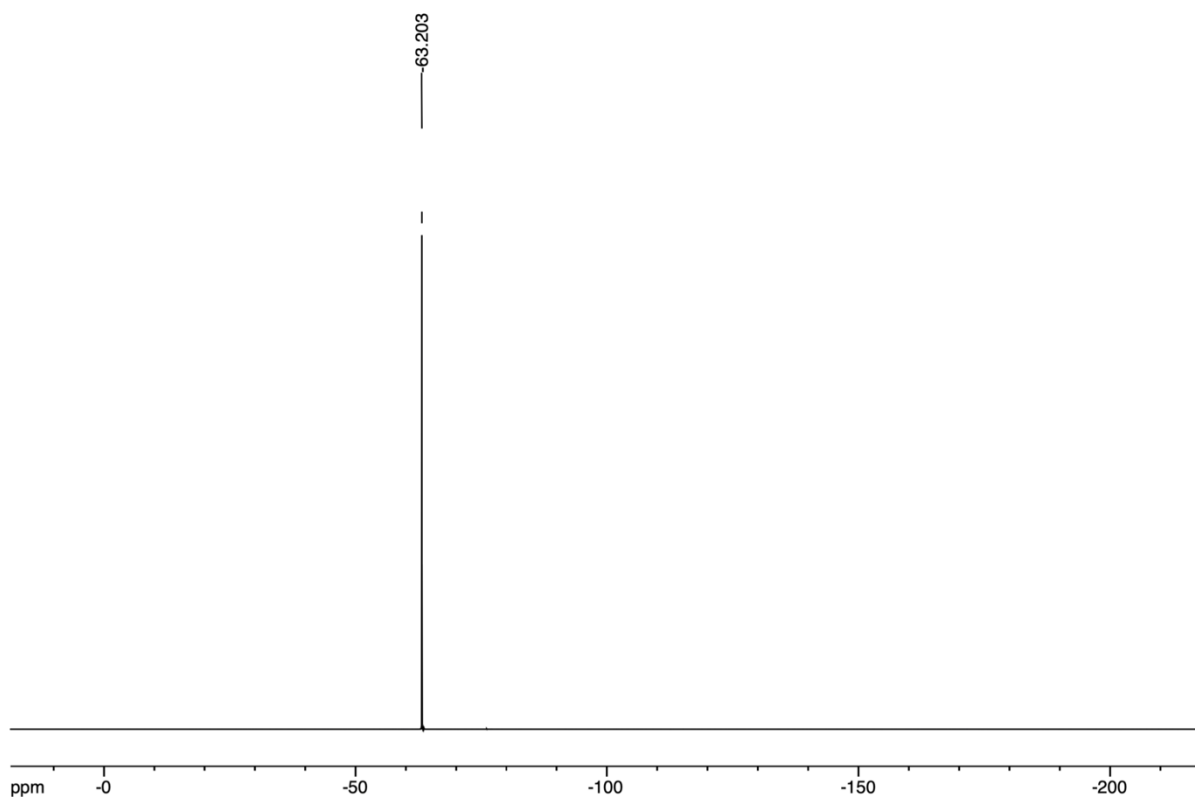


Figure S55. ^{19}F NMR spectrum of $[\mathbf{2bZn}](\text{TFPB})_2$ (376 MHz, CD_3CN).

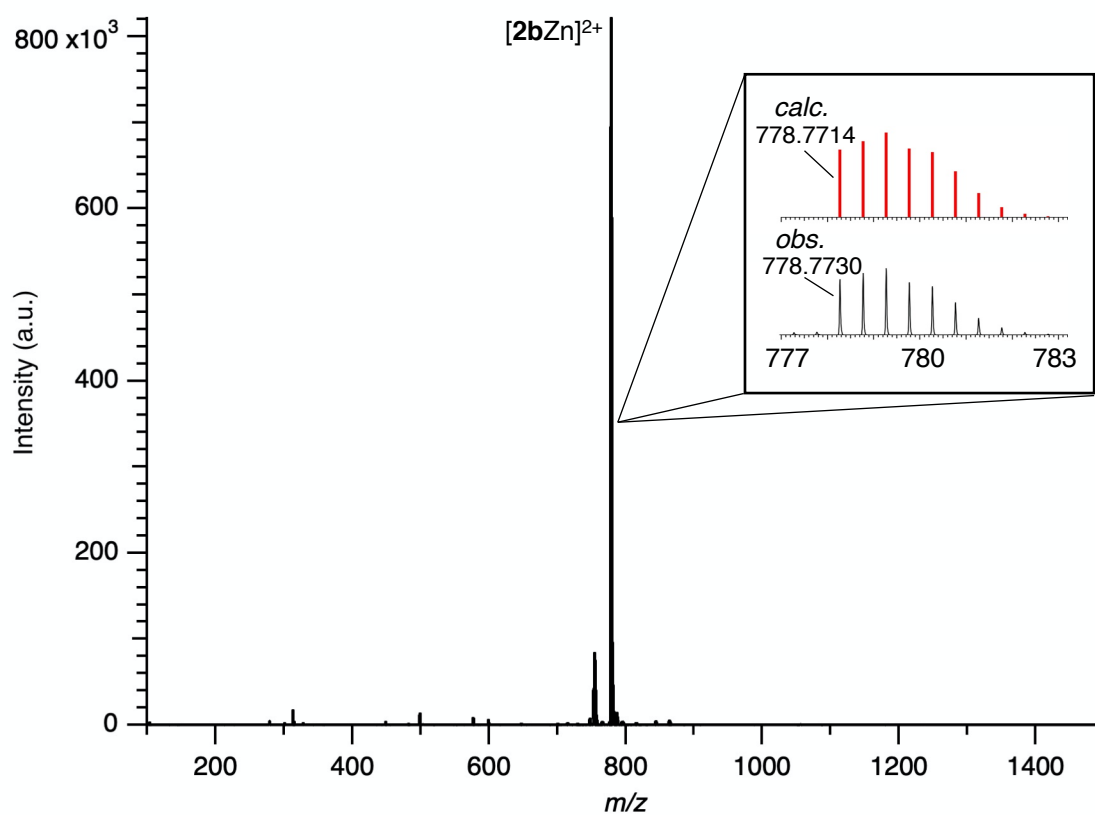


Figure S56. ESI mass spectrum of $[\mathbf{2bZn}](\text{TFPB})_2$ (solv. CH_3CN).

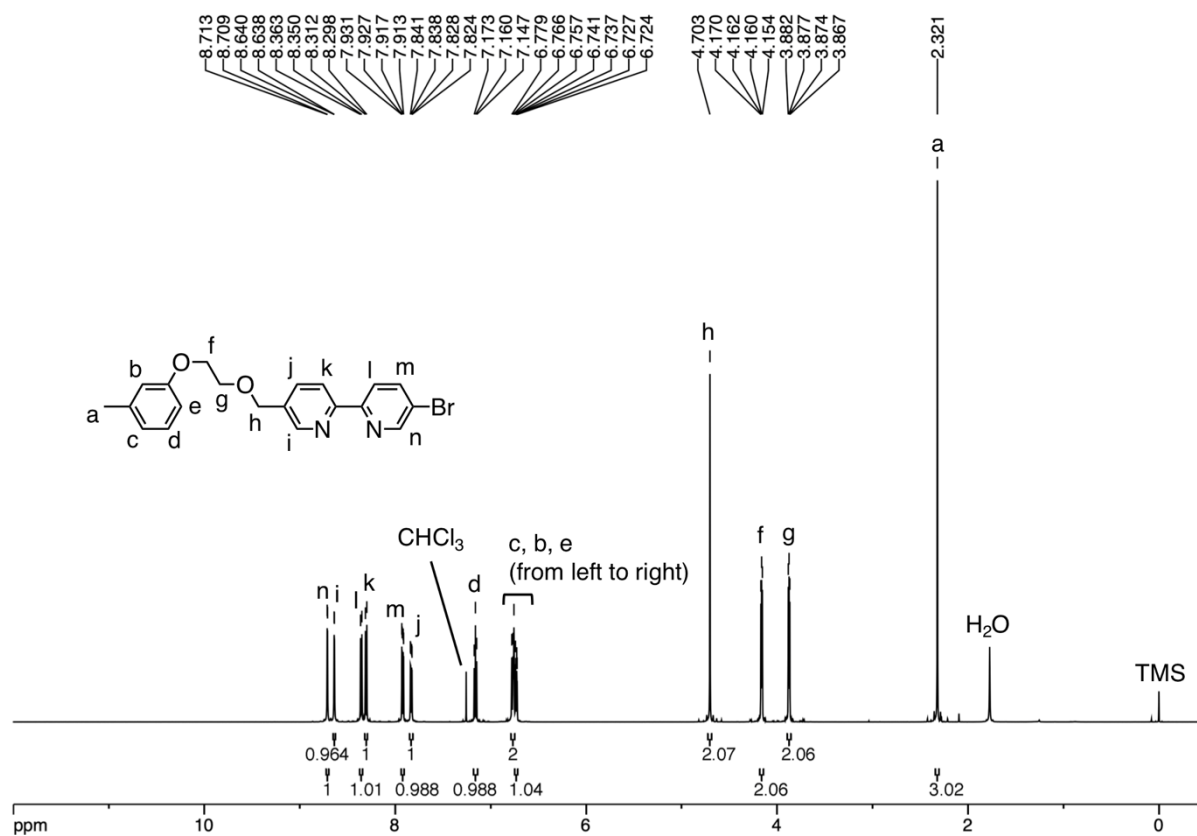


Figure S57. ¹H NMR spectrum of **3a** (600 MHz, CDCl₃).

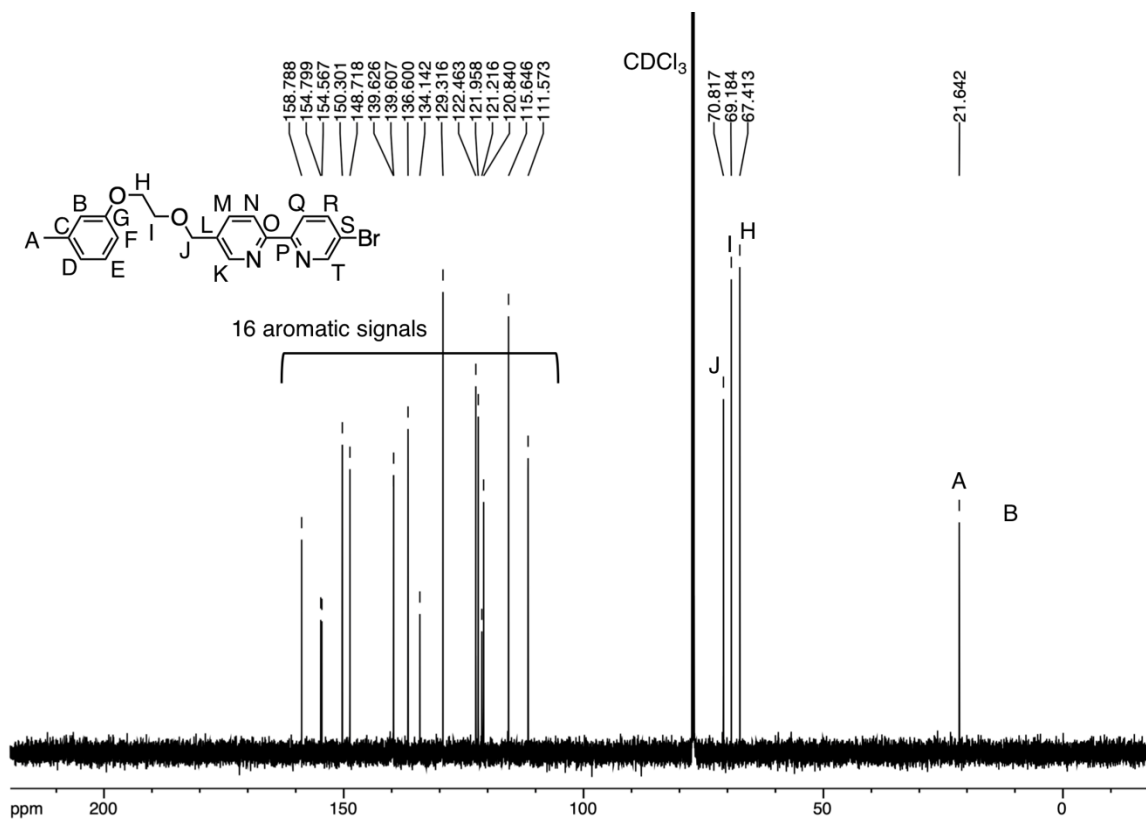


Figure S58. ¹³C NMR spectrum of **3a** (151 MHz, CDCl₃).

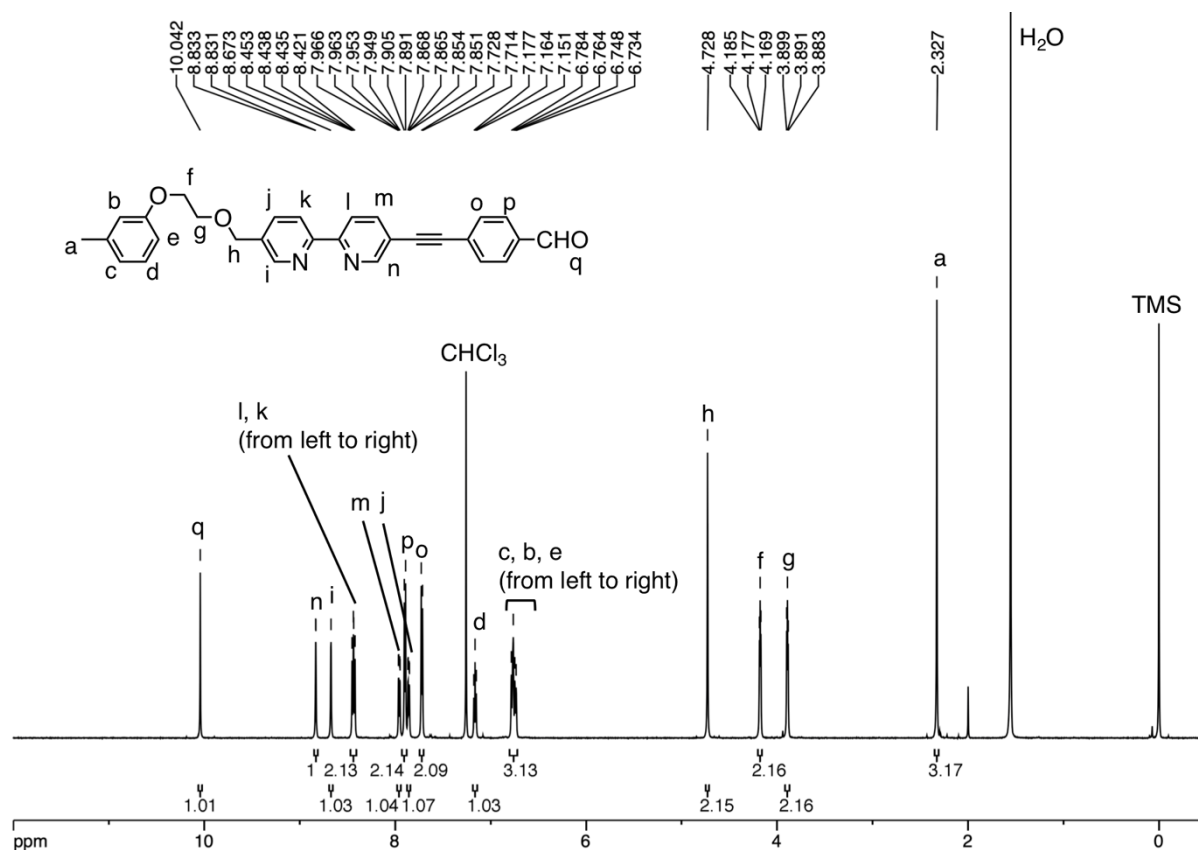


Figure S59. ^1H NMR spectrum of **3b** (600 MHz, CDCl_3).

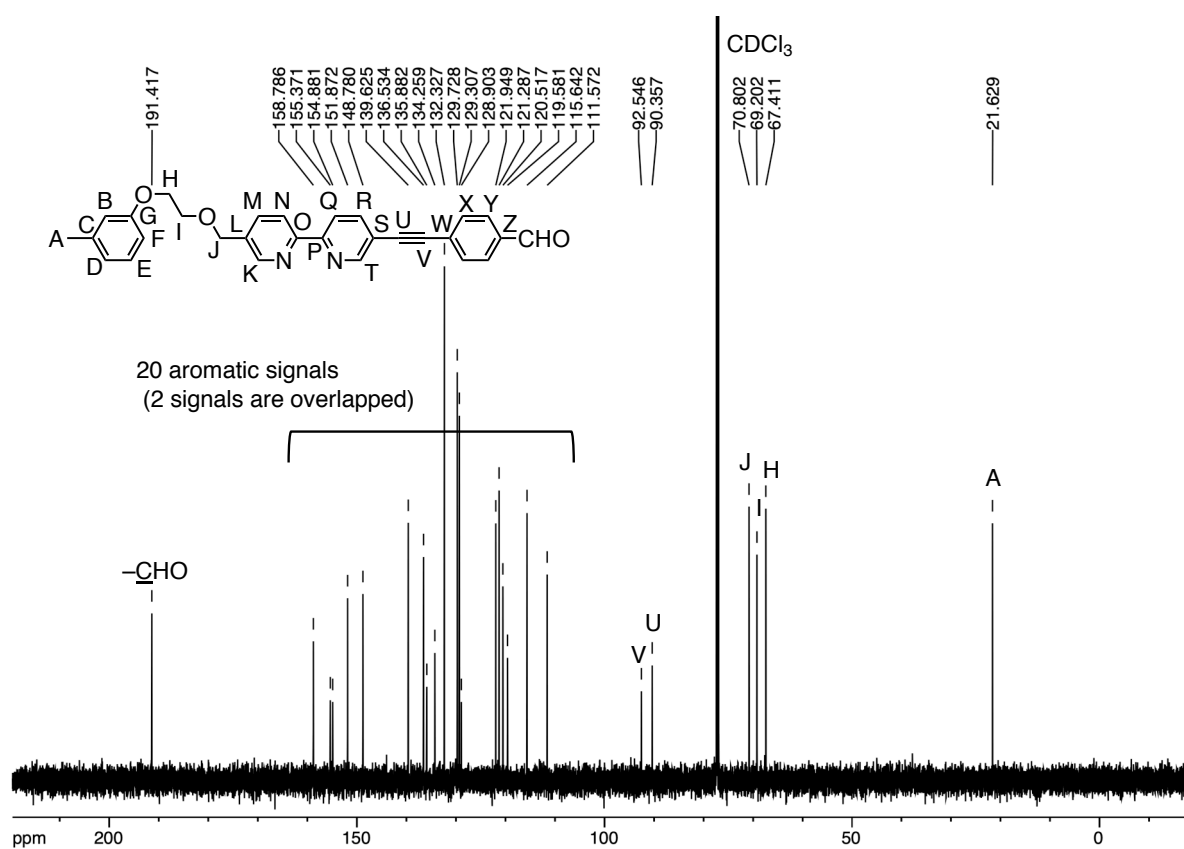


Figure S60. ^{13}C NMR spectrum of **3b** (151 MHz, CDCl_3).

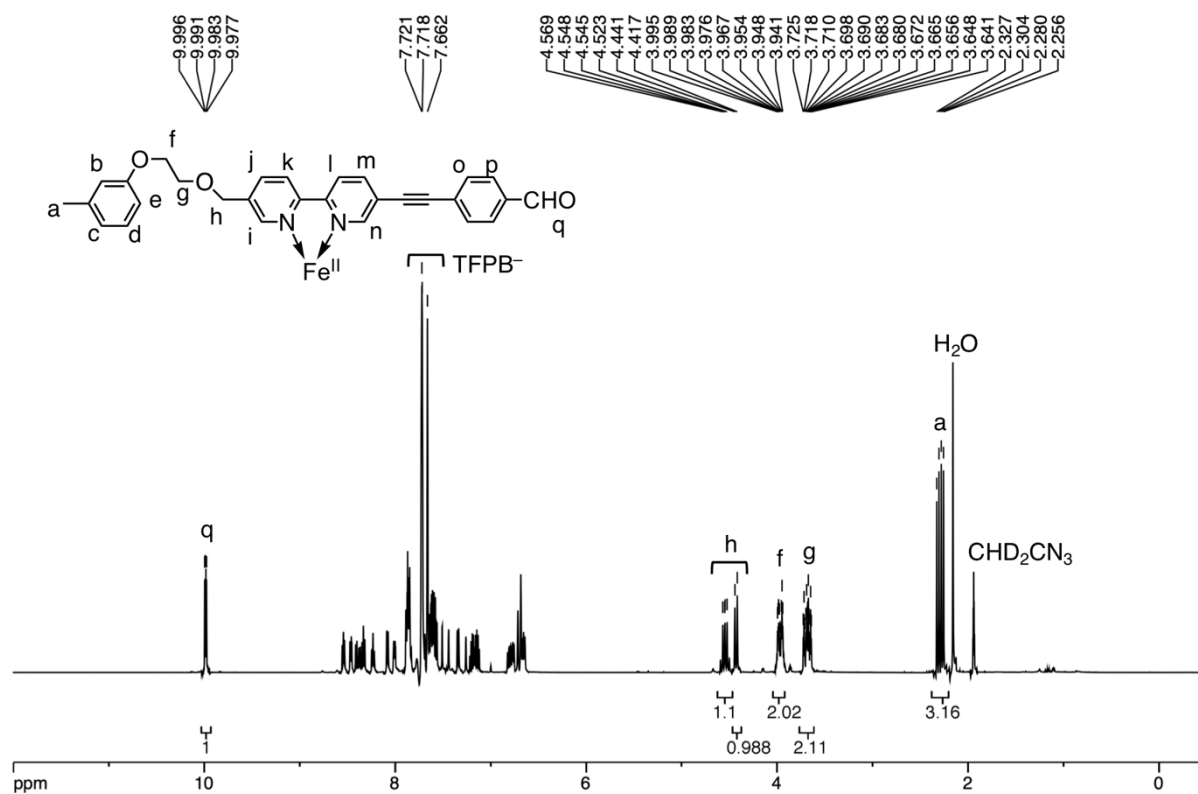


Figure S61. ¹H NMR spectrum of [(**3b**)₃Fe](TFPB)₂ (600 MHz, CD₃CN).

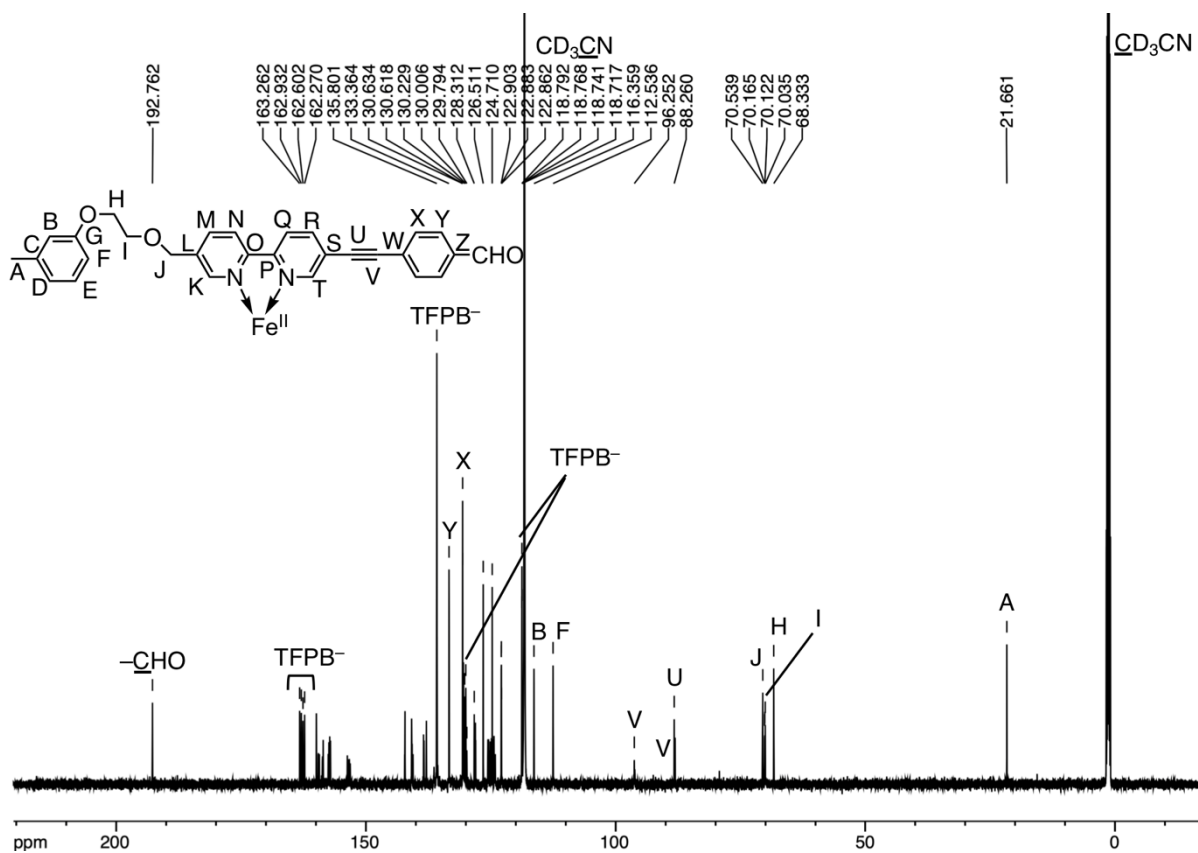


Figure S62. ¹³C NMR spectrum of [(**3b**)₃Fe](TFPB)₂ (151 MHz, CD₃CN).

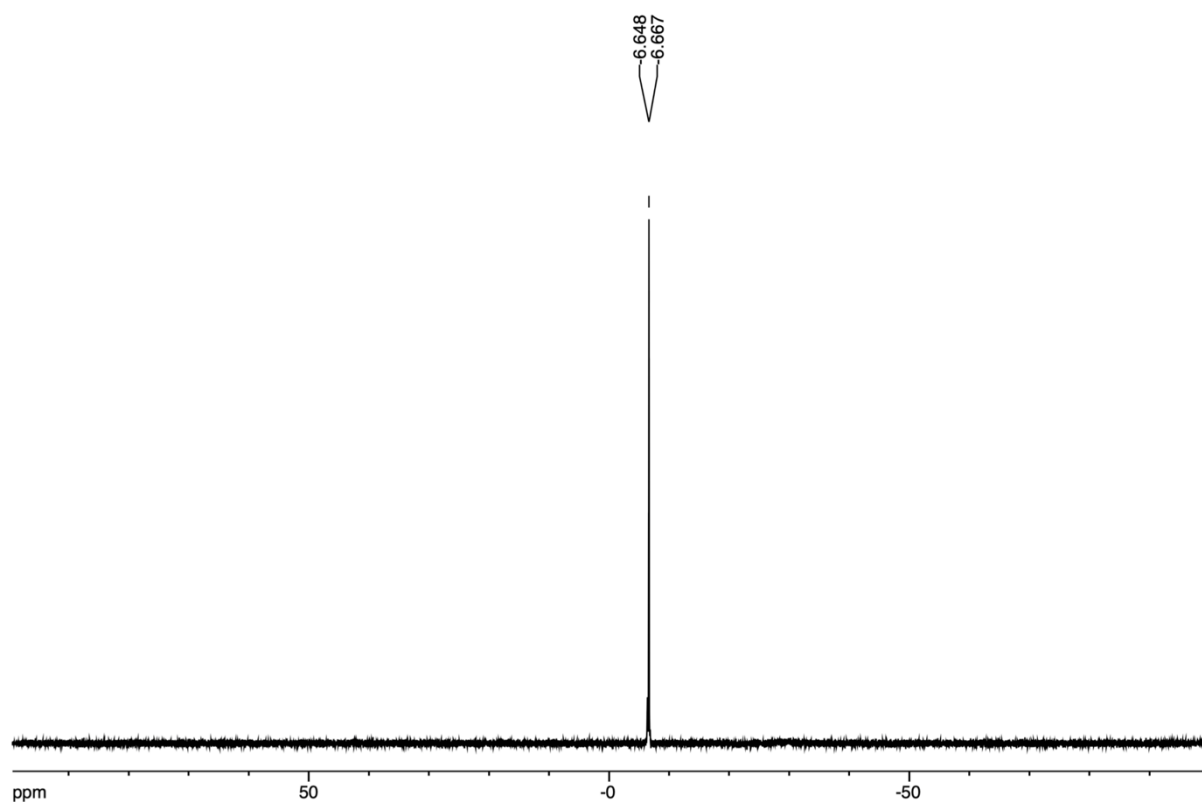


Figure S63. ^{11}B NMR spectrum of $[(\mathbf{3b})_3\text{Fe}](\text{TFPB})_2$ (192 MHz, CD_3CN).

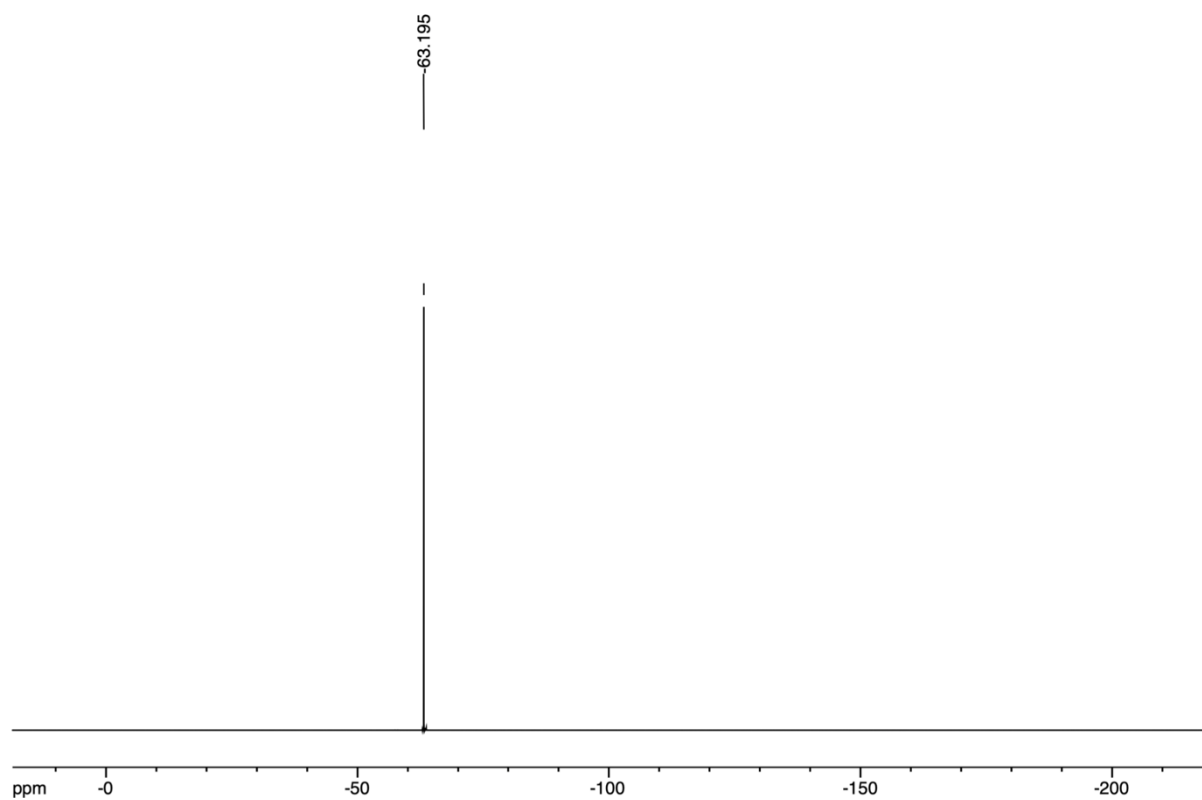


Figure S64. ^{19}F NMR spectrum of $[(\mathbf{3b})_3\text{Fe}](\text{TFPB})_2$ (376 MHz, CD_3CN).

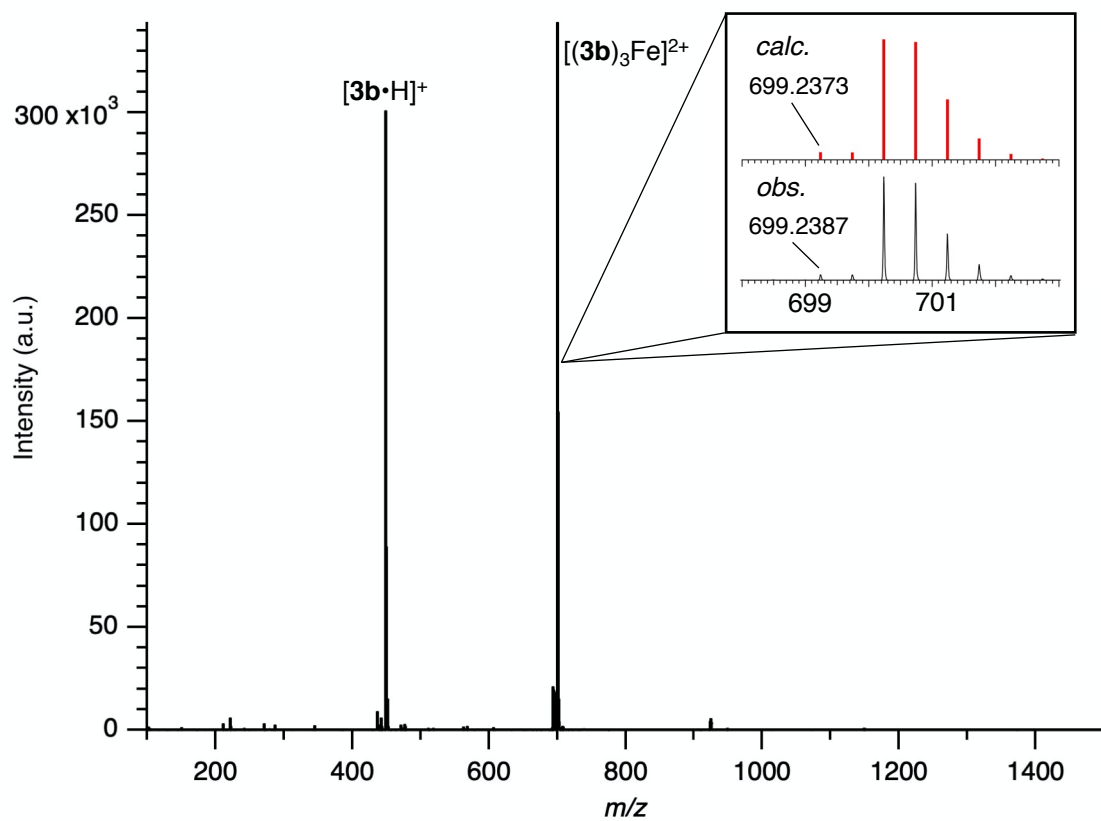


Figure S65. ESI mass spectrum of $[(\mathbf{3b})_3\text{Fe}](\text{TFPB})_2$ (solv. CH_3CN).

Solvent dependence in the *fac/mer*-isomerization of complexes

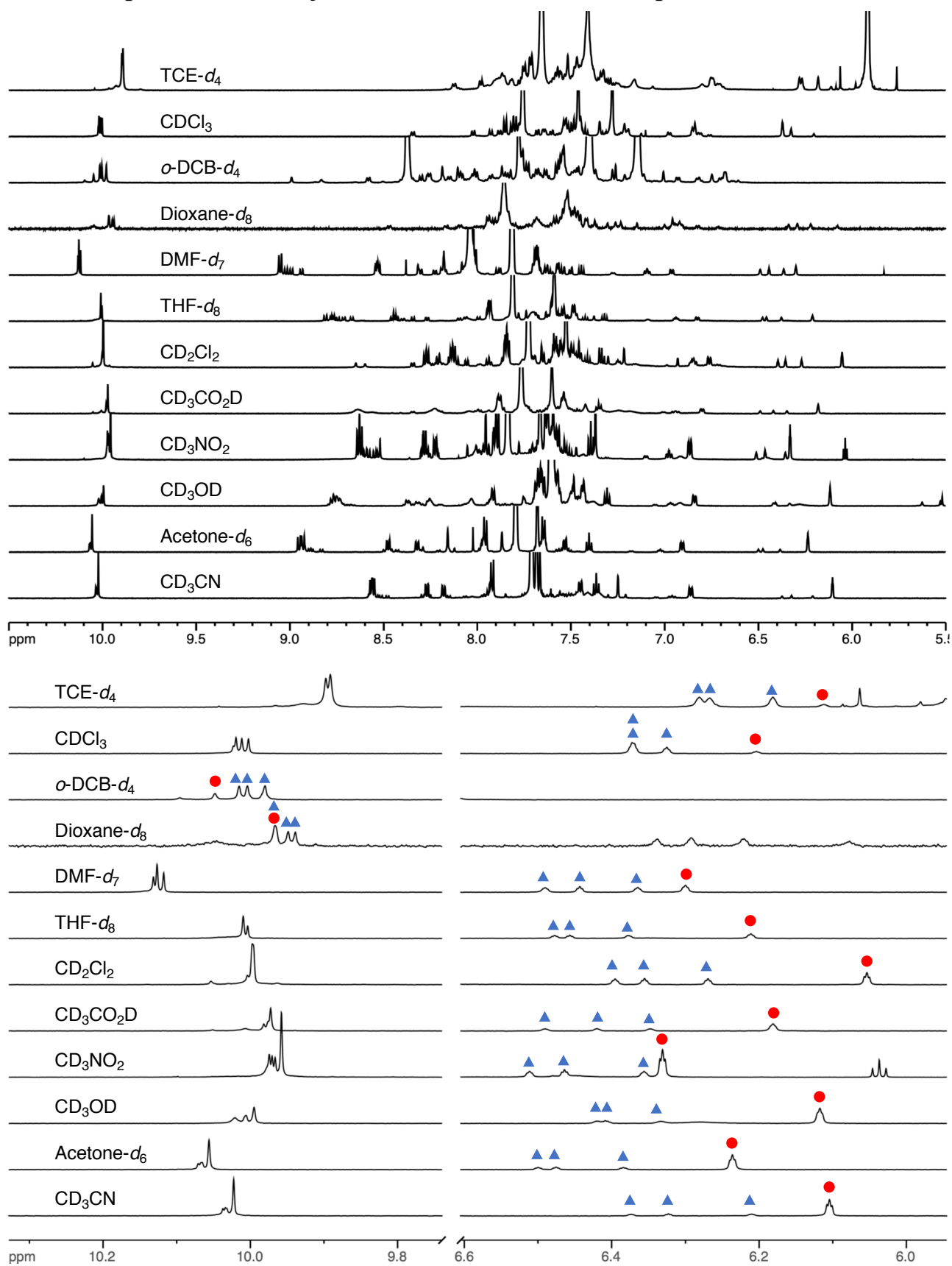


Figure S66. (Top) ¹H NMR spectra of [2bFe](TFPB)₂ in various solvents. (Bottom) Enlarged ¹H NMR spectra. Signals used for the determination of *fac/mer* ratios were denoted in the same way as Fig. 2a (600 MHz, 1.0 mM, measured in 12 h after dissolution).

Table S1. Solvent effects on the *fac/mer*-isomerization equilibrium of [2bFe](TFPB)₂ (298 K) and various parameters for solvents.^a

Solvent	<i>fac/mer</i> ^b	ΔG^c (kJ/mol)	ϵ	μ (D)	DN (kcal/mol)	AN (kcal/mol)	V_m (cm ³ /mol)	δ_d (MPa ^{1/2})	δ_p (MPa ^{1/2})	δ_h (MPa ^{1/2})
TCE- <i>d</i> ₂	10:90	5.5	8.0	1.31	–	–	105.2	18.8	5.1	5.3
CDCl ₃	10:90	5.5	4.7	1.1	4	23.1	80.7	17.8	3.1	5.7
<i>o</i> -DCB- <i>d</i> ₄	13:87	4.8	9.9	2.14	3	–	112.8	19.0	6.3	3.3
Dioxane- <i>d</i> ₈	20:80	3.4	2.2	0.4	14.8	10.8	85.7	17.5	1.8	7.4
DMF- <i>d</i> ₇	32:68	1.8	36.7	3.86	26.6	16.0	77.4	17.4	13.7	11.3
THF- <i>d</i> ₈	34:66	1.7	7.4	1.7	20	8.0	81.7	16.8	5.7	8.0
CD ₂ Cl ₂	40:60	1.1	8.9	1.5	1	20.4	63.9	18.2	6.3	6.1
CD ₃ CO ₂ D	53:47	–0.31	6.2	1.73	10	52.9	57.1	14.5	8.0	13.5
CD ₃ NO ₂	57:43	–0.70	36.7	3.57	2.7	20.5	54.3	15.8	18.8	5.1
CD ₃ OD	64:36	–1.5	32.6	1.71	19	41.3	40.7	15.1	12.3	22.3
Acetone- <i>d</i> ₆	69:31	–2.0	20.7	2.88	17	12.5	74.0	15.5	10.4	7.0
CD ₃ CN	71:29	–2.2	36	3.44	14.1	19.3	52.6	15.3	18.0	6.1

a: ϵ : dielectric constant^[S8a]; μ : dipole moment^[S8a]; DN: donor number^[S8a, b]; AN: acceptor number^[S8b]; V_m : molar volume^[S8c]; δ_d , δ_p , and δ_h : the terms of Hansen solubility parameters^[S8c]. δ_d : the dispersion term; δ_p : the dipole interaction term; δ_h : the hydrogen bonding term.

b: Determined from signals of proton *f* (pivot unit) (For *o*-DCB-*d*₄ and dioxane-*d*₈, signals of proton *r* (formyl group) were used. see **Fig. S46**).

c: $\Delta G = -RT \ln([fac]/[mer])$ (R : gas constant, T : temperature, $[fac]$: concentration of *fac*-isomer, $[mer]$: concentration of *mer*-isomer).

van't Hoff analysis of the *fac/mer*-isomerization in various solvents

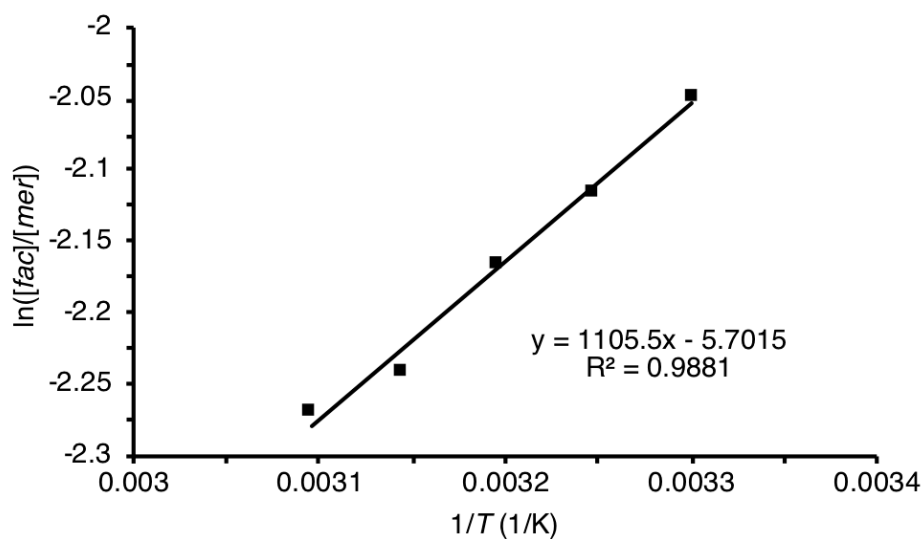


Figure S67. A van't Hoff plot of the *fac/mer* ratio of $[2bFe](TFPB)_2$ in $CDCl_3$.

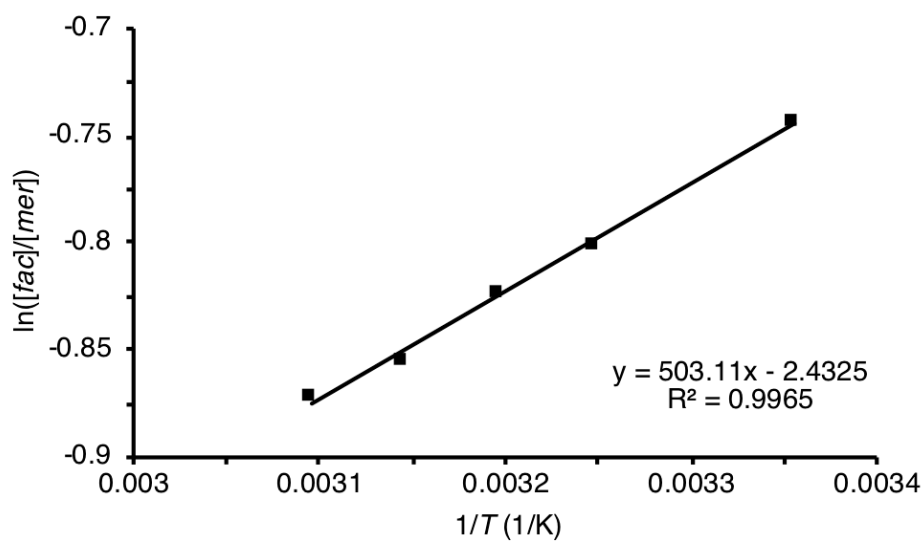


Figure S68. A van't Hoff plot of the *fac/mer* ratio of $[2bFe](TFPB)_2$ in $DMF-d_7$.

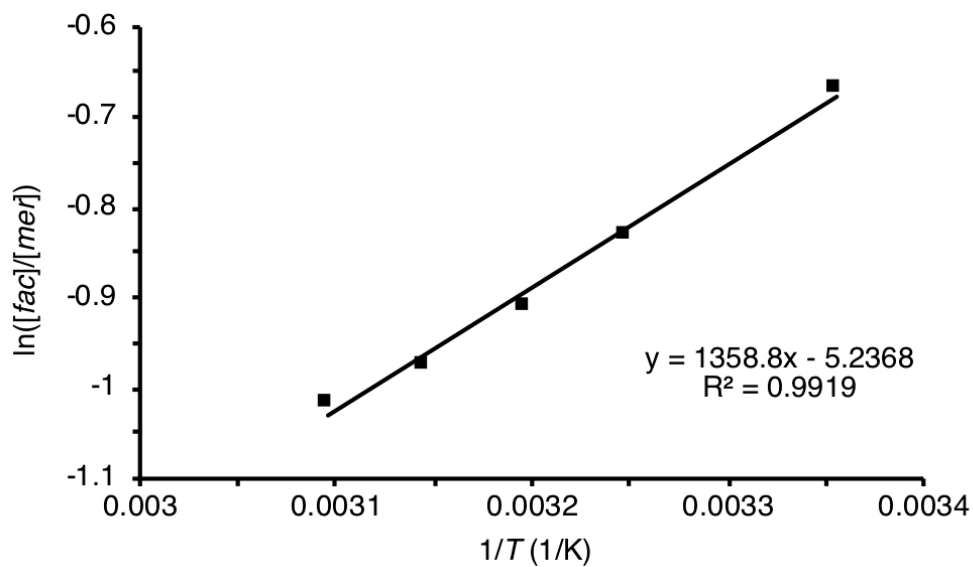


Figure S69. A van't Hoff plot of the *fac/mer* ratio of $[2bFe](TFPB)_2$ in THF- d_8 .

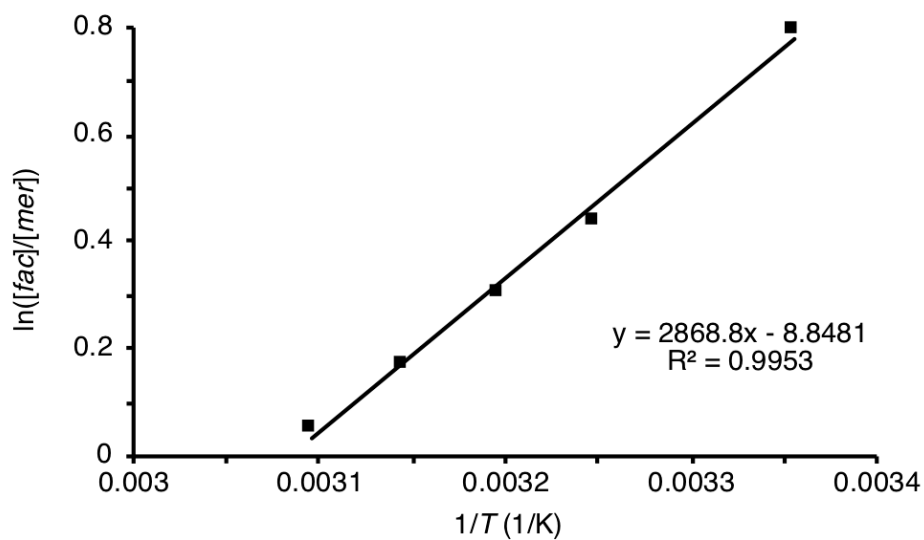


Figure S70. A van't Hoff plot of the *fac/mer* ratio of $[2bFe](TFPB)_2$ in acetone- d_6 .

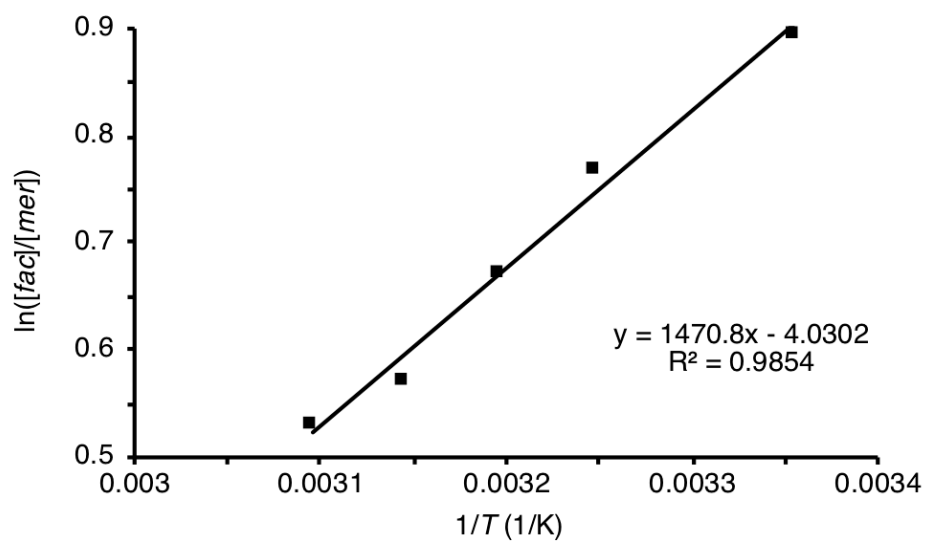


Figure S71. A van't Hoff plot of the *fac/mer* ratio of $[2bFe](TFPB)_2$ in CD_3CN .

DOSY NMR spectra of $[2bFe](TFPB)_2$ in CD_3CN or $CDCl_3$

The hydrodynamic radii of $[2bFe](TFPB)_2$ were evaluated by 1H DOSY measurements (Table S2, Fig. S72, S73). The hydrodynamic radii of the *facial* isomer and the *meridional* isomers in the same solvent were almost the same. However, the hydrodynamic radius of $[2bFe]^{2+}$ was approximately 9 Å in CD_3CN , but 14–15 Å in $CDCl_3$. Difference in hydrodynamic radius between CD_3CN and $CDCl_3$ was approximately 5 Å, which was roughly corresponding to the hydrodynamic radius of $TFPB^-$ in CD_3CN (5.7 Å). It was suggested that the ion pair of $[2bFe]^{2+}$ and $TFPB^-$ formed in $CDCl_3$, while it did not in CD_3CN . Thus, it must be cautioned that the solvent dependency of *fac/mer* isomerism discussed in this paper contains the effect of ion pair formation between $[2bFe]^{2+}$ and $TFPB^-$, and should be treated as the result of ionic complex $[2bFe](TFPB)_2$ as a whole.

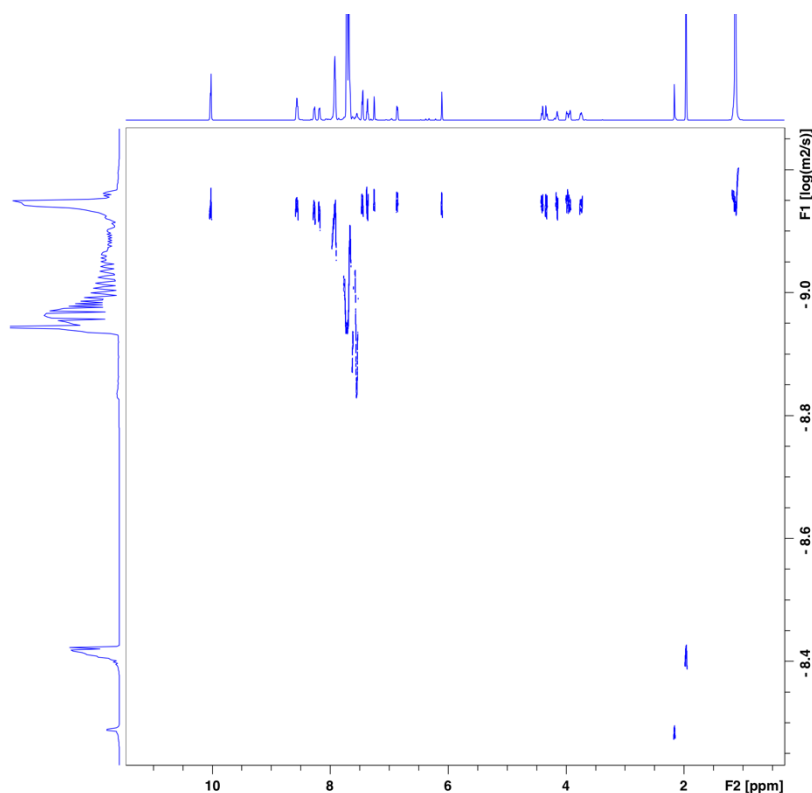


Figure S72. 1H DOSY NMR spectrum of $[2bFe](TFPB)_2$ (600 MHz, CD_3CN).

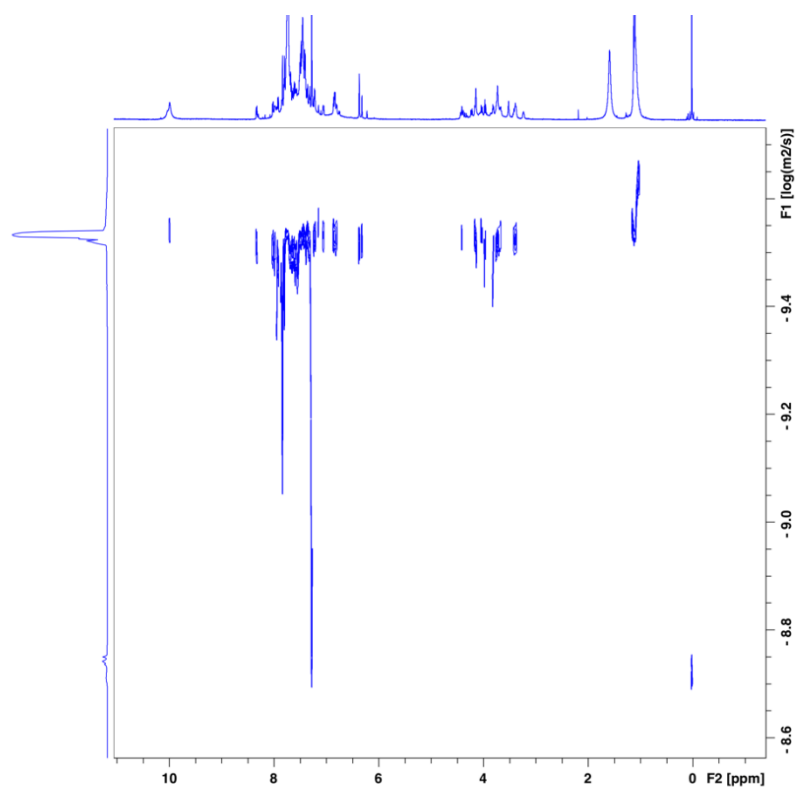


Figure S73. ^1H DOSY NMR spectrum of $[\mathbf{2bFe}](\text{TFPB})_2$ (600 MHz, CDCl_3).

Table S2. Diffusion constants and hydrodynamic radii of $[\mathbf{2bFe}](\text{TFPB})_2$ in CD_3CN and CDCl_3 .

Solvent	Species	Diffusion constant (m^2/s)	Hydrodynamic radius (\AA)
CD_3CN	<i>fac</i> -isomer	6.9×10^{-10}	9.3
	<i>mer</i> -isomer	7.2×10^{-10}	8.9
	TFPB^-	1.1×10^{-9}	5.7
CDCl_3	<i>fac</i> -isomer	2.8×10^{-10}	15
	<i>mer</i> -isomer	2.9×10^{-10}	14
	TFPB^-	2.9×10^{-10}	14

Comparison of solvent dependence of [2bFe](TFPB)₂ and the other complexes

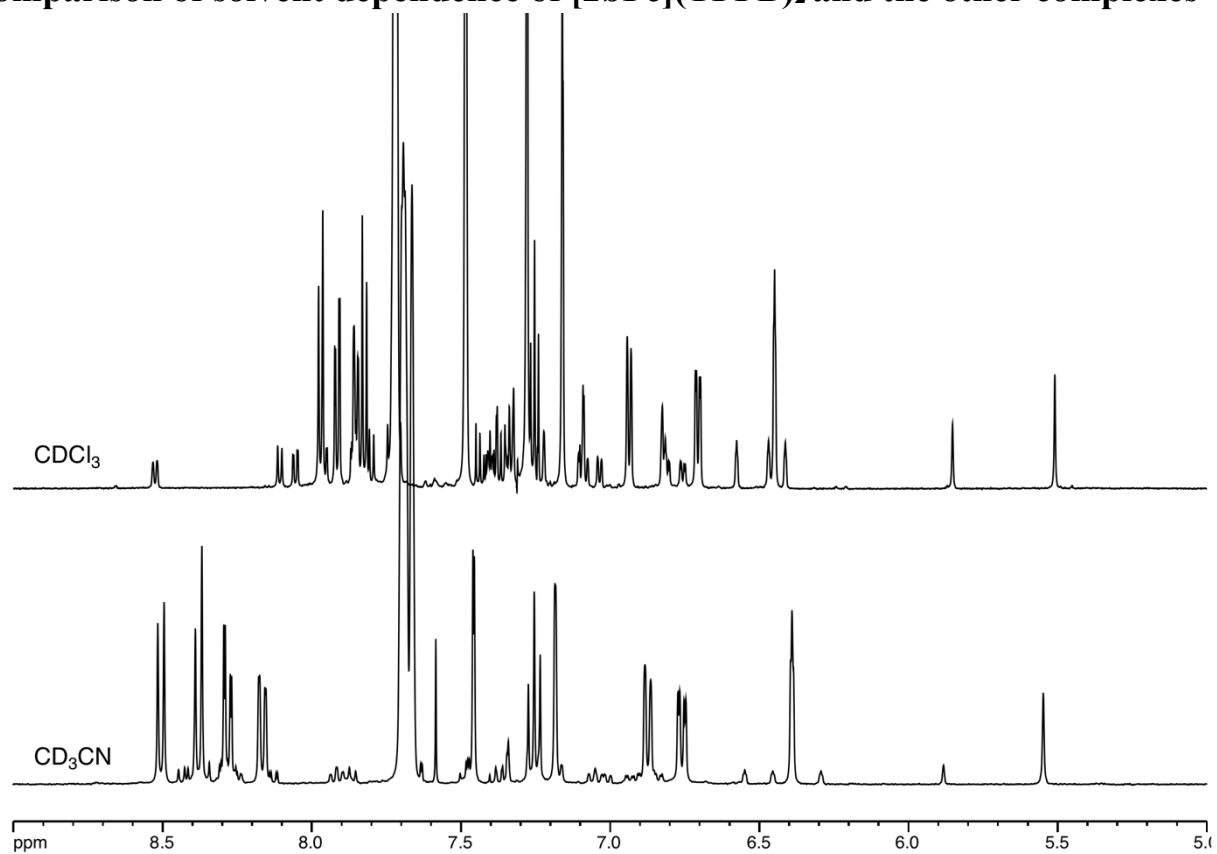


Figure S74. ¹H NMR spectra of [1aFe](TFPB)₂ (600 MHz).

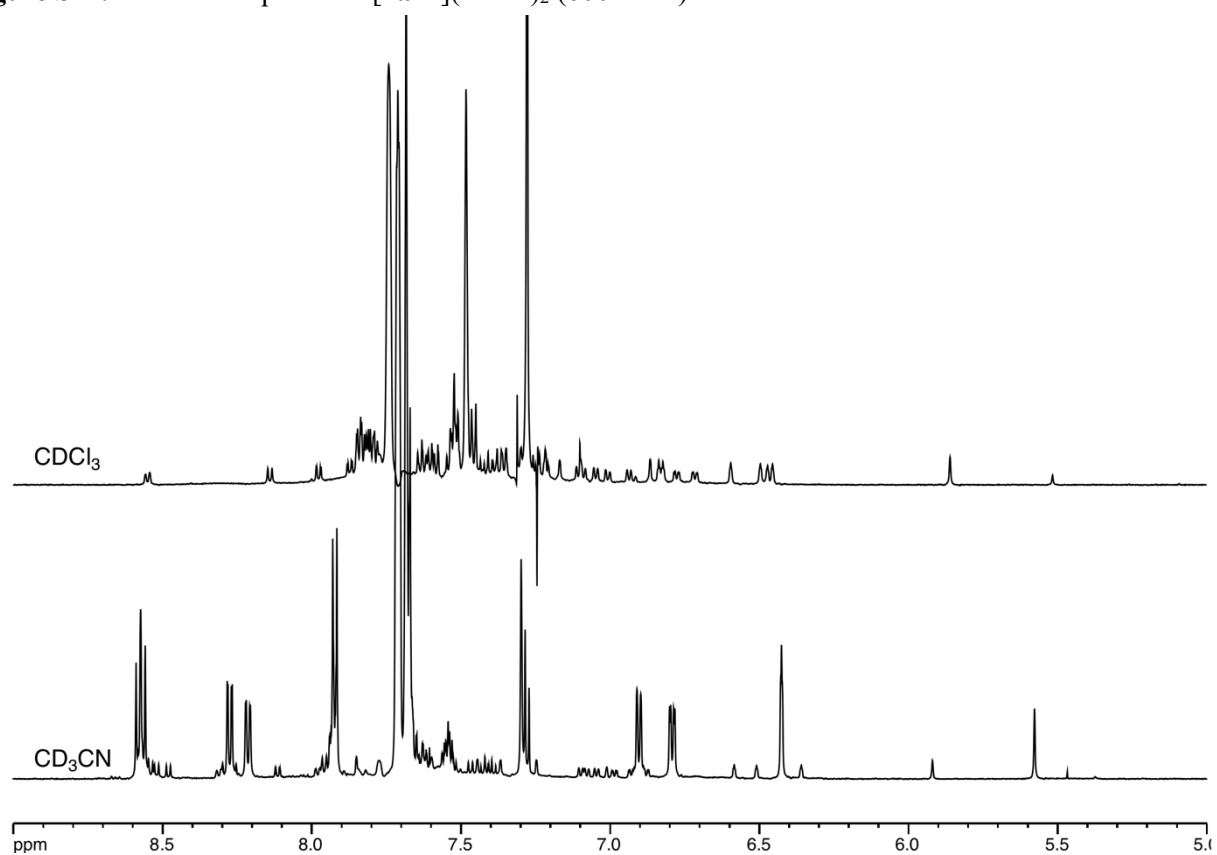


Figure S75. ¹H NMR spectra of [1bFe](TFPB)₂ (600 MHz).

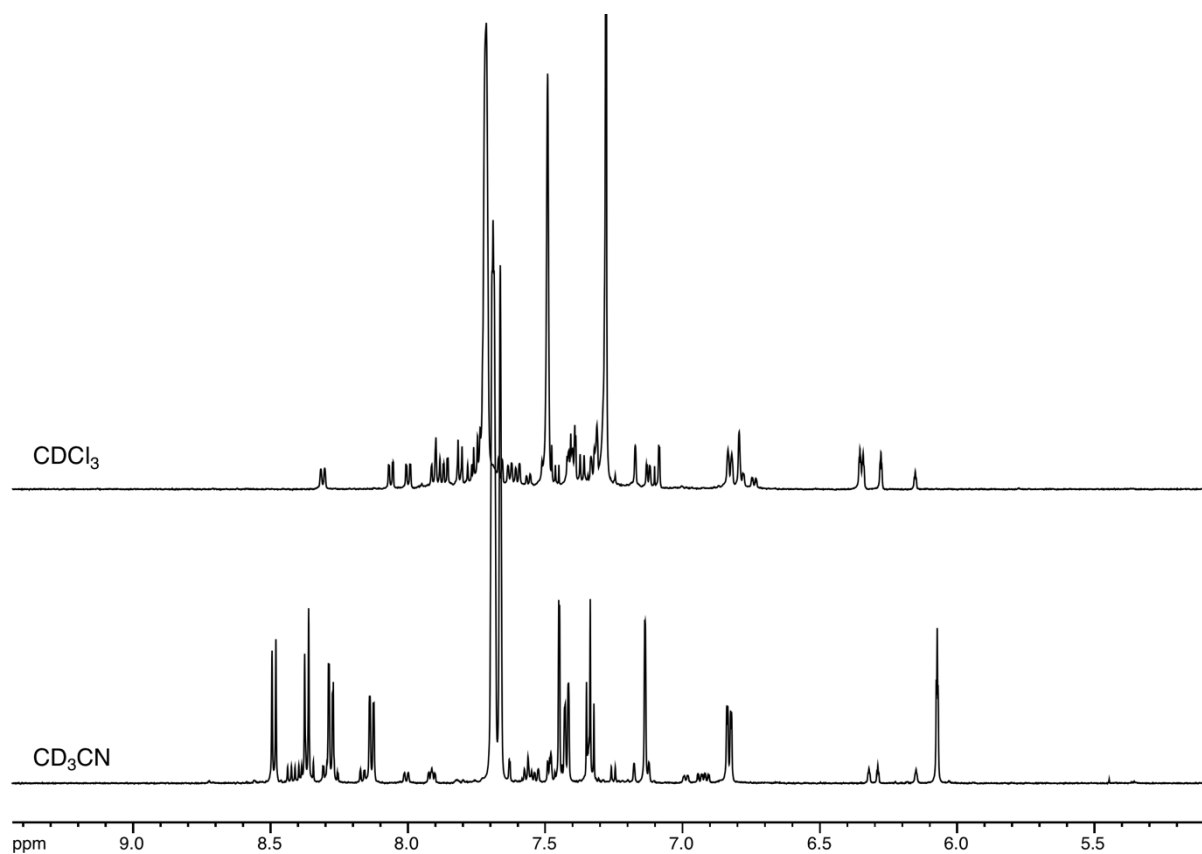


Figure S76. ¹H NMR spectra of [2aFe](TFPB)₂ (600 MHz).

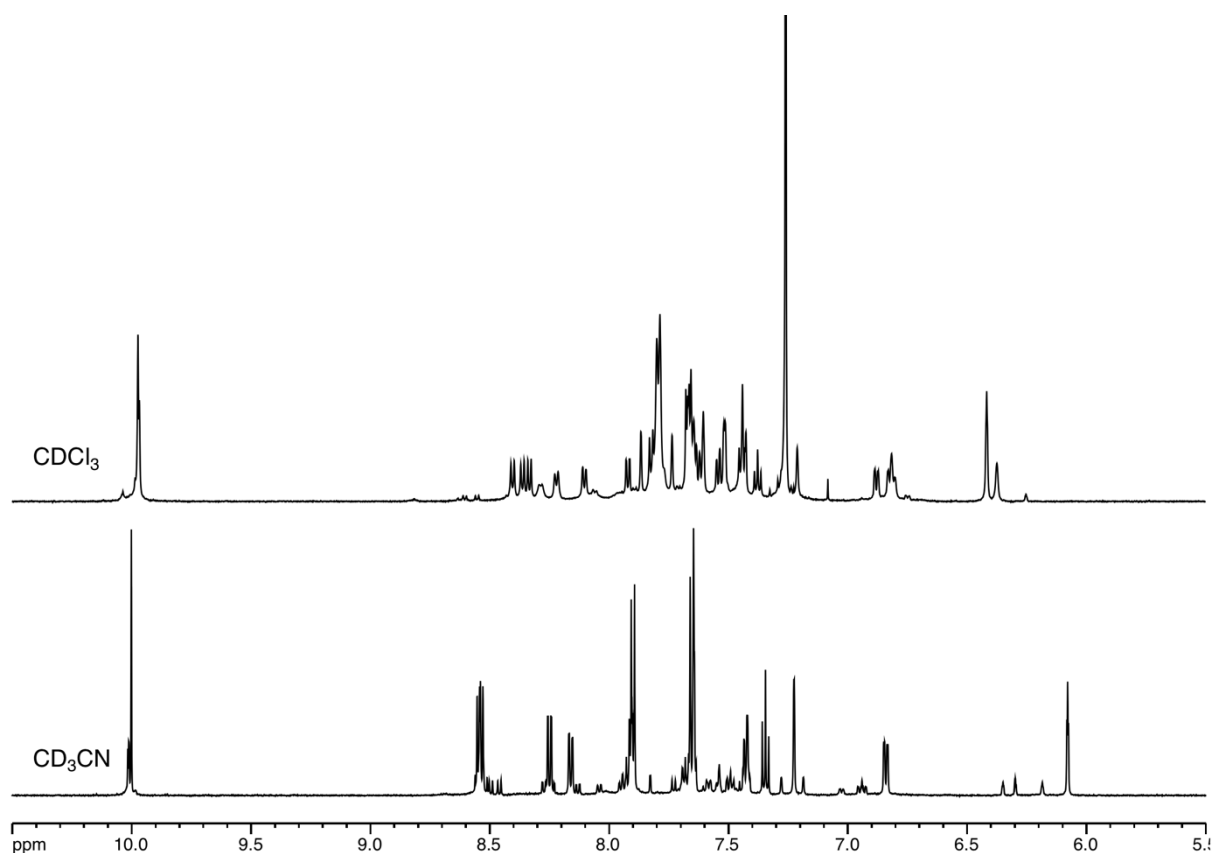


Figure S77. ¹H NMR spectra of [2bFe](PF₆)₂ (600 MHz).

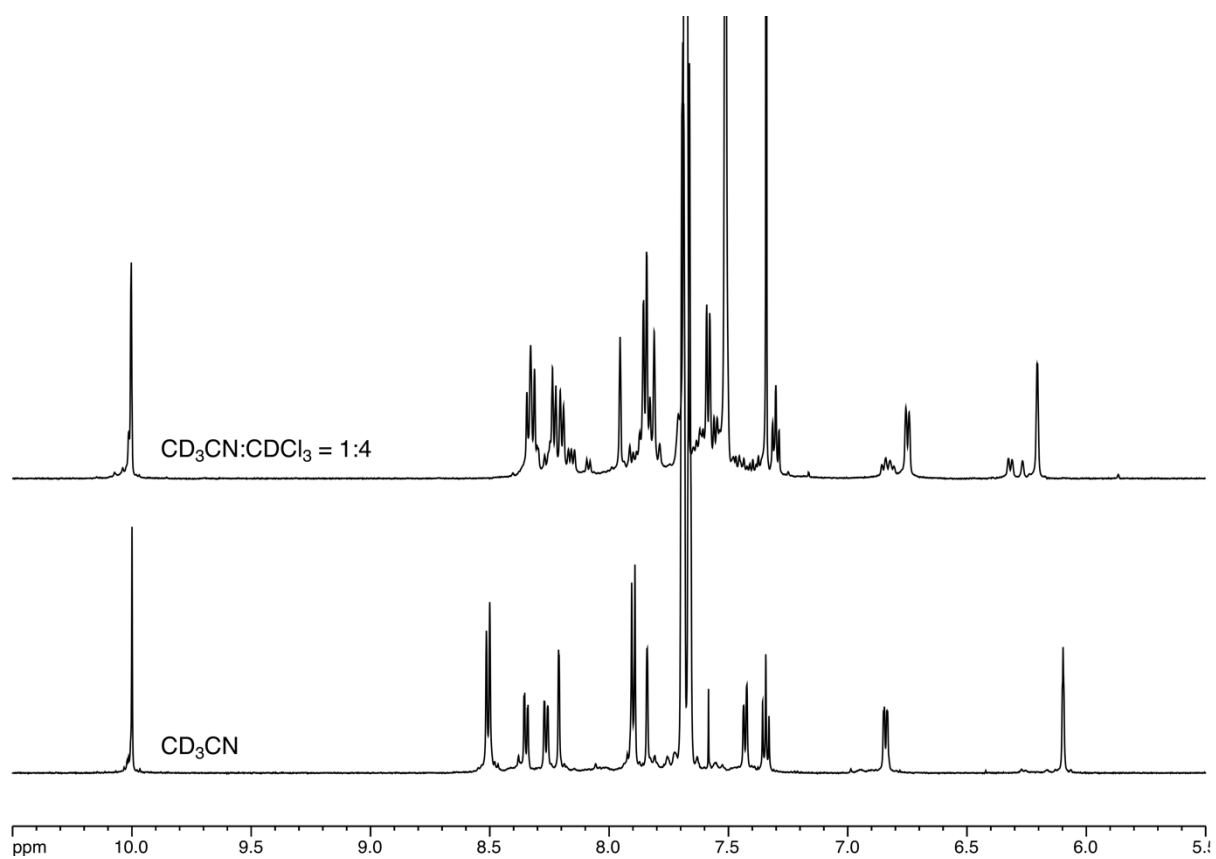


Figure S78. ^1H NMR spectra of $[\mathbf{2bZn}](\text{TFPB})_2$ (600 MHz).

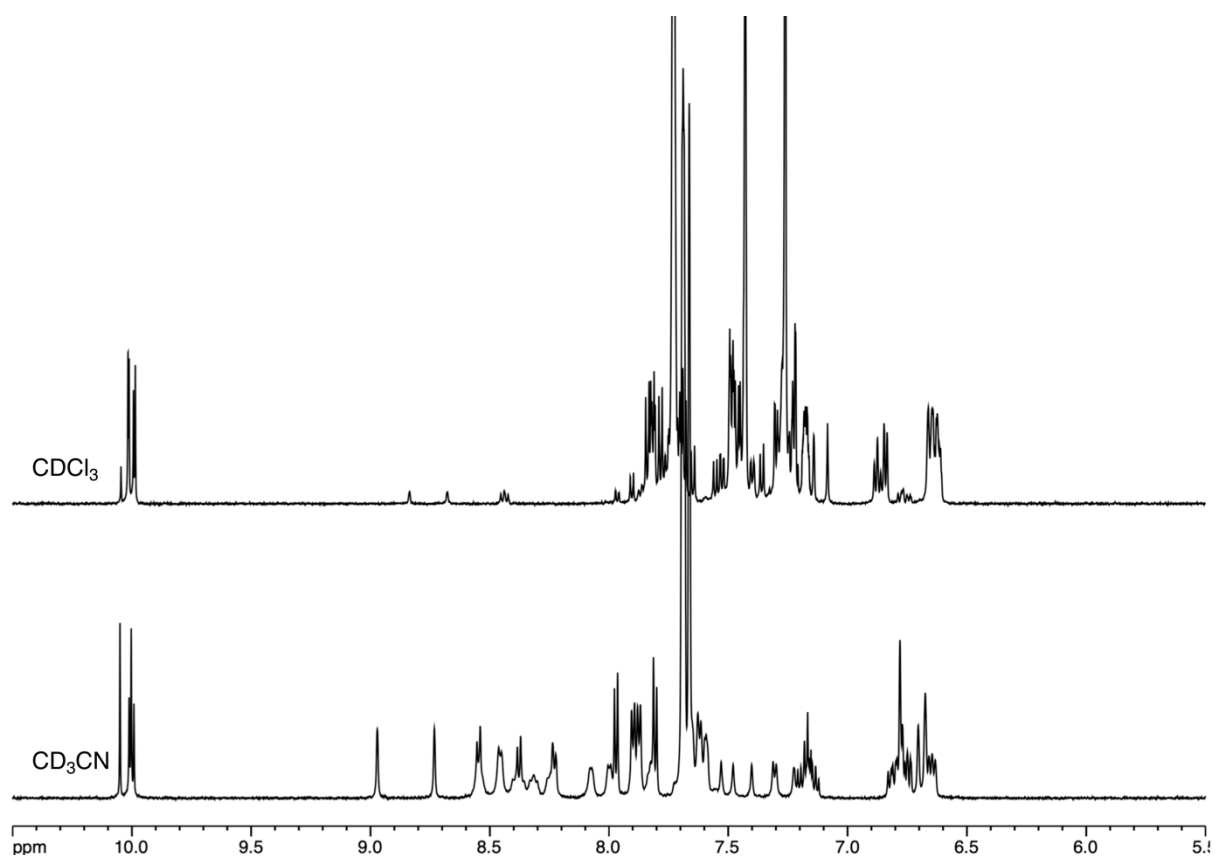


Figure S79. ^1H NMR spectra of $[(\mathbf{3b})_3\text{Fe}](\text{TFPB})_2$ (600 MHz).

Regression analyses with various solvent parameters

Table S3. Results of regression analyses between ΔG of (*mer* to *fac* isomerization) of $[\mathbf{2bFe}](\text{TFPB})_2$ and thermodynamic parameters of solvents. See also Table S1.

Parameter	(Multiple) correlation coefficient R	adjusted R-squared R_{adj}^2	Standard error σ (kJ/mol)
ε	-0.64	0.34	2.3
μ	-0.54	0.23	2.5
DN	-0.29	-0.015	2.7
AN	0.26	-0.049	2.5
V_m	0.83	0.66	1.6
δ_d	0.87	0.72	1.5
δ_p	-0.73	0.48	2.0
δ_h	-0.42	0.10	2.7
ε, μ	0.64	0.27	2.4
DN, AN	0.33	-0.14	2.7
V_m, δ_d	0.89	0.75	1.4
$\delta_d, \delta_p, \delta_h$	0.91	0.77	1.4
δ_d, δ_p	0.91	0.79	1.3

R_{adj}^2 was defined as this equation (R : the correlation coefficient, n : the sample size, p : the total number of explanatory variables).

$$R_{\text{adj}}^2 = 1 - (1 - R^2) \frac{n - 1}{n - p - 1}$$

R_{adj}^2 is one of the extended coefficients of determination considered the number of explanatory variables and can be compared even when different numbers of variables are used.

X-ray diffraction analysis

A single crystal of $[\mathbf{1aFe}](\text{PF}_6)_2 \cdot 4(\text{CH}_3)_2\text{CO}$ suitable for the X-ray diffraction analysis was obtained by the slow diffusion of diethyl ether vapor into an acetone solution of $[\mathbf{1aFe}](\text{PF}_6)_2$.

Crystal data for $[\mathbf{1aFe}](\text{PF}_6)_2 \cdot 4(\text{CH}_3)_2\text{CO}$: $\text{C}_{70}\text{H}_{73}\text{Br}_3\text{FeN}_6\text{O}_{10}\text{P}_2$, $F_w = 1743.86$, hexagonal red plate, $0.14 \times 0.17 \times 0.02 \text{ mm}^3$, rhombohedral, space group $R\bar{3}$, $a = 13.982(3) \text{ \AA}$, $c = 67.108(15) \text{ \AA}$, $V = 11362(6) \text{ \AA}^3$, $Z = 6$, $R_1 = 0.0643$, $wR_2 = 0.1997$, $\text{GOF} = 1.068$. CCDC 2067281.

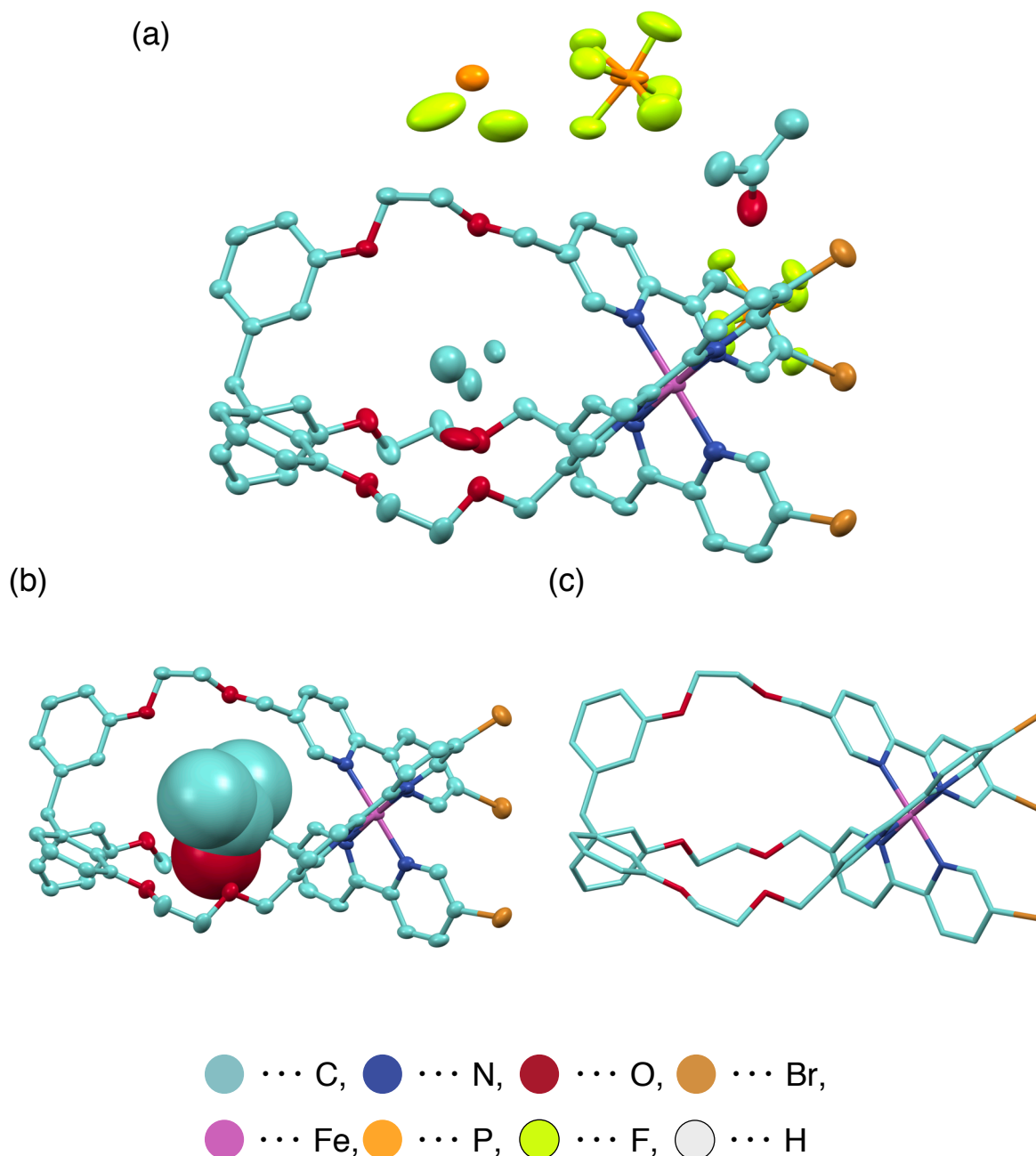


Figure S80. The structure of $[\mathbf{1aFe}](\text{PF}_6)_2 \cdot 2(\text{CH}_3)_2\text{CO} \cdot 2\text{PF}_6$ determined by X-ray diffraction analysis. Hydrogen atoms were omitted for clarity. a) An ellipsoidal model (50% probability). One of the disordered structures is shown. b) An ellipsoid model for $[\mathbf{1aFe}]^{2+}$ and a space-filling model for the included acetone. c) A stick model of $[\mathbf{1aFe}]^{2+}$.

Cycle characteristics of exchanging solvent

[**2b**Fe](TFPB)₂ (2.32 mg, 1.25 μmol) was dissolved in CD₃CN (500 μL). The solution was heated at 50 °C for 12 h, cooled to r.t., and then ¹H NMR spectrum was measured. After the measurement, the solution was concentrated *in vacuo*, and the residue was dissolved in CDCl₃ (500 μL). The solution was heated at 50 °C for 12 h, cooled to r.t., and then ¹H NMR spectrum was measured. These operations were repeated for 5 times with the same sample.

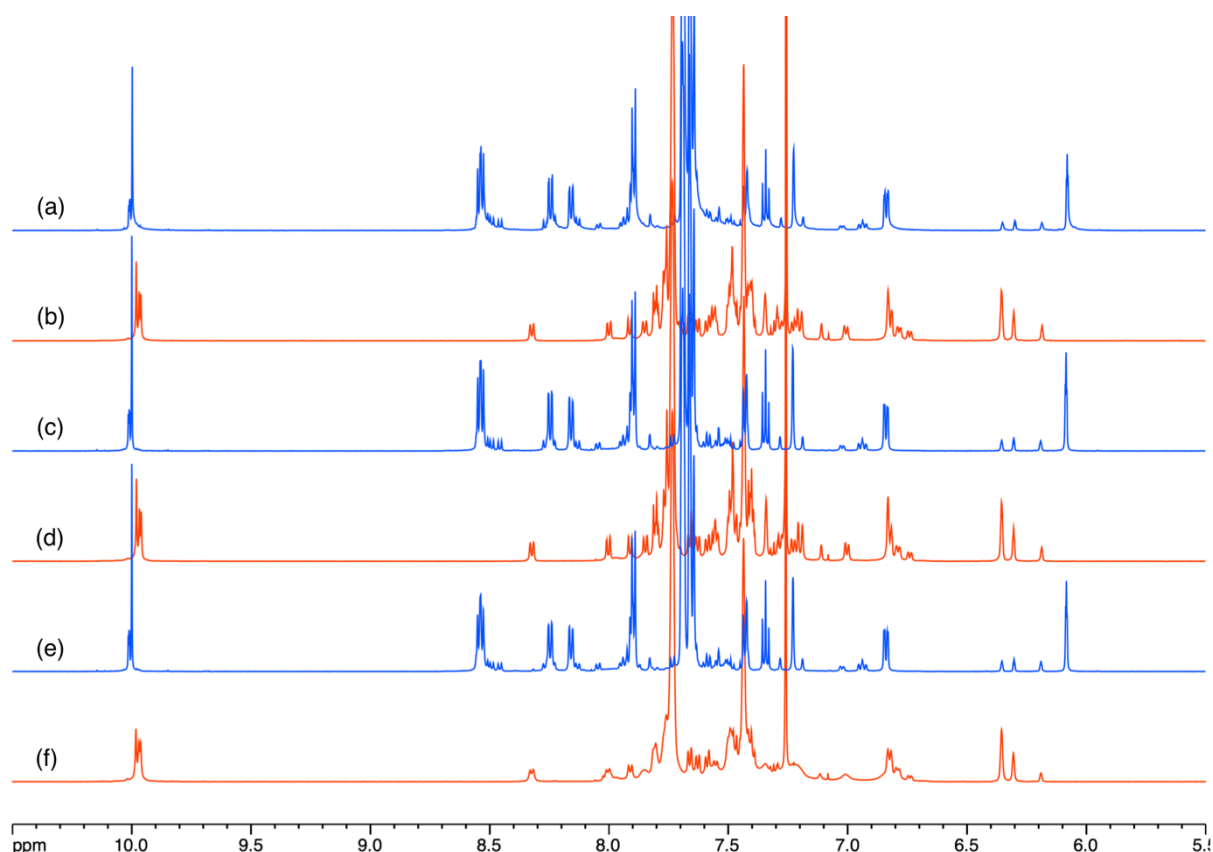


Figure S81. ¹H NMR spectra of [**2b**Fe](TFPB)₂ at 1st, 2nd, and 5th cycle in the solvent exchange experiment (600 MHz). (a) 1st cycle in CD₃CN. (b) 1st cycle in CDCl₃. (c) 2nd cycle in CD₃CN. (d) 2nd cycle in CDCl₃. (e) 5th cycle in CD₃CN. (f) 5th cycle in CDCl₃.

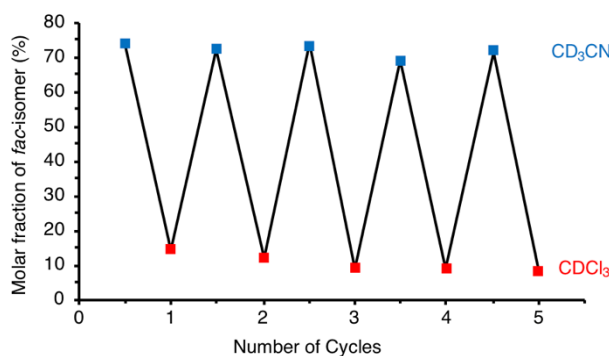


Figure S82. Reversibility of the *fac/mer* isomerization of [**2b**Fe](TFPB)₂.

Synthesis of imine-linked dimer and tetramer

Synthesis of **D-PPD**(PF₆)₄

To a solution of [2**b**Fe](PF₆)₂ (0.92 mg, 0.50 μmol) in a mixed solvent of CD₃CN (250 μL) and CDCl₃ (250 μL) was added a solution of 1,3-propanediamine (60.0 mM, 12.5 μL) in a mixed solvent of CD₃CN/CDCl₃ = 1/1. The mixture was heated at 50 °C for 24 h, and then was subjected to the spectroscopic measurements.

D-PPD(PF₆)₄: ¹H NMR (600 MHz, CD₃CN/CDCl₃ = 1/1) δ 8.53 (d, *J* = 8.4 Hz, 6H), 8.52 (d, *J* = 8.4 Hz, 6H), 8.31 (s, 6H), 8.22 (dd, *J* = 8.4, 1.8 Hz, 6H), 8.17 (d, *J* = 8.4 Hz, 6H), 7.71 (d, *J* = 7.8 Hz, 12H), 7.53–7.49 (m, 18H), 7.45 (d, *J* = 7.8 Hz, 6H), 7.32 (dd, *J* = 7.8, 7.8 Hz, 6H), 7.19 (br s, 6H), 6.80 (dd, *J* = 7.8, 1.8 Hz, 6H), 6.12 (br s, 6H), 4.39 (dd, *J* = 64.2, 12.6 Hz, 12H) 4.17–4.11 (m, 6H), 3.99–3.92 (m, 12H), 3.77–3.72 (m, 6H), 3.68 (t, *J* = 5.4 Hz, 12H), 1.15–1.09 (m, 42H); ¹⁹F NMR (376 MHz, CD₃CN/CDCl₃ = 1/1) δ –72.8 (d, ¹*J*_{F-P} = 709 Hz); ³¹P NMR (243 MHz, CD₃CN/CDCl₃ = 1/1) δ –144.5 (d, ¹*J*_{P-F} = 709 Hz); HRMS (ESI): *m/z* calcd for (**D-PPD**⁴⁺): 801.8202; found: 801.8176.

Synthesis of **D-CHZ**(PF₆)₄

To a solution of [2**b**Fe](PF₆)₂ (0.90 mg, 0.49 μmol) in a mixed solvent of CD₃CN (250 μL) and CDCl₃ (250 μL) was added a solution of carbohydrazide in water (375 mM, 2.0 μL). The mixture was heated at 50 °C for 24 h, and then was subjected to the spectroscopic measurements.

D-CHZ(PF₆)₄: ¹H NMR (600 MHz, CD₃CN/CDCl₃ = 1/1) δ 9.36 (br s, 6H), 8.54–8.46 (m, 12H), 8.19–8.13 (m, 12H), 8.00 (br s, 6H), 7.73 (dd, *J* = 9.0, 9.0 Hz, 12H), 7.54 (s, 6H), 7.48 (dd, *J* = 45.6, 8.4 Hz, 12H), 7.43 (d, *J* = 7.8 Hz, 6H), 7.30 (d, *J* = 7.4 Hz, 6H), 7.17 (d, *J* = 18.6 Hz, 6H), 6.80–6.76 (m, 6H), 6.11 (td, *J* = 7.4, 2.4 Hz, 12H), 4.37 (ddd, *J* = 60.0, 12.6, 8.4 Hz, 12H), 4.14–4.01 (m, 12H), 3.96–3.89 (m, 12H), 3.75–3.70 (m, 12H), 1.16–1.04 (m, 42H); HRMS (ESI): *m/z* calcd for (**D-CHZ**⁴⁺): 813.7975; found: 813.7981.

Synthesis of **T**(PF₆)₈

To a solution of [2**b**Fe](PF₆)₂ (4.60 mg, 2.50 μmol) in a mixed solvent of CD₃CN (250 μL) and CDCl₃ (250 μL) was added a solution of *trans*-1,4-cyclohexanediamine (37.5 mM, 10.0 μL) in a mixed solvent of CD₃CN/CDCl₃ = 1/1. The mixture was heated at 50 °C for 12 h, and then was subjected to the spectroscopic measurements.

T(PF₆)₈: ¹H NMR (600 MHz, CD₃CN/CDCl₃ = 1/1) δ 8.55–8.46 (m, 24H), 8.33 (s, 12H), 8.21 (br dd, *J* = 7.2, 7.2 Hz, 12H), 8.15 (br d, *J* = 7.2 Hz, 12H), 7.70 (d, *J* = 7.2 Hz, 24H), 7.53–7.46 (m, 36H), 7.42 (d, *J* = 7.8 Hz, 12H), 7.29 (dd, *J* = 7.8, 7.8 Hz, 12H), 7.12–7.14 (m, 12H), 6.77 (d, *J* = 7.8 Hz, 12H), 6.11 (br s, 12H), 4.37 (dd, *J* = 66.0, 12.0 Hz, 24H) 4.15–4.07 (m, 12H), 3.97–3.88 (m, 24H), 3.76–3.69 (m, 12H), 3.28 (br s, 12H), 1.73 (d, *J* = 52.8 Hz, 48H), 1.15–1.09 (m, 84H); ¹⁹F NMR (376 MHz, CD₃CN/CDCl₃ = 1/1) δ –72.7 (d, ¹*J*_{F-P} = 709 Hz); ³¹P NMR (243 MHz, CD₃CN/CDCl₃ = 1/1) δ –144.5 (d, ¹*J*_{P-F} = 709 Hz); HRMS (ESI): *m/z* calcd for (**T**⁸⁺): 832.2185; found: 832.2175.

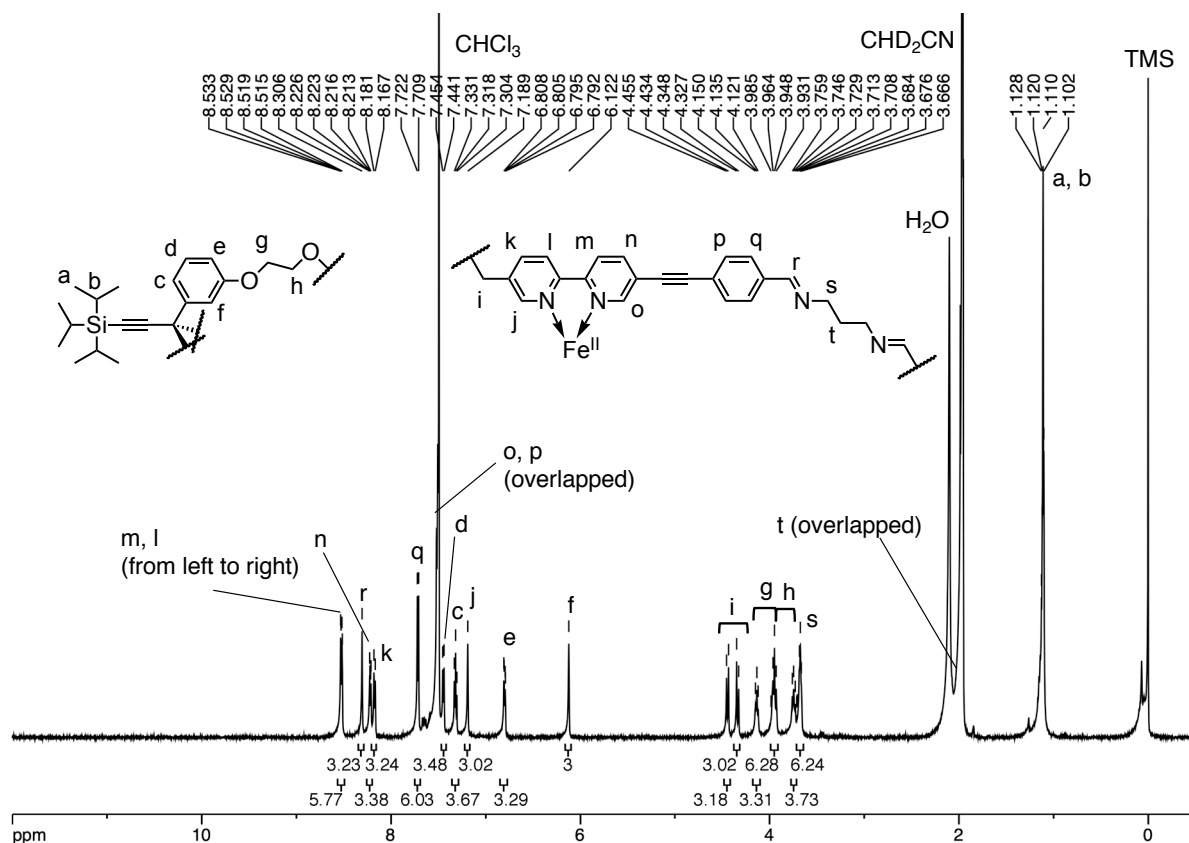


Figure S83. ^1H NMR spectrum of **D-PPD**(PF₆)₄ (600 MHz, CD₃CN/CDCl₃ = 1/1).

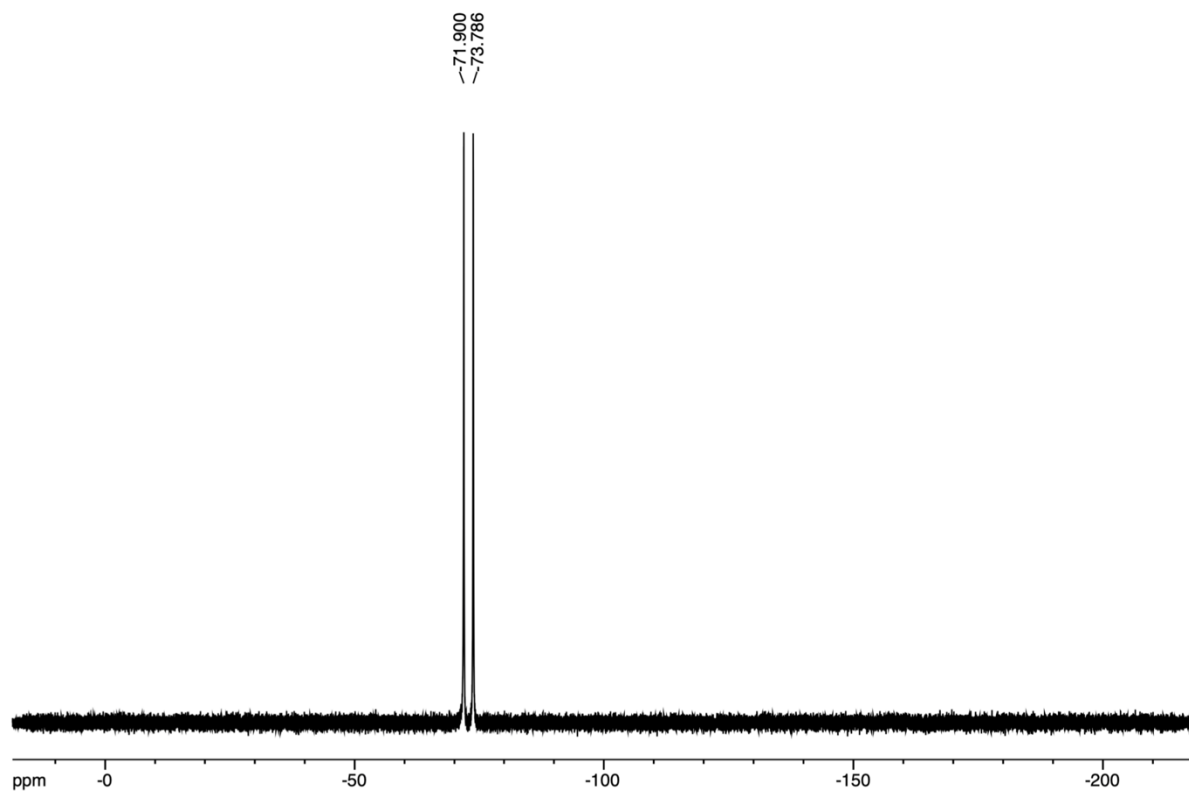


Figure S84. ^{19}F NMR spectrum of **D-PPD**(PF₆)₄ (376 MHz, CD₃CN/CDCl₃ = 1/1).

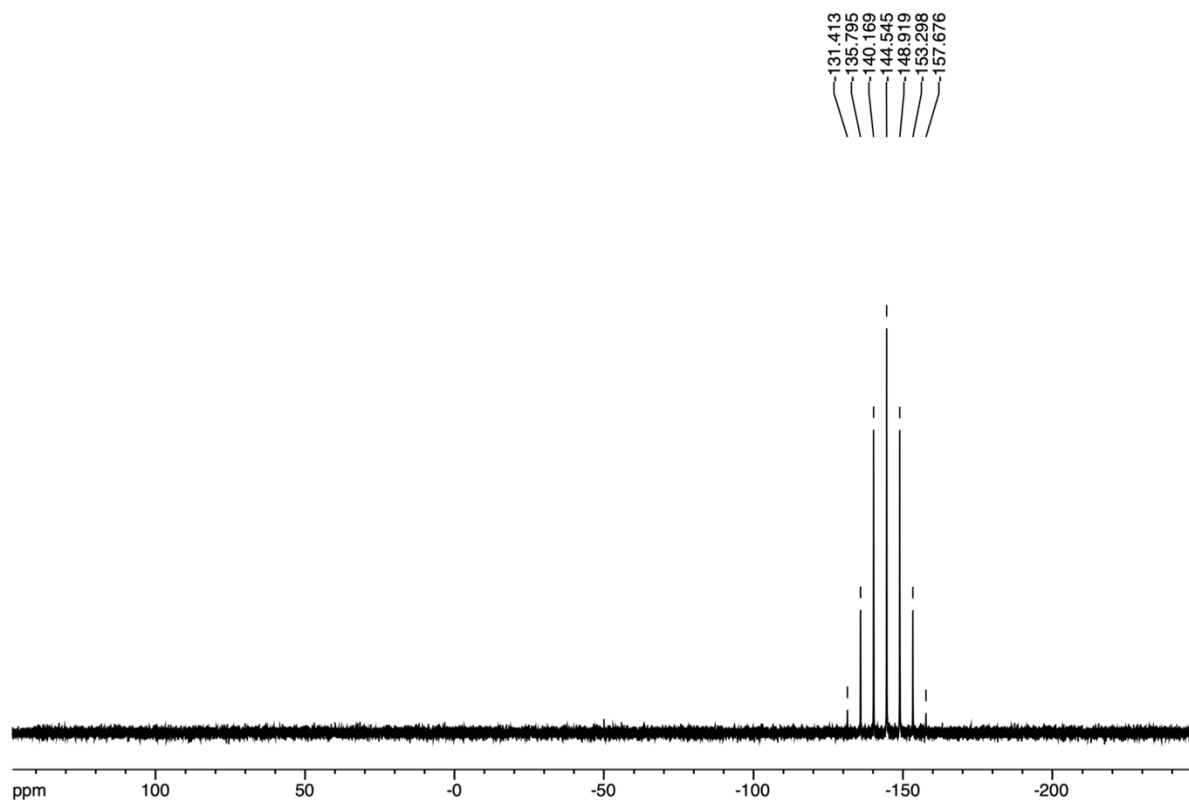


Figure S85. ^{31}P NMR spectrum of **D-PPD**(PF₆)₄ (162 MHz, CD₃CN/CDCl₃ = 1/1).

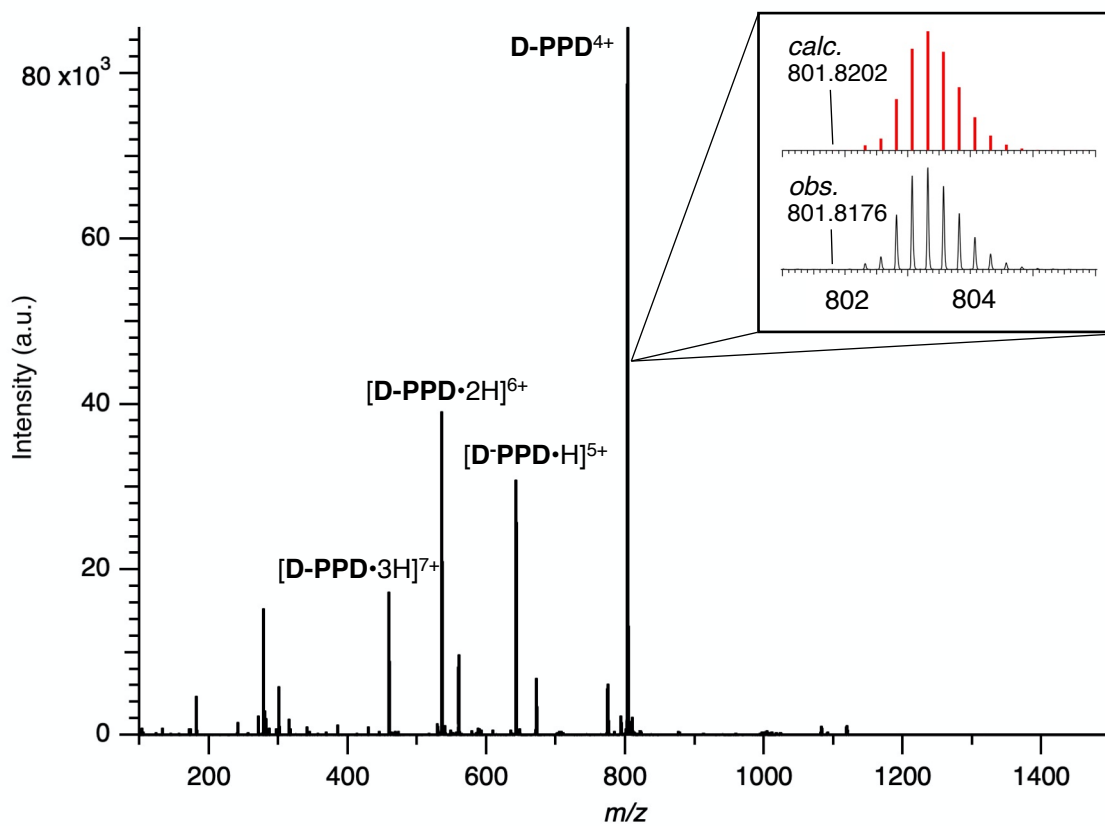


Figure S86. ESI mass spectrum of **D-PPD**(PF₆)₄ (solv. CH₃CN).

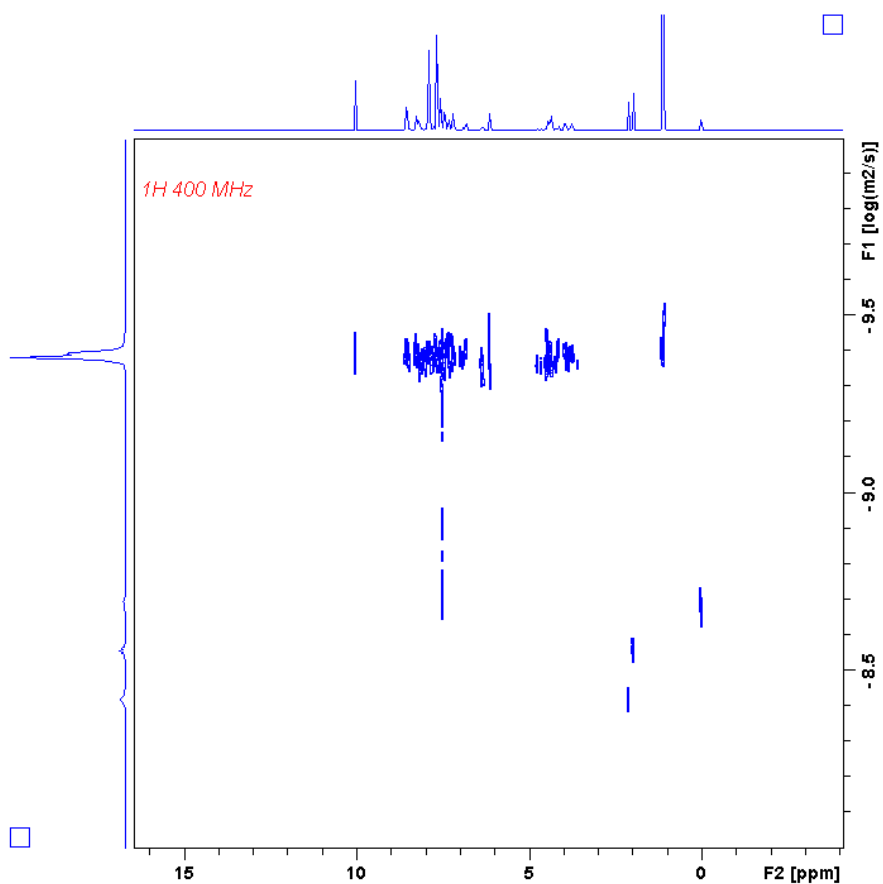


Figure S87. ^1H DOSY spectrum of **D-PPD**(PF₆)₄ (400 MHz, CD₃CN/CDCl₃ = 1/1).

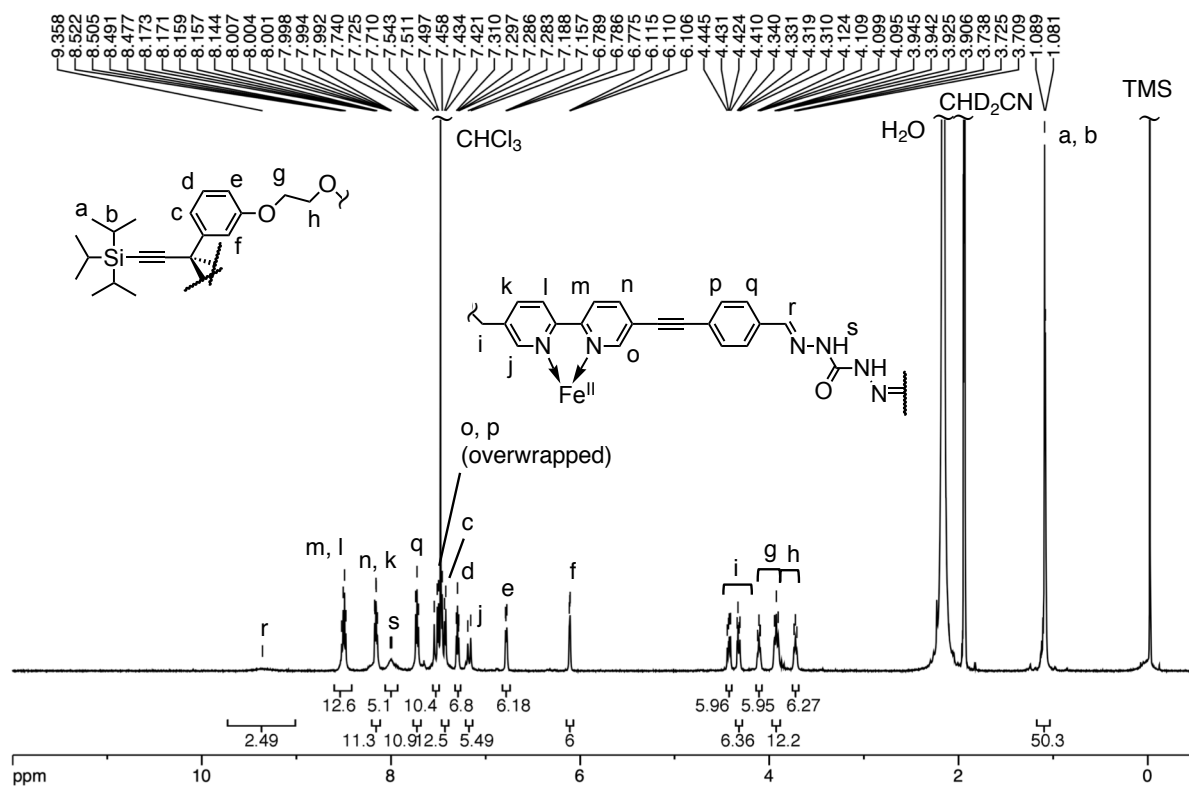


Figure S88. ^1H NMR spectrum of **D-CHZ**(PF₆)₄ (600 MHz, CD₃CN/CDCl₃ = 1/1).

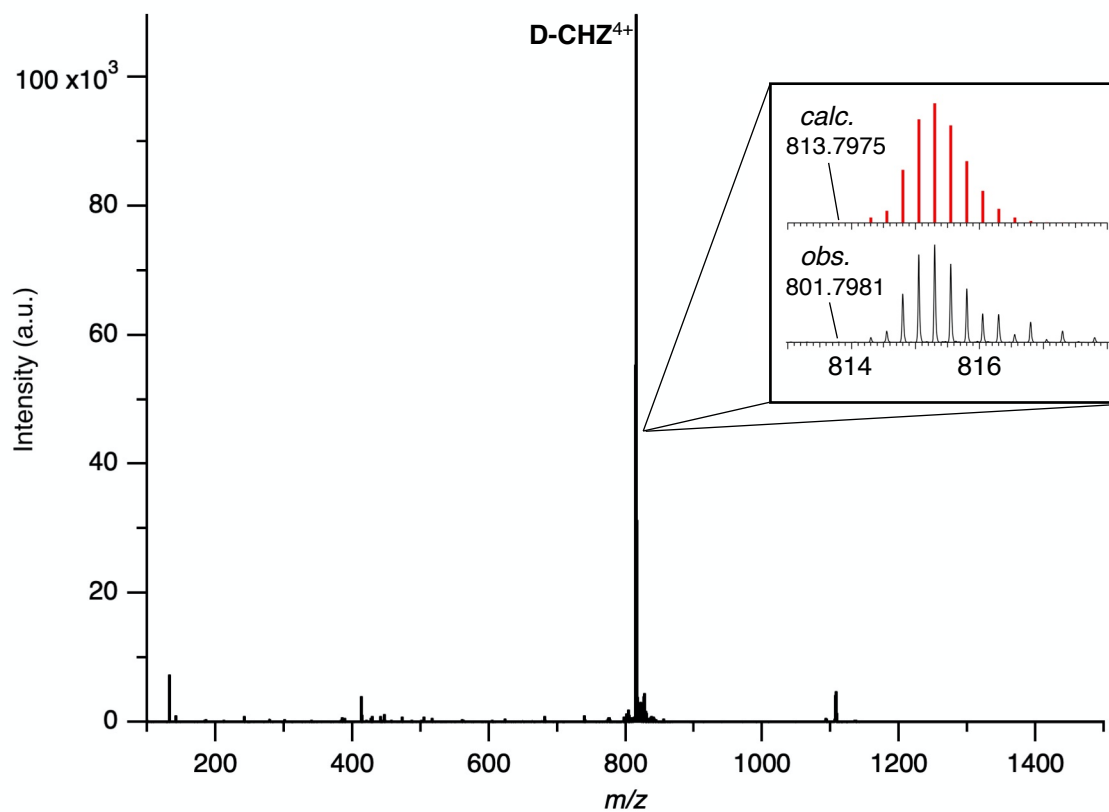


Figure S89. ESI mass spectrum of **D-CHZ**(PF₆)₄ (solv. CH₃CN).

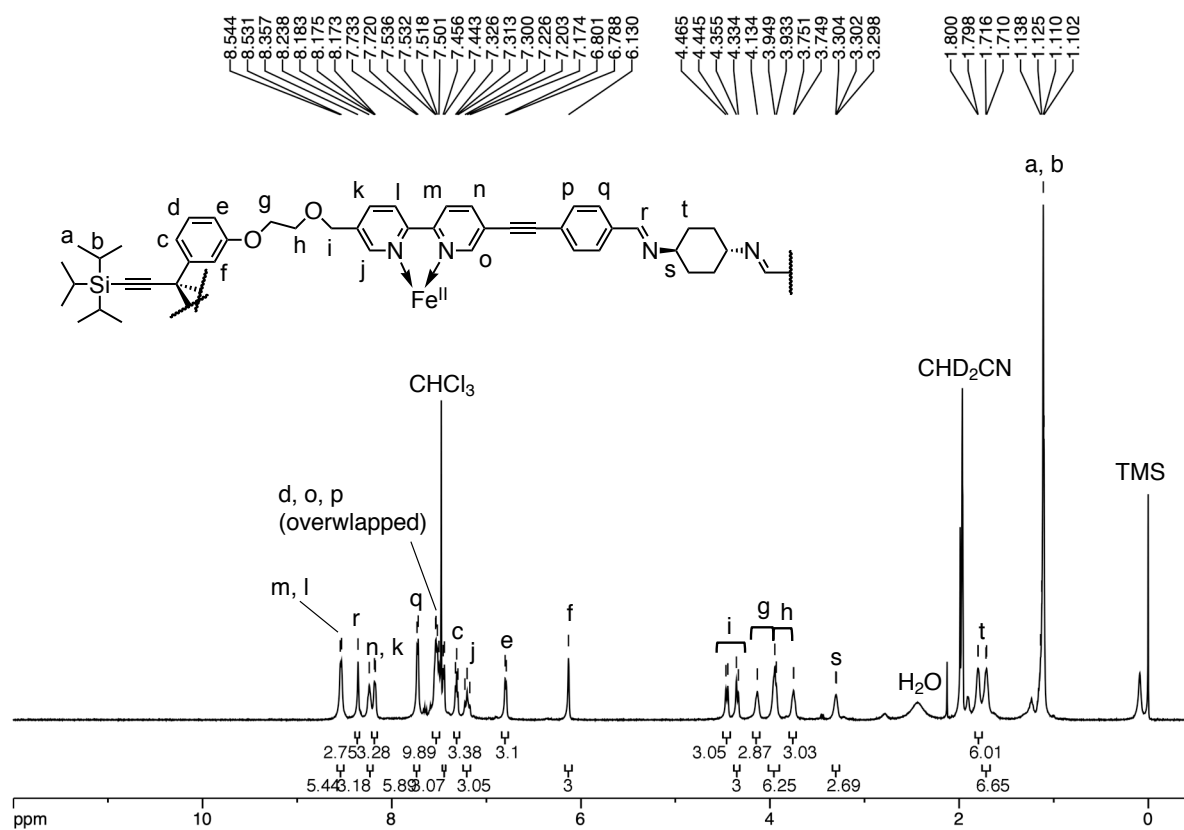


Figure S90. ¹H NMR spectrum of **T**(PF₆)₈ (600 MHz, CD₃CN/CDCl₃ = 1/1).

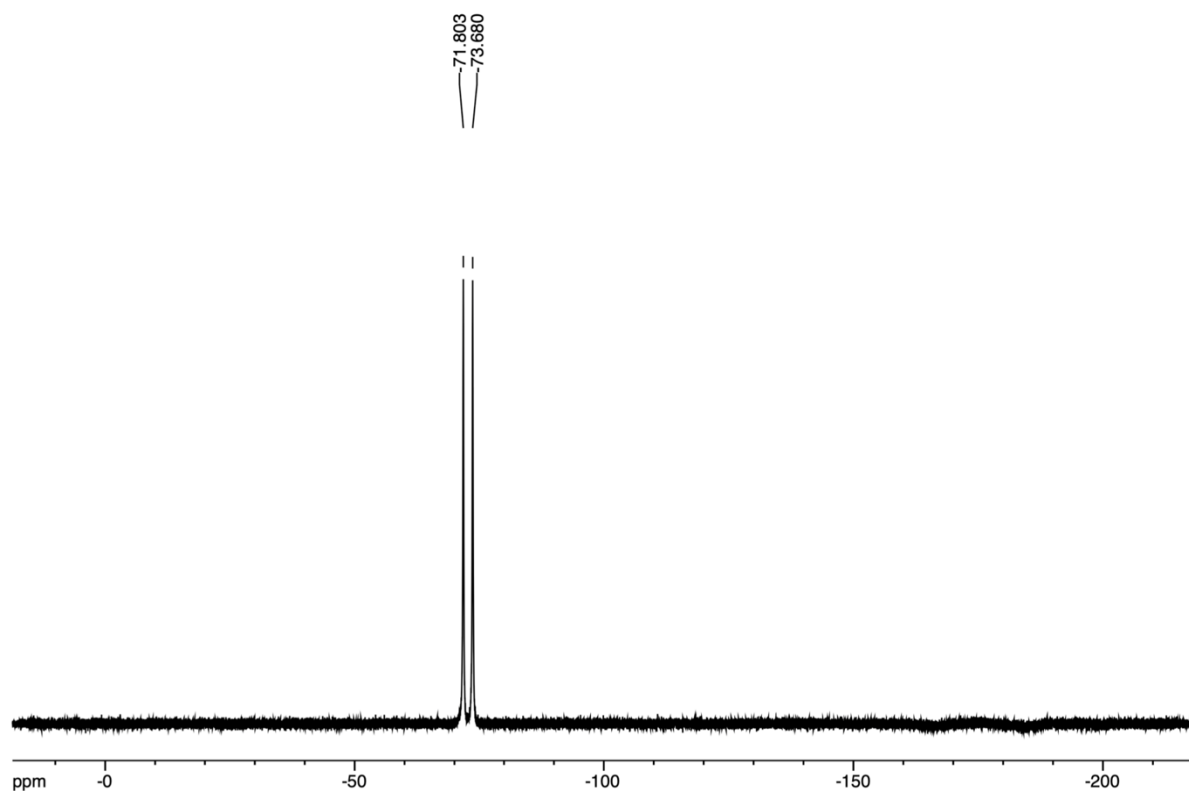


Figure S91. ^{19}F NMR spectrum of $\text{T}(\text{PF}_6)_8$ (376 MHz, $\text{CD}_3\text{CN}/\text{CDCl}_3 = 1/1$).

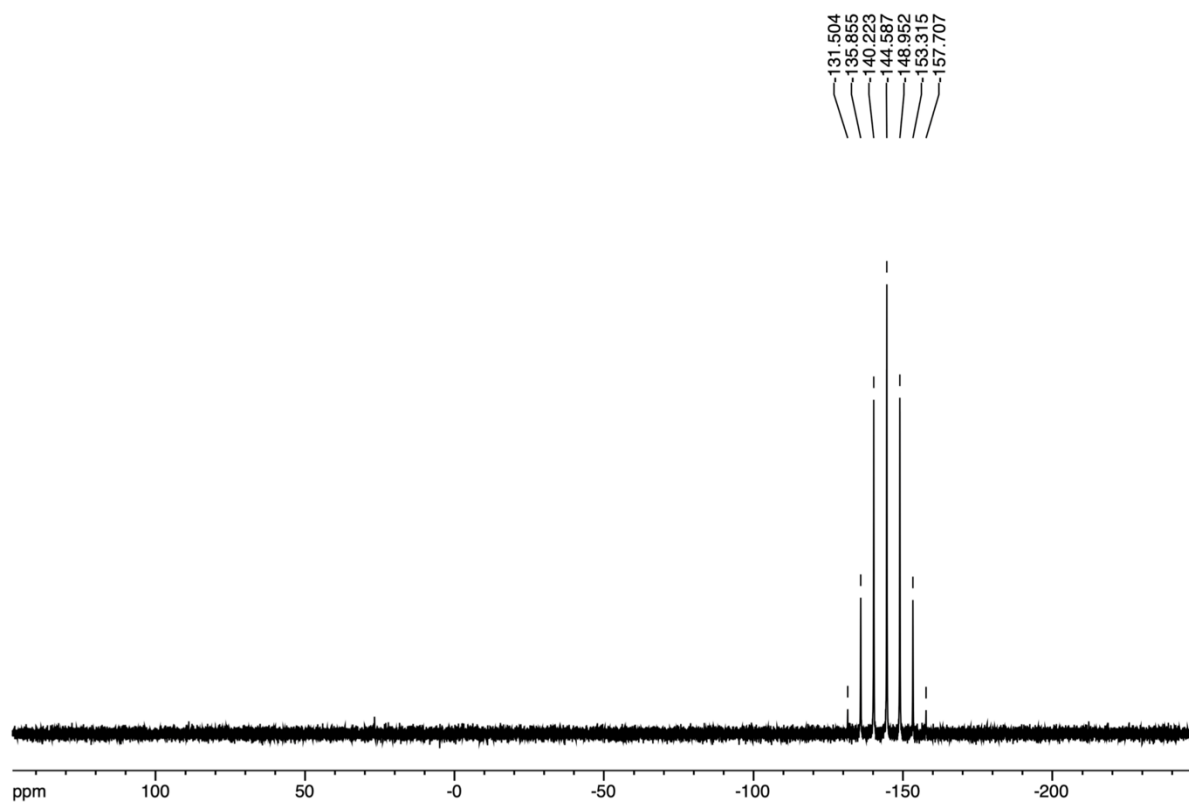


Figure S92. ^{31}P NMR spectrum of $\text{T}(\text{PF}_6)_8$ (162 MHz, $\text{CD}_3\text{CN}/\text{CDCl}_3 = 1/1$).

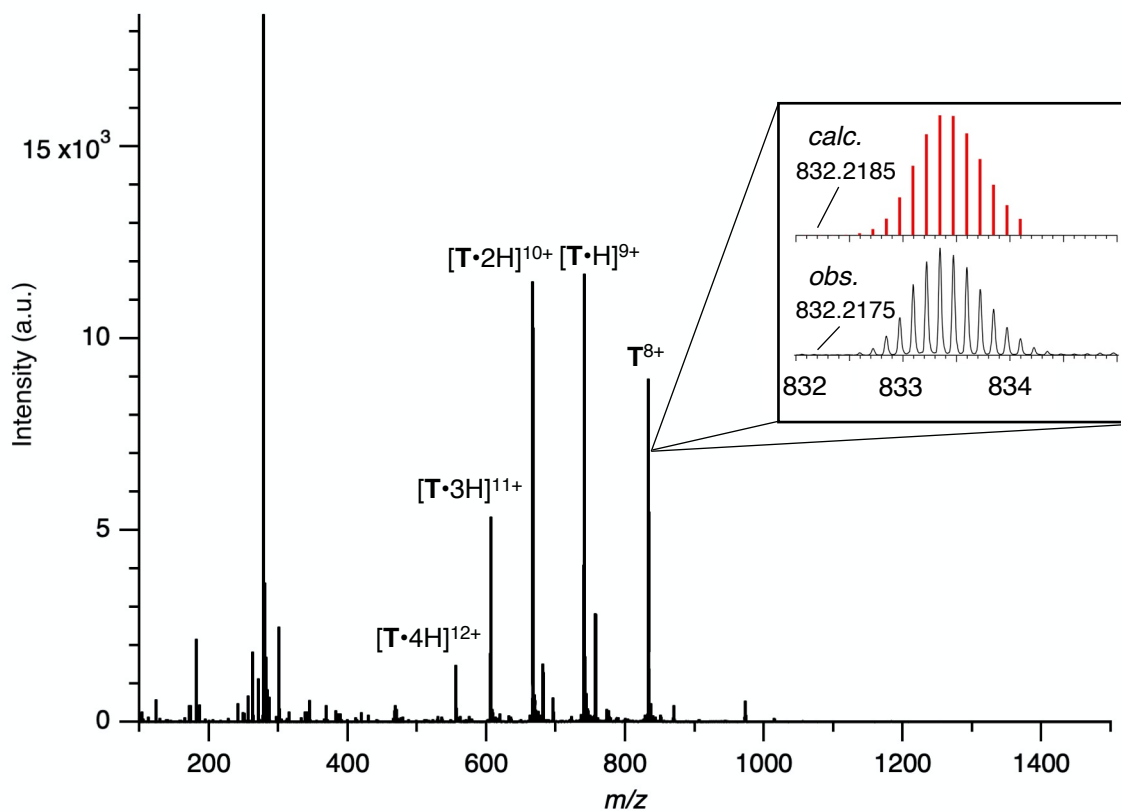


Figure S93. ESI mass spectrum of $T(PF_6)_8$ (solv. CH_3CN).

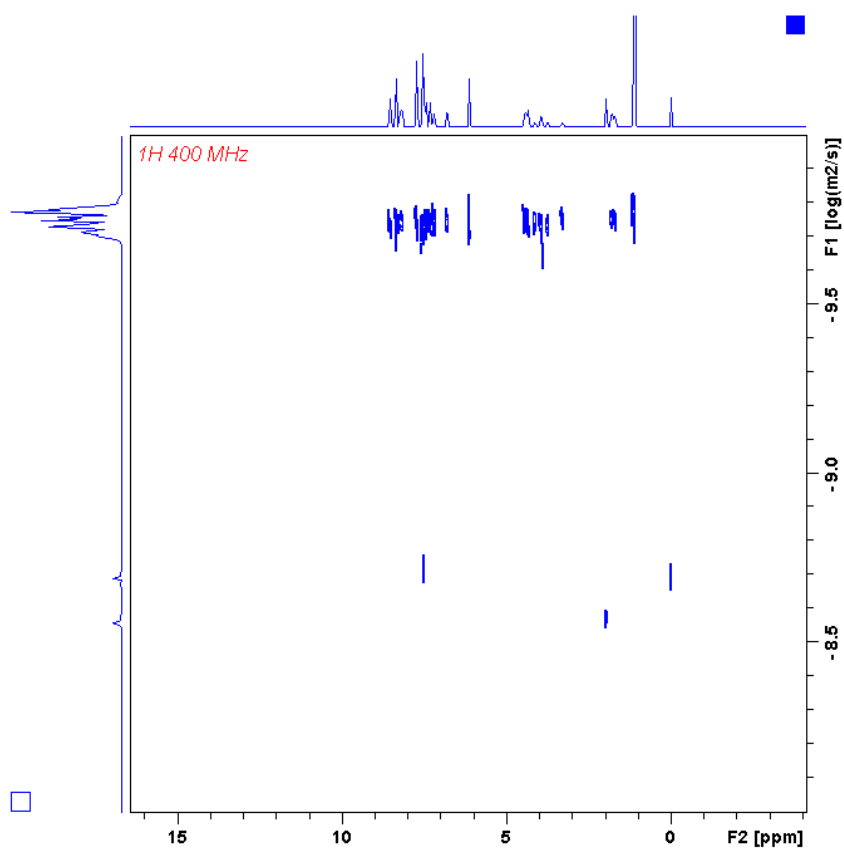


Figure S94. 1H DOSY spectrum of $T(PF_6)_8$ (400 MHz, $CD_3CN/CDCl_3 = 1/1$).

Table S4. Diffusion constants determined by ^1H DOSY measurements and the hydrodynamic radii calculated by the Stokes-Einstein Equation.

Structure	Diffusion constant (m^2/s)	Hydrodynamic radius (\AA)
[2bFe](PF₆)₂	4.0×10^{-10}	12
D-PPD(PF₆)₄	2.8×10^{-10}	17
T(PF₆)₈	1.8×10^{-10}	25

References for the Supporting Information

- S1. G. M. Sheldrick, *Acta Cryst.*, 2008, **A64**, 112–122.
- S2. G. M. Sheldrick, *Acta Cryst.*, 2015, **C71**, 3–8.
- S3. (a) K. Wakita, *Yadokari-XG, Software for Crystal Structure Analyses*, 2001; (b) C. Kabuto, S. Akine, T. Nemoto and E. Kwon, *J. Cryst. Soc. Jpn.*, 2009, **51**, 218–224.
- S4. T. Nakamura, H. Kimura, T. Okuhara, M. Yamamura and T. Nabeshima, *J. Am. Chem. Soc.*, 2016, **138**, 794–797.
- S5. J. E. Nunez, T.-A. V. Khuong, L. M. Campos, N. Farfan, H. Dang, S. D. Karlen and M. A. Garcia-Garibay, *Cryst. Growth Des.*, 2006, **6**, 866–873.
- S6. S. T. Bowden, *J. Chem. Soc.*, 1957, 4235–4239.
- S7. W. B. Austin, N. Bilow, W. J. Kelleghan and K. S. Y. Lau, *J. Org. Chem.*, 1981, **46**, 2280–2286.
- S8. (a) U. Mayer, V. Gutmann and W. Gerger, *Monatsh. Chem.*, 1975, **106**, 1235–1257; (b) F. Cataldo, *Eur. Chem. Bull.*, 2015, **4**, 92–97; (c) C. M. Hansen, *Hansen Solubility Parameters: A User's Handbook*, 2nd ed.; CRC Press LLC: Boca Raton, Florida, USA, 2007.